MULTICOLOR PHOTOELECTRIC PHOTOMETRY OF BRIGHT EXTRAGALACTIC SYSTEMS

Thesis by

William Grant Tifft

In Partial Fulfillment of the Requirements

For the Degree of

Doctor of Philosophy

California Institute of Technology

Pasadena, California

1958

ACKNOWLEDGEMENTS

The author wishes to acknowledge the advice and encouragement of Dr. Arthur D. Code who suggested this thesis and served as advisor during the investigation. Acknowledgement is also due to Dr. Code for the use of some unpublished observations, and to Dr. William A. Baum in connection with the selection of photoelectric filters, and the selection of Coma and Virgo cluster galaxies for observation.

The author is particularly grateful to the staff and council of the Mount Wilson and Palomar Observatories for the use of the equipment at Mount Wilson. The research and study program leading to the doctorate degree has been greatly facilitated by fellowships from the National Science Foundation; for this support the author is very grateful.

The author's wife, Carol N. Tifft, is due a special vote of thanks for having typed this thesis.

ABSTRACT

57 galaxies and 52 stars have been observed in four colors using a blue sensitive phototube. The response bands of the photometric system have effective reciprocal wave lengths of (micron units) 2.66, 2.39, 2.07, and 1.68. In addition to the blue measurements 8 galaxies and 19 stars have been observed in four colors using a red sensitive photocell. The effective reciprocal wave lengths of the red response bands are 1.55, 1.26, 1.14, and 1.00. From one to five different aperture sizes have been used in the photometry of each galaxy, with an average of three per galaxy. The entire eight color photometric system has been calibrated to place color index measurements on an absolute energy basis.

Correlations between nuclear color index and inclination, spectral class, and nebular type indicate that most of the observed galaxies fall into fairly distinct groups. Radial color variations are also found to correlate with group membership. The dominant characteristics of the groups are as follows: spectral type A, spectral type F, spectral type FG, nebular type Sa, nebular type E, nebular type S0, nebular type Sb.

The correlation between nuclear color and inclination (axis ratio) is found to show a distinct separation of Sa, Sb, and elliptical galaxies, probably due in part to differences in internal absorption. The correlation of nuclear color and spectral type shows that FG galaxies, while later in spectral class than F galaxies, have nuclei bluer than those in F galaxies. A possible explanation is offered which interprets the inversion in terms of the relative numbers of normal and low metal abundance stars in each type of galaxy. Radial color investigations reveal the existence of blue nuclei in three galaxies.

Synthetic models are given for five distinct types of extragalactic nuclei. K nuclei can be represented with a mixture of old population I and II stars. F, FG, and probably AF nuclei can be produced by adding various numbers of young blue stars to K galaxies. A type galaxies appear to be completely dominated by young stars.

TABLE OF CONTENTS

I INTRODUCTION

1.1 Purpose

The first objective of this photometric study of extragalactic systems has been to provide a set of basic color measurements for a wide range of extragalactic structural types. The second objective has been the attempted interpretation of the colors in terms of the relative numbers and types of constituent stars, and the investigation of various correlations between color and other properties of the systems studied. Emphasis has been placed on color measurement and not on the determination of magnitudes since appreciable portions of many of the systems studied could not be included within the largest diaphragm acceptable by the photometric equipment.

1.2 Selection of Objects

Galaxies were selected for observation according to the following restrictions:

1. With the exception of M31, M32, M33 and NGC 205, all galaxies lie between galactic latitude $+30°$ and $+90°$. More extensive observations than were possible would be required to investigate dependence of color on galactic latitude or systematic differences between the polar caps.
2. The majority of the galaxies observed are bright non-cluster field galaxies with small redshifts. A few representative galaxies from the Coma and Virgo clusters were also included.
3. All the Hubble extragalactic types are represented, including examples over the full range of inclination from edge-on to face-on.
4. With one accidental exception, all galaxies are free from interference by superimposed bright field stars.
5. Whenever possible, galaxies were selected from the list of systems for which Morgan (1) has given spectral classes. To complete representation of structural types, additional galaxies were selected from the Humason, Mayall and Sandage (2) redshift catalog.
6. A number of elliptical galaxies in the Coma and Virgo clusters were selected to provide photometry on galaxies which have also been measured by Baum (3) and/or Whitford (4).

In addition to the galaxies a selection of standard stars was observed to determine stellar colors on the photometric system. The

MAJORITY OF THE STARS RANGE FROM SPECTRAL CLASS F TO M AND INCLUDE REPRESENTATIVES OF THE MAIN SEQUENCE, NORMAL AND HIGH VELOCITY GIANTS, AND SUBDWARFS. A FEW BLUE STARS WERE ALSO MEASURED.

1.3 Color System

Some measurements have been made in eight colors using two photocells, however the vast majority of the observations were taken in four colors using a blue sensitive type 6094 EMI photocell. Toward the end of the observing program, a red photometer employing a type 16PM-1 Farnsworth photomultiplier became available and a small amount of data in four colors in the red and infrared was obtained. Details concerning the instruments and filters employed, as well as their calibration, are included in the following section.

II INSTRUMENTATION AND TECHNIQUES

2.1 Instruments Used, Their Calibration

The blue sensitive type 6094 EMI employed is an eleven-stage end-on photocell and operates unrefrigerated. The output of the photocell passes to ground through one of eleven load resistors arranged in half magnitude steps from 1M to 100M. The potential across the load resistor is fed into a D.C. amplifier and the amplifier output recorded on a Brown recorder. The same box which houses the amplifier contains the electronic power supply to provide the high voltage to operate the photocell. For faint work the photocell normally operates with a total applied voltage of 1300 volts; however, provision is made for division of the voltage to reduce the voltage on the photocell to a total of 700 volts to introduce a 4 1/2 magnitude coarse sensitivity step. For a short period after a coarse sensitivity switch the photocell sensitivity tends to drift slightly, necessitating small corrections which are determined by observations of a standard luminous source. The load resistors, referred to the smallest resistor as standard, have slightly different temperature coefficients and slow time changes. The resistors were calibrated near the middle of the period during which observations were being made. The calibration was done at two temperatures using a Wheatstone bridge circuit. The coarse sensitivity step was determined every time it was used by means of the known load resistor calibration and standard source measurements. The slight difference in the coarse step for stars and the standard source, due to different imaging on the cathode, was determined on two occasions by comparing both star and source deflections under high and low sensitivity conditions. The small correction, amounting to +0.016 magnitude, was then added to each determination of the coarse step from standard source measurements.

Red and infrared observations were obtained with a red sensitive type 16PM-1 Farnsworth photomultiplier tube. The thirteen-stage end-on photocell was operated under dry ice refrigeration. Throughout the use of the Farnsworth photocell it was operated with total applied voltage of 2200 volts from an electronic power supply. The first observations were obtained with the Farnsworth photocell operated in conjunction with a chopper stabilized amplifier. The photocell output passed to ground through one of seventeen load resistors arranged in magnitude and half magnitude steps from 0.063M to 25M. The potential across the load resistor was fed into the chopper amplifier and the output read on a Brown recorder. A selector switch permitted the output to be taken as 100, 10, or 1 mv full scale to provide additional sensitivity control. Unfortunately the amplifier has positional sensitivity dependence; however, since the sensitivity variation was generally small in the course of observation on any one object it was possible to assume the variation was linear with time and to derive color measurements with very little loss of accuracy. Since color measurement was the major objective, reduction of data on magnitudes was not attempted. Because all deflections on any given object were made without switching output scale sensitivity, there was no need to calibrate the sensitivity steps between the output scales. The load resistors were calibrated immediately following their use by means of a Wheatstone bridge circuit. Since all the resistors have identical materials, hence identical temperature coefficients, the resistance values, referred to the smallest resistor as standard, were assumed to be independent of temperature.

For applications of the Farnsworth photocell subsequent to the initial use, a new electrometer tube amplifier was available. In this case the photocell output was dropped to ground through one of six load resistors in 2 1/2 magnitude steps from 10^5 to 10^{10} ohms. Seven half magnitude steps were provided by eight attenuation resistors in the feedback circuit. The amplifier output was recorded as usual on a Brown recorder with 10 mv full scale. The attenuation resistor steps were calibrated by feeding in known relative signals from a battery source operating through a precision Wolf potentiometer and recording the output on a Brown recorder. The load resistors were calibrated by sending in a constant current signal and comparing adjacent load steps by means of the calibrated attenuation steps.

The sensitivity curves of the EMI and Farnsworth phototubes were determined as a function of wave length for use in absolute energy calibration of the color system. The calibration was carried out by comparing the response of the photocells with that of a thermocouple. The source of illumination was either a tungsten ribbon filament lamp or a high amperage tungsten coil filament lamp viewed through a Hilger-Muller double-pass quartz monochrometer. The ribbon filament lamp was operated through a voltage regulator and a Powerstat variable output

TRANSFORMER. THE LAMP CURRENT WAS CONTINUOUSLY MONITORED AND ADJUSTED TO MAINTAIN CONSTANCY WITHIN ABOUT 0.03 AMP. THE LAMP IS RATED AT NINE AMPERES AND WAS OPERATED SLIGHTLY BELOW THAT VALUE. THE COIL FILAMENT LAMP, USED ONLY FOR THE ULTRAVIOLET, WAS OPERATED AT EITHER 28 OR 32 AMPS THROUGH A 45 AMP VARIAC OFF THE 110 VOLT LINE. THE CURRENT WAS CONTINUOUSLY MONITORED, BUT SINCE NO VOLTAGE REGULATOR WAS AVAILABLE FOR THE LARGE CURRENT INVOLVED, THE LAMP CURRENT COULD NOT BE REGULATED AS ACCURATELY AS FOR THE SMALLER AMPERAGE LAMP.

THE CALIBRATION OF THE TWO PHOTOCELLS WAS CARRIED OUT IN THREE SESSIONS; THE FARNSWORTH PHOTOCELL (UNDER DRY ICE REFRIGERATION) BETWEEN λ5500 AND λ16000, THE EMI PHOTOCELL BETWEEN λ4500 AND λ8000, AND THE EMI PHOTOCELL BETWEEN λ3500 AND λ4900. FOR THE FIRST TWO CALIBRATIONS THE LAMP FILAMENT WAS IMAGED ON THE MONOCHROMETER ENTRANCE SLIT BY MEANS OF THREE LENSES. BECAUSE OF CHROMATIC ABBERATION THE IMAGE FOCUS IN THE INFRARED WAS DETERMINED EMPIRICALLY TO GIVE MAXIMUM RESPONSE FROM THE THERMOCOUPLE WHEN THE MONOCHROMETER WAS SET AT A WAVE LENGTH NEAR THE MIDDLE OF THE RANGE INVESTIGATED. FOR THE ULTRAVIOLET CALIBRATION THE LENSES WERE REPLACED BY TWO ALUMINIZED PARABOLIC MIRRORS. BECAUSE OF THE MUCH GREATER RESPONSE SENSITIVITY OF THE PHOTOCELLS COMPARED TO THE THERMOCOUPLE, IT WAS NECESSARY TO INTRODUCE APPRECIABLE ATTENUATION INTO THE LIGHT BEAM WHEN THE PHOTOCELLS WERE IN PLACE. IN THE CASE OF THE LENS IMAGING OPTICS THE LAMP FILAMENT WAS PLACED AT THE FOCUS OF THE FIRST LENS TO PRODUCE A COLLIMATED BEAM. WHEN THE PHOTOCELLS WERE IN PLACE AT THE MONOCHROMETER A PINHOLE DIAPHRAGM WAS INTRODUCED INTO THE COLLIMATED BEAM. FOR THE MIRROR OPTICS A HARTMANN-LIKE SCREEN WAS PLACED DIRECTLY IN FRONT OF THE FINAL MIRROR IN THE IMAGING TRAIN TO PRODUCE THE NECESSARY ATTENUATION.

THROUGHOUT THE CALIBRATION THE ENTRANCE AND EXIT SLITS OF THE HILGER-MULLER DOUBLE-PASS MONOCHROMETER WERE SET EQUAL, AND THE CENTRAL SLIT AT ABOUT TWICE THE WIDTH OF THE OTHER TWO. SLIT WIDTHS WERE NOT CHANGED DURING THE COURSE OF A CALIBRATION RUN. FOR THE FARNSWORTH PHOTOCELL CALIBRATION THE EXIT SLIT WIDTH CORRESPONDED TO 240 ANGSTROMS IN THE EMERGENT SPECTRUM AT λ5850. THE SAME SLIT SETTINGS WERE USED FOR THE LONGER WAVE LENGTH CALIBRATION OF THE EMI PHOTOCELL. FOR THE ULTRAVIOLET CALIBRATION THE EXIT SLIT WIDTH CORRESPONDED TO 260 ANGSTROMS IN THE EMERGENT SPECTRUM AT λ4045. THE EFFECTIVE SLIT WIDTH AT OTHER WAVE LENGTHS CAN BE DETERMINED FROM THE DISPERSION PROPERTIES OF QUARTZ. THE

WAVE LENGTH SCALE OF THE HILGER-MULLER MONOCHROMETER WAS CALIBRATED BY VISUAL OBSERVATIONS BETWEEN λ4045 AND λ6700, AND BY PHOTOELECTRIC SCANNING IN THE ULTRAVIOLET AND INFRARED. MERCURY AND NEON LINE SOURCES WERE USED FOR THE CALIBRATION. THE STRONGEST INFRARED LINE EMPLOYED WAS THE λ10113 NITROGEN LINE PRESENT AS AN IMPURITY IN THE MERCURY SOURCE. SYSTEMATIC DIFFERENCES WERE FOUND IN THE WAVE LENGTH CALIBRATION AT DIFFERENT TIMES. POSSIBLE ERRORS RESULTING FROM THESE DIFFERENCES ARE ABOUT 5 ANGSTROMS AT λ4500 AND AS MUCH AS 50 ANGSTROMS AT λ10,000.

BOTH THE THERMOCOUPLE AND PHOTOCELL ENTRANCE WINDOWS WERE PLACED IN THE SAME POSITION AS CLOSE AS POSSIBLE TO THE EXIT SLIT OF THE MONOCHROMETER. THE THERMOCOUPLE OUTPUT WAS READ BY MEANS OF A SENSITIVE GALVANOMETER, AND THE PHOTOCELL OUTPUT WAS FED THROUGH AN AMPLIFIER AND RECORDED ON EITHER A BROWN OR VARIAN RECORDER. THE PHOTOCELLS WERE OPERATED WITH TOTAL APPLIED VOLTAGES OF 500 VOLTS TAKEN FROM AN ELECTRONIC SUPPLY. BECAUSE OF TIME DELAYS AND THE CHANCE OF DISTURBING THE CALIBRATION IT WAS NOT FEASIBLE TO ALTERNATE BETWEEN THE PHOTOCELL AND THERMOCOUPLE VERY FREQUENTLY. CONSEQUENTLY THE ENTIRE RANGE OF INTEREST IN A GIVEN MEASUREMENT SESSION WAS SCANNED WITH THE THERMOCOUPLE, THEN THE SCAN WAS REPEATED WITH THE PHOTOCELL, AND FINALLY REPEATED AGAIN WITH THE THERMOCOUPLE. THE TWO THERMOCOUPLE SCANS AGREED SATISFACTORILY IN ALL CASES. WHEN SCANNING WITH EITHER THE THERMOCOUPLE OR PHOTOCELL FREQUENT REMEASUREMENTS WERE MADE AT A SELECTED WAVE LENGTH TO CORRECT FOR ANY SLIGHT DRIFT DURING THE CALIBRATION.

IN VIEW OF THE TECHNIQUE EMPLOYED IN CALIBRATION OF THE PHOTOCELLS THE ONLY IMPORTANT DIFFERENCES IN THE LIGHT SEEN BY THE THERMOCOUPLE AND PHOTOCELL ARISE FROM THE LIGHT ATTENUATION DIAPHRAGMING, AND SLIGHT DIFFERENCES IN THE VIEWING AT THE EXIT SLIT, PARTICULARLY THE VIEWING OF LIGHT SCATTERED FROM THE JAWS OF THE EXIT SLIT. BOTH OF THESE EFFECTS ARE PROBABLY RELATIVELY SMALL. VISUAL INSPECTION OF THE EMERGENT LIGHT SUGGESTS THAT A SMALL AMOUNT OF LIGHT IS SCATTERED INTO THE BEAM FROM ADJACENT SPECTRAL REGIONS, PROBABLY BY SCATTERING AT THE JAWS OF THE CENTRAL SLIT. THE EFFECT APPEARS TO BE VERY SMALL AND IN ANY CASE THE WAVE LENGTH DIFFERENCE OF THE LIGHT FROM THE MAIN BUNDLE IS NOT VERY LARGE. PHOTOELECTRIC SCANNING IN THE ULTRAVIOLET BEYOND THE PHOTOTUBE CUTOFF AND IN THE FAR INFRARED GIVES ZERO RESPONSE IMPLYING THAT SCATTERING OVER LARGE WAVE LENGTH RANGES IS VIRTUALLY ZERO. TABLE 1 GIVES THE MEASURED PHOTOTUBE RESPONSE RELATIVE TO THE THERMOCOUPLE AS A

FUNCTION OF RECIPROCAL WAVE LENGTH. THE RESPONSE VALUES ARE NORMALIZED TO READ 1.000 AT MAXIMUM SENSITIVITY. THE VALUES WERE NOT CORRECTED FOR THE EFFECT OF FINITE SLITWIDTH.

TABLE 1

NORMALIZED RESPONSE OF PHOTOCELLS

EMI PHOTOCELL

$1/\lambda$	P	$1/\lambda$	P	$1/\lambda$	P	$1/\lambda$	P
2.925	.587	2.500	.993	2.075	.808	1.650	.0673
2.900	.626	2.475	.997	2.050	.776	1.625	.0385
2.875	.663	2.450	1.000	2.025	.742	1.600	.0224
2.850	.699	2.425	1.000	2.000	.707	1.575	.0133
2.825	.731	2.400	.999	1.975	.670	1.550	.00790
2.800	.763	2.375	.998	1.950	.632	1.525	.00453
2.775	.793	2.350	.994	1.925	.594	1.500	.00234
2.750	.821	2.325	.988	1.900	.550	1.475	.00108
2.725	.846	2.300	.980	1.875	.502	1.450	.00059
2.700	.869	2.275	.972	1.850	.447	1.425	.00033
2.675	.890	2.250	.962	1.825	.387	1.400	.000157
2.650	.910	2.225	.950	1.800	.328	1.375	.000065
2.625	.928	2.200	.933	1.775	.274	1.350	.000033
2.600	.946	2.175	.915	1.750	.222	1.325	.0000145
2.575	.962	2.150	.895	1.725	.183	1.300	.0000068
2.550	.974	2.125	.868	1.700	.144	1.275	.0000029
2.525	.985	2.100	.839	1.675	.106	1.250	.0000012

FARNSWORTH PHOTOCELL

$1/\lambda$	P	$1/\lambda$	P	$1/\lambda$	P	$1/\lambda$	P
1.725	.288	1.450	.512	1.175	.939	0.900	.159
1.700	.297	1.425	.547	1.150	.966	0.875	.075
1.675	.310	1.400	.587	1.125	.989	0.850	.026
1.650	.323	1.375	.629	1.100	1.000	0.825	.0113
1.625	.339	1.350	.675	1.075	.990	0.800	.00275
1.600	.356	1.325	.717	1.050	.953	0.775	.00050
1.575	.375	1.300	.761	1.025	.878	0.750	.00013
1.550	.397	1.275	.801	1.000	.767	0.725	.000062
1.525	.420	1.250	.840	0.975	.624	0.700	.000015
1.500	.448	1.225	.876	0.950	.468		
1.475	.478	1.200	.909	0.925	.302		

2.2 The Filter System

Conventional Corning and Schott glass filters or filter combinations were used in conjunction with the EMI photocell. Special interference filters made by Federal Engineering were used for three of the four red and infrared pass bands. Two of the interference filters were combined with glass filters, in one case to cut out a second transmission maximum in the blue and in the other case to sharpen the blue side of the transmission band. The furthest infrared response band was defined by means of a Heimann No. 205 filter consisting of a special infrared transmitting coating on glass. In the case of the longest wave length bands with both photocells the phototube sensitivity cutoff provided the long-wave boundary. Clear glass was cemented to three of the four glass filters and the far infrared filter to bring them all to the same thickness as the thickest glass filter. The interference filters were not adjusted but are quite close to the same thickness. The glass added to the ultraviolet filter cuts out light below λ3450 normally transmitted by the filter; the glass does not affect transmission significantly in any other cases. Table 2 lists the filter components and gives thicknesses when they differ from stock values. The interference filters were custom made hence have no special designation. The filters and the response bands they define are designated by serial numbers from 1 to 8 in order of wave length.

TABLE 2

Filter System

Band	Filters
1	Corning 9863 + approximately Corning 7380
2	Schott BG-12 + Schott GG-13
3	Corning 5030 (1.6 mm) + Corning 3387
4	Corning 3480
5	Federal Engineering special interference filter
6	Federal Engineering special interference filter + Corning 2434
7	Federal Engineering special interference filter + Schott RG-10
8	Heimann No. 205

Filter transmissions were determined as a function of wave length with a Hilger-Muller double-pass quartz monochrometer. Filters were placed in the filter slide of the photohead and the emergent beam of the monochrometer viewed by the photocell alternately through a filter and directly. The monochrometer exit slit was narrow, about 40 angstroms in the emergent spectrum at λ5850, for all filter calibrations. Table 3 lists the filter transmissions, including of course surface reflection effects, as a function of reciprocal wave length. The values were read from smoothed curves of the actual measurements. All the filters in conjunction with the photocells provide well defined response bands with the exception of number 5. This filter has a small secondary maximum that requires the application of small corrections to the observations. This correction is discussed in the section concerned with calibration of the color system. The number 5 filter also tends to show appreciable non-uniformity of transmission in certain zones; however for the central portion employed in this program the non-uniformity is probably quite small.

2.3 Technique of Observation

All observations were made at the Newtonian focus of the 60-inch and 100-inch telescopes at Mount Wilson Observatory. Observations with the EMI photocell were obtained on 23 of 38 scheduled nights between February 1957 and November 1957. The Farnsworth phototube was used on 6 of 13 scheduled nights between December 1957 and February 1958. All the red observations were obtained at the 100-inch telescope. All observations were made using a base frame in which the filters are placed in a ring which may be rotated to bring any given filter into position for observation. Between the filter ring and the photohead, a similar ring carries a set of diaphragms used to define the observed field. During observation the diaphragms lie in the focal plane of the telescope. Five diaphragms were employed in the program, from 0.8mm to 7.0mm in diameter in steps of about three in area. The diameters, measured in a measuring engine, are given in Table 4 along with their actual angular size in the focal planes of the 60-inch and 100-inch telescopes.

Most settings were made visually by swinging the photocell out and replacing it with an eyepiece focussed on the diaphragm ring. Since settings are made through the filter, and none of the filters used were

TABLE 3

FILTER TRANSMISSIONS

EMI

1/λ	1	2	3	4
2.925	.004			
2.900	.016			
2.875	.052			
2.850	.121			
2.825	.212			
2.800	.313	.000		
2.775	.415	.004		
2.750	.510	.016		
2.725	.574	.045		
2.700	.608	.092		
2.675	.618	.150		
2.650	.605	.217		
2.625	.569	.285		
2.600	.515	.358		
2.575	.430	.429		
2.550	.317	.487		
2.525	.209	.525		
2.500	.130	.550	.00001	
2.475	.071	.568	.00002	
2.450	.035	.580	.00004	
2.425	.016	.587	.00005	
2.400	.0082	.590	.00006	
2.375	.0045	.587	.00007	
2.350	.0024	.576	.00008	
2.325	.00153	.558	.00013	
2.300	.00109	.534	.010	
2.275	.00079	.506	.112	
2.250	.00058	.473	.281	
2.225	.00042	.435	.420	
2.200	.00031	.391	.515	
2.175	.00020	.337	.578	
2.150	.00015	.271	.621	
2.125	.00010	.203	.649	
2.100	.00005	.132	.663	
2.075	.00003	.072	.665	
2.050	.00001	.033	.656	
2.025		.015	.634	
2.000		.0063	.605	
1.975		.0024	.568	
1.950		.00055	.525	
1.925		.00007	.473	
1.900		.000005	.413	
1.875			.360	
1.850			.296	.00000
1.825			.237	.00002
1.800			.184	.0061

1/λ	1	2	3	4
1.775			.136	.033
1.750			.098	.235
1.725			.068	.571
1.700			.0455	.728
1.675			.0278	.791
1.650			.0128	.809
1.625			.0061	.813
1.600			.0044	.812
1.575			.0034	.809
1.550			.0028	.804
1.525	.00001		.0022	.797
1.500	.0033		.0021	.789
1.475	.023		.0025	.780
1.450	.140		.0043	.769
1.425	.302		.0096	.757
1.400	.410		.067	.744
1.375	.426		.250	.730
1.350	.385		.485	.715
1.325	.324		.675	.700
1.300	.260		.752	.683
1.275	.210			
1.250	.172			

FARNSWORTH

1/λ	5	6	7	8
1.7250	.0005			
1.7125	.006			
1.7000	.029			
1.6875	.114			
1.6750	.264			
1.6625	.434			
1.6500	.572			
1.6375	.653			
1.6250	.681			
1.6125	.685			
1.6000	.678			
1.5875	.640			
1.5750	.588			
1.5625	.535			
1.5500	.483			
1.5375	.456			
1.5250	.458			
1.5125	.484			
1.5000	.578			
1.4875	.611			
1.4750	.570	.000		
1.4625	.415	.003		
1.4500	.225	.011		
1.4375	.113	.032		
1.4250	.059	.068	.00000	

1/λ	5	6	7	8
1.4125	.032	.130	.00001	
1.4000	.020	.212	.00006	
1.3875	.013	.315	.00028	
1.3750	.0094	.424	.00071	
1.3625	.0065	.535	.00151	
1.3500	.0047	.616	.00264	
1.3375	.0037	.670	.00451	
1.3250	.0030	.684	.0065	
1.3125	.0025	.683	.0105	
1.3000	.00215	.668	.018	
1.2875	.00193	.670	.029	
1.2750	.00175	.695	.050	
1.2625	.00163	.722	.084	
1.2500	.00157	.748	.131	.000005
1.2375	.00152	.768	.201	.000006
1.2250	.00152	.761	.288	.000008
1.2125	.00157	.736	.380	.000011
1.2000	.00162	.676	.466	.000019
1.1875	.00172	.560	.550	.000115
1.1750	.00190	.445	.581	.00042
1.1625	.00218	.330	.567	.00149
1.1500	.00261	.213	.524	.00585
1.1375	.00332	.126	.470	.0148
1.1250	.00436	.072	.418	.0355
1.1125	.00589	.040	.366	.0727
1.1000	.00750	.0236	.320	.132
1.0875	.00875	.0142	.302	.212
1.0750	.00944	.0092	.307	.302
1.0625	.00945	.0063	.330	.391
1.0500	.00895	.0044	.355	.478
1.0375	.00821	.0033	.325	.562
1.0250	.00743	.0025	.235	.615
1.0125	.00665	.0020	.140	.658
1.0000	.00583	.0016	.067	.683
0.9875	.00519	.0014	.033	.703
0.9750	.00459	.0012	.0178	.717
0.9625	.00413	.0010	.0098	.726
0.9500	.00378	.0010	.0056	.733
0.9375	.00368	.0009	.00305	.740
0.9250	.00385	.0008	.00150	.745
0.9125	.0042	.0008	.00070	.750
0.9000	.005	.0008	.00033	.756
0.8875	.006	.0008	.00019	.760
0.8750	.007	.0009	.00012	.765
0.8625	.009	.0010	.00008	.769
0.8500	.010	.0012	.00005	.773
0.8375	.014	.0015		.778
0.8250	.018	.0019		.782
0.8125	.027	.0052		.786
0.8000	.047	.0120		.790
0.7875	.080	.0189		.794
0.7750	.126	.0254		.797
0.7625	.212	.0284		.800

1/λ	5	6	7	8
0.7500	.328	.0290		.804
0.7375	.445	.0281		.807
0.7250	.557	.0265		.810
0.7125	.674	.0247		.813
0.7000	.782	.0229		.815

TABLE 4

MEASURING DIAPHRAGMS

DIAMETER IN MM	DIAMETER IN MINUTES OF ARC	
	60-INCH	100-INCH
0.809	0.365	0.216
1.328	0.600	0.354
2.264	1.023	0.604
4.032	1.822	1.075
7.028	3.177	1.874

particularly satisfactory for visual work, a clear window the same thickness as the filters was used. All stars were centered visually in the diaphragm selected for use. Galaxies with sufficiently well defined nuclei were also centered visually. In a few cases special regions of galaxies were measured by offsetting from the nucleus, or in one case, from a nearby reference star. Nearly all galaxy measurements were made directly above sky by offsetting between the galaxy and a pre-selected clear sky region. Sky was placed near the bottom of the Brown recorder scale and the sensitivity adjusted to make the galaxy deflection above sky as large as possible or practical. A typical observing run on each galaxy with each diaphragm size employed consisted of five deflections, one in each of the four colors in order of increasing wave length followed by a repetition of the first color as a check. For faint galaxies where small or particularly noisy deflections were obtained, double and sometimes triple deflections were taken in each color to increase accuracy. Throughout each measurement run an offset guide star was used in order to keep the object centered while being measured and to permit recentering after offset to sky. Depending upon the faintness of any given galaxy a run with one diaphragm size required from twenty minutes to an hour, not counting the time for initial setting up for offset guiding.

Two stars were used as primary reference and extinction stars when using the EMI photocell. Eight other stars were used as secondary standards. One star was used as standard for work in the red. Identifications, magnitudes, colors, and observational probable errors of these stars are given in Part III. The principal reference star pair consists of the very blue star Feige 95 (5) and a nearby reddish star. They were selected because of their convenient location for the program, the extreme color range available for determination of extinction color dependence, and because the magnitudes were such as to permit measurement at the same general sensitivity level as the galaxies. This last point was of particular importance because of the sensitivity drift in the EMI phototube when a voltage switch is made to measure bright objects. Similar considerations applied to the selection of the secondary pair of stars, Feige 36 (5) and a nearby companion. The other stars were selected primarily on the basis of their locations. Extinction measurements generally were taken at the beginning and end of each night and at intervals of one to three hours throughout the night. Stellar measures were occasionally made above sky but more often above dark current with separate observations of sky following the stellar observations.

2.4 Technique of Reduction of Observations

The observations were reduced by fairly standard procedures. The deflections above sky were read off the tracings directly and converted to instrumental magnitudes. Reduction to one sensitivity was then accomplished by means of additive corrections determined from known sensitivity ratios. Time marks were placed on the tracing several times throughout a night making it possible to determine the sidereal time and hour angle for each deflection within a few seconds. Values of the secant of the zenith distance were then computed for each individual deflection. When using the EMI photocell for colors 1 to 4, band 3 was taken as standard. In the red, band 6 was used for standard. Using a preliminary determination of the extinction coefficient in the standard response band for each night, the instrumental magnitudes in the standard color were referred to the time of measurement of each other color. This was done by adding to the standard magnitude the correction

$$\Delta = (\text{extinction coeff.})(\text{sec.}Z - \text{sec.}Z_{STD}). \qquad (1)$$

This correction was particularly necessary for galaxy measurements where appreciable time was required to record all the colors.

After referring instrumental magnitudes in the standard response bands to each of the other response bands, instrumental colors were formed. The instrumental colors, three in both the blue and red, as well as the two standard instrumental magnitudes, were then tabulated with their individual values of the secant of the zenith distance preparatory to determination of atmospheric extinction corrections.

Theoretically if there is no variation in total response sensitivity in the telescope-filter-photocell system, a unique set of instrumental magnitudes would exist except for the effect of atmospheric extinction. It follows that once a unique "outside atmosphere" instrumental magnitude has been determined, each subsequent observation of the same object provides an "instantaneous" determination of the extinction coefficient, α, according to the relation

$$\alpha = \frac{M_{OBS.} - M_{OUT.ATMO.}}{SEC.Z} \quad . \tag{2}$$

UNFORTUNATELY THE TOTAL RESPONSE SENSITIVITY OF THE TELESCOPE-FILTER-PHOTOCELL SYSTEM IS SUBJECT TO VARIATION, AT LEAST OVER PERIODS OF SEVERAL WEEKS, SO UNIQUE OUTSIDE ATMOSPHERE MAGNITUDES CANNOT BE SAFELY ASSUMED FOR ANY VERY LONG PERIOD OF TIME. AS LONG AS THE <u>RELATIVE</u> RESPONSE OF THE OBSERVING SYSTEM DOES NOT CHANGE HOWEVER, THIS OBJECTION DOES NOT APPLY TO COLOR MEASUREMENTS SINCE THE SENSITIVITY VARIATION CANCELS OUT. THUS COLOR EXTINCTION COEFFICIENTS, β, MAY BE EASILY DETERMINED, ONCE OUTSIDE ATMOSPHERE COLORS HAVE BEEN FOUND, BY THE RELATION

$$\beta = \frac{C_{OBS.} - C_{OUT.ATMO.}}{SEC.Z} \quad . \tag{3}$$

EXTINCTION COEFFICIENTS ARE GENERALLY NOT SIMPLE CONSTANTS, AND MAY VARY WITH THE COLOR OF THE OBJECT OBSERVED, TIME, OR POSITION. COLOR DEPENDENCE ARISES BECAUSE OF THE CHANGE IN EFFECTIVE WAVE LENGTHS OF OBSERVATION WHEN DIFFERENT OBSERVED ENERGY DISTRIBUTIONS ARE FOLDED INTO THE RESPONSE BANDS. TO THE FIRST ORDER THE DEPENDENCE OF EXTINCTION ON COLOR OF OBJECTS OBSERVED IS REMOVED BY WRITING THE EXTINCTION COEFFICIENT AS A CONSTANT PLUS A SECOND CONSTANT TIMES THE OUTSIDE ATMOSPHERE COLOR. THUS

$$\beta = K_1 + K_2 C \quad , \tag{4}$$

THEN

$$C_{OBS.} - (K_1 + K_2 C) SEC.Z = C \quad , \tag{5}$$

SO

$$C = \frac{C_{OBS.} - K_1 SEC.Z}{1 + K_2 SEC.Z} \quad . \tag{6}$$

THE SAME SORT OF EQUATIONS CAN BE WRITTEN FOR MAGNITUDE EXTINCTION EXCEPT OF COURSE WE MUST DERIVE THE OUTSIDE ATMOSPHERE COLOR BEFORE THE EQUATIONS CAN BE SOLVED. IT IS OBVIOUS FROM EQUATION 4 THAT DETERMINATIONS OF β FOR TWO OR MORE STARS OF DIFFERENT COLOR ARE NECESSARY TO DETERMINE THE SET OF EXTINCTION CONSTANTS.

IN VIEW OF THE ABOVE CONSIDERATIONS THE FOLLOWING PROCEDURES WERE

USED IN DERIVING EXTINCTION. FOR THE COLORS 1-3, 2-3, AND 3-4 ALL THE OBSERVATIONS ON EACH EXTINCTION STAR WERE PLOTTED AGAINST SECANT Z. FOR EACH OF THE TWO FUNDAMENTAL REFERENCE STARS ABOUT SEVENTY INDIVIDUAL OBSERVATIONS WERE AVAILABLE. USING THE BEST QUALITY NIGHTS OUT OF THE ENTIRE SET, PRELIMINARY VALUES OF THE OUTSIDE ATMOSPHERE COLORS WERE DERIVED FOR THE REFERENCE STARS. THESE COLORS WERE THEN USED TO DERIVE INSTANTANEOUS EXTINCTION COEFFICIENTS FOR EACH OBSERVATION OF EACH STAR.

ON THE BASIS OF THE INSTANTANEOUS COLOR EXTINCTION COEFFICIENTS IT WAS FOUND THAT SIGNIFICANT VARIATION OF EXTINCTION WITH STAR COLOR WAS PRESENT ONLY FOR THE COLOR 2-3. FURTHERMORE, ANALYSIS OF THE 2-3 EXTINCTION DATA DEMONSTRATED A TENDENCY FOR K_2/K_1 TO BE CONSTANT. SINCE INDIVIDUAL NIGHT DETERMINATIONS OF K_2 WERE NOT OF HIGH ACCURACY A CONSTANT MEAN RATIO WAS DERIVED AND USED FOR ALL NIGHTS. THE ERRORS CAUSED BY THIS PROCEDURE APPEAR TO BE WELL WITHIN OBSERVATIONAL ERROR. UPON THE DERIVATION OF A VALUE OF K_2/K_1 FOR 2-3, THE COLOR EXTINCTION PROBLEM WAS REDUCED TO DERIVATION OF K_1 VALUES FOR EACH NIGHT. TO THIS END THE INSTANTANEOUS K_1 VALUES FOR ALL EXTINCTION OBSERVATIONS WERE CONSIDERED. IF THE INSTANTANEOUS K_1 VALUES SHOWED NO SYSTEMATIC DRIFTS WITH TIME THE MEAN VALUE WAS TAKEN FOR THE NIGHT. IF SIGNIFICANT VARIATION OF K_1 WITH TIME APPEARED TO BE PRESENT, K_1 WAS PLOTTED AS A FUNCTION OF TIME AND A SMOOTH CURVE DRAWN TO FIT THE POINTS. THE MAJORITY OF THE NIGHTS YIELDED CONSTANT COEFFICIENTS, ALTHOUGH THE VALUE OF THE CONSTANT OFTEN VARIED SIGNIFICANTLY FROM NIGHT TO NIGHT. USING THE K_2/K_1 RATIO AND THE K_1 DETERMINATION FOR EACH NIGHT ALL THE EXTINCTION STAR OBSERVATIONS WERE REDUCED TO OUTSIDE THE ATMOSPHERE.

UPON PLOTTING THE OUTSIDE ATMOSPHERE EXTINCTION STAR COLORS AS A FUNCTION OF SECANT Z, A SMALL RESIDUAL DEPENDENCE OF COLOR ON SECANT Z WAS FOUND IN ALL CASES. THIS DEPENDENCE, CAUSED BY SLIGHT ERRORS IN THE INITIAL DETERMINATIONS OF OUTSIDE ATMOSPHERE COLORS, PROVIDED IMPROVED VALUES FOR THE EXTINCTION STAR OUTSIDE COLORS. USING THE IMPROVED COLORS THE ENTIRE PROCESS OF COMPUTING INDIVIDUAL NIGHT EXTINCTION WAS REPEATED, INCLUDING INVESTIGATION OF THE K_2/K_1 RATIO FOR 2-3, AND A SECOND SET OF OUTSIDE ATMOSPHERE COLORS COMPUTED FOR ALL EXTINCTION STAR OBSERVATIONS. WITH THE EXCEPTION OF THE COLOR 3-4 FOR WHICH A THIRD ITERATION WAS CARRIED OUT THE SECOND COMPUTATION OF EXTINCTION REMOVED ALL SIGNIFICANT DEPENDENCE OF OUTSIDE ATMOSPHERE COLOR ON SECANT Z, AND PROVIDED FINAL VALUES FOR THE COLOR EXTINCTION COEFFICIENTS USED TO REDUCE THE COLORS

OF THE GALAXIES OBSERVED.

FOR DETERMINATION OF EXTINCTION COEFFICIENTS TO APPLY TO MAGNITUDES IN RESPONSE BAND 3, ONE OUTSIDE ATMOSPHERE MAGNITUDE COULD NOT BE ASSUMED TO APPLY TO ALL NIGHTS. INSTEAD EACH INDIVIDUAL OBSERVING RUN WAS REDUCED AS A UNIT BY ASSUMING A UNIQUE OUTSIDE ATMOSPHERE VALUE FOR THE RUN, BUT ALLOWING THE VALUE TO VARY BETWEEN RUNS. WITH THIS ASSUMPTION THE MAGNITUDES IN EACH GROUP WERE CORRECTED FOR EXTINCTION IN A MANNER VERY SIMILAR TO THE COLORS DISCUSSED ABOVE, INCLUDING A DEFINITE DEPENDENCE OF THE EXTINCTION COEFFICIENT ON THE COLOR 2-3. IN ORDER TO REMOVE DIFFERENCES BETWEEN THE FINAL MAGNITUDES IN EACH GROUP, THE MAGNITUDES WERE REFERRED TO ONE BASIS BY MEANS OF A COLOR EQUATION OF THE FORM

$$M_{STD.} = M + A + B(2-3) \quad . \qquad (7)$$

THE COLOR COEFFICIENT IN EQUATION 7 WAS GENERALLY NEGLIGIBLE.

IN THE INFRARED EACH OF THREE RUNS OF TWO NIGHTS WAS REDUCED SEPARATELY USING THE BEST AVAILABLE DETERMINATIONS OF OUTSIDE ATMOSPHERE COLORS AND THE MAGNITUDE IN RESPONSE BAND 6. COLOR DEPENDENCE OF EXTINCTION WAS NOT INVESTIGATED IN VIEW OF THE RATHER SMALL VALUES OF THE EXTINCTION COEFFICIENTS AND THE FACT THAT NONE OF THE NIGHTS WERE OF REALLY EXCELLENT QUALITY. FINAL COLORS AND THE STANDARD BAND MAGNITUDES FROM THE DIFFERENT OBSERVING RUNS WERE TRANSFORMED TO ONE BASIS WITH EQUATIONS SIMILAR TO EQUATION 7. TABLE 5 GIVES MEAN VALUES FOR EXTINCTION COEFFICIENTS IN ALL COLORS AND THE TWO STANDARD MAGNITUDES.

TABLE 5

MEAN EXTINCTION COEFFICIENTS, $\alpha = K_1 + K_2C$

COLOR OR MAGNITUDE	K_1	K_2	C
1 - 3	0.269	0.00	
2 - 3	0.101	0.033	2 - 3
3	0.246	0.032	2 - 3
3 - 4	0.053	0.00	
5 - 6	0.054	-	
6	0.159	-	
6 - 7	0.006	-	
6 - 8	0.005	-	

2.5 Calibration of the Color System

Once atmospheric extinction has been removed from photoelectric measures, instrumental magnitudes can be represented by

$$m = -2.5\log\int E(1/\lambda)P(1/\lambda)F(1/\lambda)M^2(1/\lambda)d(1/\lambda) + \text{const.} \quad . \quad (8)$$

E is the absolute energy curve of the object observed, P is the relative photocell sensitivity including the transmission of the optics in the photohead, F is the filter transmission, and M is the reflectivity of the telescope mirror. Two aluminum reflections enter for Newtonian focus measurements. Now define

$$x = 1/\lambda \quad (9)$$

$$P(x)F(x)M^2(x) = G(x) \quad (10)$$

and expand E(x) in a Taylor series about some $x = x_o$.

$$m = -2.5\log\left(\int\left[E(x_o) + \frac{dE}{dx}\bigg|_{x_o}(x-x_o) + \frac{1}{2}\frac{d^2E}{dx^2}\bigg|_{x_o}(x-x_o)^2 + \ldots\right]G(x)dx\right) + C \quad (11)$$

$$m = -2.5\log\left[E(x_o)\int G(x)dx + \frac{dE}{dx}\bigg|_{x_o}\left[\int xG(x)dx - x_o\int G(x)dx\right] + \frac{1}{2}\frac{d^2E}{dx^2}\bigg|_{x_o}\int(x-x_o)^2G(x)dx + \ldots\right] + C. \quad (12)$$

Now define the set of moments γ

$$\gamma_1 = x_o \;, \quad \gamma_1\int G(x)dx = \int xG(x)dx \quad (13)$$

$$\gamma_N\int G(x)dx = \int(x-x_o)^N G(x)dx \;, \qquad N = 2,3,4,\ \ldots \quad . \quad (14)$$

Inserting the moments in equation 12 the first derivative term of the Taylor expansion vanishes so we have

$$m = -2.5\log[E(\gamma_1) + \frac{1}{2}\frac{d^2E}{dx^2}\bigg|_{\gamma_1}\gamma_2 + \ldots] - 2.5\log\int G(x)dx + C \quad . \quad (15)$$

To the extent that terms in γ_2 and higher moments may be neglected we have

$$m = -2.5\log E(\gamma_1) - 2.5\log\int G(x)dx + C \quad . \quad (16)$$

Thus, given the integrals of the G functions, we can determine the shape of the energy curve. It is of course obvious that observations with response functions G cannot show detail in the energy distribution over intervals of x significantly less than the bandwidth of the G functions.

As the monochromatic energy distribution E is smoothed over larger and larger intervals Δx, until Δx approaches the bandwidth of the G functions, values of $E(\gamma_1)$ computed from equation 16 will be better and better approximations to the energies read from the smoothed energy curve at the γ_1 points. This is the case since smoothing E reduces the higher derivatives of E and thus reduces the terms neglected in equation 16. Except possibly in the ultraviolet and violet, most observed energy distributions smoothed over intervals Δx comparable to the G function bandwidths have fairly small second and higher derivatives. For illustration, using the solar energy curve according to Minnaert (6), the second derivative term in equation 15 was observed to change m by 0.09 magnitudes in band 2. However, the Minnaert energy curve still has much less smoothing than introduced by the G functions. Actually, the value of $E(\gamma_1)$ given by equation 16 when m is computed precisely from equation 8, is found to lie very close to the Minnaert curve smoothed over Δx intervals comparable to the G function bandwidths. Thus relative energies, computed from equation 16, generally give a good determination of the shape of the true smoothed energy distribution. Errors in the determinations of G functions have proved in practice to be unfortunately large and limit the accuracy attainable rather severely.

Transposing equation 16 and writing

$$m_E = -2.5\log E(\gamma_1) \quad , \quad (17)$$

we have

$$m_E = m_{obs.} + 2.5\log\int G(x)dx + C \quad . \quad (18)$$

Define

$$\Delta = 2.5\log\int G(x)dx \ , \qquad H(a,b) = \Delta(a) - \Delta(b) \quad , \quad (19)$$

THEN COLORS MAY BE PUT ON AN ABSOLUTE ENERGY BASIS BY TAKING

$$C_E(A,B) = m_{OBS.}(A) - m_{OBS.}(B) + H(A,B) \quad . \qquad (20)$$

Values of Δ, H, γ_1, and γ_2 for the photometric system used in this thesis are given in Table 6. The values were determined by performing the operations indicated in equations 10, 13, 14, and 19. P and F were taken from data given on previous pages of the section, while values of M were determined from data given by Allen (7). All integrations were performed by Simpson's rule using intervals of 0.025 or 0.0125 in $1/\lambda$. The absolute values of Δ have no particular significance since no attempt was made to determine C in equation 18. The Δ values do show, however, the relative "constant energy" areas of the bands. The constant C in equation 18 is different for the EMI and Farnsworth photocell observations, consequently the value of H(3,6) cannot be determined according to equation 19. The determination of H(3,6) is discussed separately later in this section.

TABLE 6

Calibration Constants of the Photometric System

Band	Δ	γ_1	γ_2	Color	H
1	2.683	2.664	0.006	1 - 3	-0.343
2	3.371	2.392	0.023	2 - 3	0.345
3	3.026	2.068	0.016		
4	0.141	1.682	0.009	3 - 4	2.885
				3 - 6	4.830
5	1.696	1.554	0.005	5 - 6	-0.922
6	2.618	1.262	0.005		
7	2.280	1.136	0.003	6 - 7	0.338
8	2.270	1.001	0.002	6 - 8	0.348

In an earlier section of this thesis it was mentioned that filter 5 has a significant secondary transmission maximum to the longwave side of the main band. An attempt has been made to correct for the light leak theoretically since an empirical calibration is not available. The response minimum of band 5 between the principal and secondary maxima occurs near $1/\lambda = 1.225$ (micron units), thus we write

$$m_5 = -2.5\log\left[\int_{\infty}^{1.225} E(x)G_5(x)dx + \int_{1.225}^{0} E(x)G_5(x)dx\right] + C \quad . \qquad (21)$$

Now we apply the notation 5 to the main band with x values greater than 1.225 and denote the secondary band by 5'. Thus

$$m_{5+5'} = -2.5\log\left[\int E(x)G_5(x)dx + \int E(x)G_{5'}(x)dx\right] + C \qquad (22)$$

$$m_{5+5'} = -2.5\log\int E(x)G_5(x)dx - 2.5\log\frac{\int E(x)G_{5+5'}(x)dx}{\int E(x)G_5(x)dx} + C \qquad (23)$$

so

$$m_{5+5'} = m_5 - \delta + C \quad , \qquad (24)$$

where

$$\delta = 2.5\log\int E(x)G_{5+5'}(x)dx - 2.5\log\int E(x)G_5(x)dx \quad . \qquad (25)$$

δ is the correction to the observed magnitude $m_{5+5'}$. In view of this representation of magnitudes in band 5 equation 20 for the energy calibrated color 5-6 becomes

$$C_E(5,6) = m_{OBS.}(5+5') - m_{OBS.}(6) + H(5,6) + \delta \quad . \qquad (26)$$

The effective wave length of the secondary maximum in response band 5 is similar to that of band 7, consequently δ has been determined as a function of the instrumental color 5-7. Four values of δ were computed using equation 25. For one determination E was taken as a black body at 20,000°K and the computed δ used in conjunction with the observed colors of 10 Lacertae. For a second value of δ the solar flux given by Minnaert (6) was used for E. This value of δ was assumed to refer to the color of a G2V star determined by interpolation among colors of observed stars. The third and fourth determinations of δ were made by integration of flux scans of the G8III star Eta Piscium and M32, made available by Dr. Code. Since neither a G8III star nor M32 had been observed in the infrared for the thesis program it was necessary to interpolate a color

FOR A G8III STAR AND TO USE THE MEAN COLOR OF THE ELLIPTICAL GALAXIES OBSERVED FOR M32. SINCE δ IS RELATIVELY SMALL, SLIGHT ERRORS IN THE DETERMINATION OF COLORS TO WHICH THE COMPUTED δ VALUES REFER ARE NOT IMPORTANT. TABLE 7 GIVES THE SMOOTHED RELATION FOUND BETWEEN δ AND THE OBSERVED INSTRUMENTAL 5-7 COLOR.

TABLE 7

CORRECTIONS FOR THE SECONDARY TRANSMISSION MAXIMUM IN BAND 5

$(5-7)_{OBS}$	δ	$(5-7)_{OBS}$	δ	$(5-7)_{OBS}$	δ
0.00	.018	0.50	.029	1.00	.065
0.10	.019	0.60	.035	1.10	.074
0.20	.020	0.70	.041	1.20	.083
0.30	.022	0.80	.049	1.30	.093
0.40	.025	0.90	.057	1.40	.102
				1.50	.111

THE VALUE OF H(3,6) GIVEN IN TABLE 6 COULD NOT BE FOUND BY APPLICATION OF EQUATIONS 18 AND 19 BECAUSE THE VALUE OF C FOR THE FARNSWORTH PHOTOCELL IS NOT THE SAME AS THE VALUE OF C FOR THE EMI PHOTOCELL. IN PARTICULAR THE C VALUES DEPEND UPON THE ABSOLUTE SENSITIVITIES OF THE PHOTOCELLS WHICH HAVE NOT BEEN DETERMINED. CONSEQUENTLY THE VALUE OF H(3,6) WAS DERIVED BY USING THE SOLAR ENERGY CURVE GIVEN BY MINNAERT (6). THE SOLAR FLUX WAS INTEGRATED OVER RESPONSE BANDS 3 AND 6 TO DERIVE THE ABSOLUTE ENERGY COLOR 3-6 FOR THE SUN.

$$(3-6)_{\odot} = -2.5\log\frac{\int E_{\odot}(x)G_3(x)dx}{\int G_3(x)dx} + 2.5\log\frac{\int E_{\odot}(x)G_6(x)dx}{\int G_6(x)dx} \quad . \quad (27)$$

INSTRUMENTAL COLORS 3-6 WERE FORMED FROM THE INSTRUMENTAL MAGNITUDES IN 3 AND 6, AND SINCE NO DIRECT OBSERVATIONS OF G2V STARS WERE AVAILABLE THE BEST POSSIBLE VALUE OF AN INSTRUMENTAL 3-6 FOR G2V WAS DETERMINED BY INTERPOLATION. THE VALUE OF H(3,6) THEN FOLLOWED DIRECTLY AS

$$H(3,6) = (3-6)_{\odot} - (3-6)_{OBS.G2} \quad . \quad (28)$$

FOLLOWING DETERMINATION OF ALL H VALUES, AND THE δ CORRECTION TO RESPONSE BAND 5, ALL INSTRUMENTAL COLORS WERE CONVERTED TO AN ABSOLUTE ENERGY BASIS WITHIN THE LIMITS, OF COURSE, OF CALIBRATION ERRORS. IT IS

IN THIS FORM THAT ALL OBSERVATIONS ARE TABULATED IN PART III OF THIS THESIS. ALL RESULTS ARE, OF COURSE, IN ENERGIES PER UNIT $1/\lambda$ INTERVAL. BECAUSE OF POSSIBLE ERRORS IN THE DETERMINATION OF THE G FUNCTIONS IT IS IMPORTANT TO INVESTIGATE POSSIBLE DEVIATIONS OF THE COLOR SYSTEM FROM A REAL ABSOLUTE ENERGY SYSTEM. TWO OF THE BEST AVAILABLE ENERGY CURVES FOR COMPARISON WITH THE OBSERVATIONAL DATA ARE THOSE OF THE SUN AND A BLACK BODY APPROXIMATION TO 10 LACERTAE. USING EQUATIONS SIMILAR TO EQUATION 27, ABSOLUTE ENERGY COLORS WERE COMPUTED USING THE SOLAR ENERGY CURVE AND A 20,000°K BLACK BODY. TABLE 8 SHOWS THE COMPARISON BETWEEN COMPUTED AND OBSERVED COLORS. THE COLORS OF 10 LACERTAE ARE DIRECT OBSERVATIONS WHILE THE COLORS COMPARED WITH THE SOLAR INTEGRATIONS ARE INTERPOLATED AMONG AVAILABLE OBSERVATIONS TO REPRESENT A G2V STAR.

TABLE 8

COMPUTED AND OBSERVED COLORS FOR THE SUN AND 10 LACERTAE

	10 LAC.			SUN			
COLOR	B(T)	OBS.	Δ	COMP.	OBS.G2	Δ	$\bar{\Delta}$
1-3	-0.255	-0.254	-0.001	1.154	1.148	0.006	0.00
2-3	-0.156	-0.156	0.000	0.506	0.492	0.014	0.01
3-4	-0.261	-0.203	-0.058	0.302	0.387	-0.085	-0.07
3-6	-0.694	-	-	0.41	0.41	0.00	0.00
5-6	-0.318	-0.314	-0.004	0.021	0.038	-0.017	-0.01
6-7	-0.174	-0.233	0.059	-0.027	-0.082	0.055	0.06
6-8	-0.388	-0.589	0.201	-0.013	-0.204	0.191	0.20

Δ = COMPUTED MINUS OBSERVED

THE AGREEMENT OF THE RESIDUALS FROM 10 LACERTAE AND THE SUN, ACCORDING TO TABLE 8, IS QUITE UNEXPECTEDLY GOOD. PARTICULARLY ENCOURAGING ARE THE SMALL VALUES INDICATED FOR THE CALIBRATION ERRORS IN ALL COLORS BUT 6-8, WITH ONLY 3-4, 6-7, AND 6-8 SHOWING SIGNIFICANT RESIDUALS. SINCE 10 LACERTAE HAS NO OBSERVED COLOR 3-6, AND THE SOLAR COLOR HAS BEEN MATCHED TO CALIBRATE 3-6 INITIALLY, THIS MATERIAL GIVES NO CHECK ON THE CALIBRATION OF 3-6.

ADDITIONAL COMPARISONS OF THE COLOR SYSTEM WITH OUTSIDE INFORMATION IS AFFORDED BY COMPARISON WITH ABSOLUTE ENERGY CALIBRATED FLUX SCANS MADE AVAILABLE BY DR. CODE. MAGNITUDES WERE READ OFF THE SCANS AT THE EFFECTIVE $1/\lambda$ POINTS, AND COLORS FORMULATED. TABLE 9 GIVES COMPARISONS

BETWEEN COLORS DERIVED FROM CODE'S MEASURE AND DIRECT OBSERVATIONS OF THE SAME OR COMPARABLE OBJECTS. THE MEAN RESIDUALS (CODE - OBSERVED) ARE IN GENERAL AGREEMENT WITH THOSE IN TABLE 8 ALTHOUGH SOME SMALL SYSTEMATIC DIFFERENCES APPEAR TO BE PRESENT.

IN MAKING COMPARISON WITH CODE'S OBSERVATIONS IN THE VIOLET AND ULTRAVIOLET, IT WAS NECESSARY TO SMOOTH OVER APPRECIABLE ENERGY FLUCTUATIONS SHOWN BY THE RELATIVELY HIGH RESOLUTION OF CODE'S DATA. IN ORDER TO INVESTIGATE HOW CLOSELY THE MEAN MAGNITUDES INTEGRATED OVER THE RESPONSE BANDS RESEMBLED THE MEAN LEVEL OF THE RADIATION IN THE IMMEDIATE VICINITY OF THE γ_1 POINTS FOR BANDS 1, 2, AND 3, DIRECT INTEGRATIONS WERE PERFORMED OVER BANDS 1, 2, AND 3 FOR TWO OBJECTS, A G8 III STAR AND M32. THE MEAN MAGNITUDES,

$$m = -2.5 \log \frac{\int E(x) G(x) dx}{\int G(x) dx} , \qquad (29)$$

WERE THEN COMPARED WITH THE LOCALLY SMOOTHED MAGNITUDES AT THE γ_1 POINTS DIRECTLY FROM CODE'S SCANS. THE AGREEMENT WAS FOUND TO BE EXCELLENT IN BANDS 1 AND 3, WHILE IN BAND 2 THE INTEGRATED MAGNITUDE WAS A FEW HUNDREDTHS OF A MAGNITUDE BRIGHTER THAN THE SMOOTHED SCAN PREDICTED. FOR THE SOLAR ENERGY CURVE, COMPARISON OF INTEGRATED MEAN MAGNITUDES IN ALL RESPONSE BANDS WITH MAGNITUDES READ DIRECTLY AT THE γ_1 POINTS SHOWED EXCELLENT AGREEMENT FOR BANDS 1, 5, 6, 7, AND 8. THE INTEGRATED MAGNITUDES FOR BANDS 2, 3, AND 4 FALL SLIGHTLY BELOW LOCAL FLUCTUATIONS IN THE MINNAERT SOLAR ENERGY CURVE. HOWEVER, THE SMOOTH CURVE DRAWN THROUGH ALL THE INTEGRATED MAGNITUDES AT THE γ_1 POINTS AVERAGES OUT LOCAL FLUCTUATIONS VERY WELL. THE GENERAL CONCLUSION WOULD SEEM TO BE THAT THE COLORS AND MAGNITUDES GIVEN IN THIS THESIS ARE QUITE REPRESENTATIVE OF THE ACTUAL ENERGIES, LOCALLY SMOOTHED, AT THE γ_1 POINTS. IT ALSO SEEMS PROBABLE THAT THE COLOR SYSTEM, INCLUDING THE MEAN CORRECTIONS IN TABLE 8, DOES NOT DEVIATE VERY APPRECIABLY FROM AN ABSOLUTE ENERGY SYSTEM.

TABLE 9

Comparison of Observed Colors with Colors from Code Scans

	10 Lac. (O9V)		55 Cyg. (B3Ia)		53 Cass. (B8Ib)	
Color	Code	Obs.	Code	Obs.	Code	Obs.
1 - 3	-0.24	-0.25	+0.39	+0.41	+0.55	+0.51
2 - 3	-0.14	-0.16	+0.22	+0.22	+0.22	+0.20
3 - 4	-0.31	-0.20	+0.29	+0.30	+0.22	+0.27
3 - 6	-0.77					
5 - 6	-0.30	-0.32				
6 - 7	-0.13	-0.23				
6 - 8	-0.25	-0.59				

	σ Boo. (F2V)		31 Com. (G0III)		β Com. (G0V)	
Color	Code	Obs.	Code	Obs.	Code	Obs.
1 - 3	+0.78	+0.73	+1.19	+1.19	+1.00	+1.06
2 - 3	+0.25	+0.28	+0.50	+0.54	+0.42	+0.45
3 - 4	+0.18	+0.23	+0.40	+0.44	+0.34	+0.36
3 - 6	+0.22	-0.01	+0.56	+0.45	+0.46	+0.35
5 - 6	+0.02	-0.05	+0.12	+0.05	+0.07	+0.02
6 - 7	+0.00	-0.11	-0.05	-0.06	-0.08	-0.09
6 - 8	+0.00	-0.30	+0.14	-0.16	+0.08	-0.19

	*	**	***	$\bar{\Delta}$		
Color	Code	Obs.	Obs.	Code - Obs.	PE	$\bar{\Delta}$ (Table 8)
1 - 3	+0.91	+0.89		+0.00	0.01	+0.00
2 - 3	+0.25	+0.35		-0.02	0.01	+0.01
3 - 4	+0.20	+0.28		-0.05	0.01	-0.07
3 - 6	+0.25		+0.15	+0.14	0.02	
5 - 6	+0.02		-0.02	+0.05	0.01	-0.01
6 - 7	+0.02		-0.10	+0.07	0.02	+0.06
6 - 8	+0.03		-0.25	+0.30	0.01	+0.20

* π^3 Ori. (F6V)
** 110 Her. (F6V)
*** θ Boo. (F7V)

III THE OBSERVATIONS

3.1 Standard Reference and Extinction Stars

Table 10 gives colors, instrumental magnitudes, probable errors of the colors and magnitudes, and the number of observations on each object, for all stars used for reference and extinction. Stars are listed in order of right ascension. Stars having no common designation are indicated by "Anon" and are identified in notes following the table.

TABLE 10

Reference and Extinction Stars

Star	1-3	pe.	2-3	pe.	3-4	pe.	3*	pe.	N
+40°129	0.967	0.0021	0.400	0.0010	0.334	0.0019	-3.633	0.0020	7
Anon 1	0.867	0.002	0.306	0.001	00.285	0.012	-2.218	0.026	2
Anon 2	0.889	0.0032	0.402	0.0018	0.329	0.0057	-0.582	0.0019	12
Feige 32	-0.220	0.0020	-0.165	0.0023	-0.260	0.0061	-1.106	0.0018	12
Feige 95	-0.236	0.0014	-0.169	0.0010	-0.260	0.0036	-0.607	0.0009	70
Anon 3	1.844	0.0019	0.792	0.0012	0.619	0.0015	-1.713	0.0009	69
ρ Boo.	2.674	0.0056	1.106	0.0020	0.854	0.0026	-9.609	0.0082	5
Anon 4	2.973	0.019	1.231	0.005	0.977	0.005	-2.886	0.005	2
Anon 5	0.827	0.0049	0.338	0.0052	0.253	0.0038	-2.306	0.0036	4
110 Her.	0.893	0.0022	0.354	0.0014	0.280	0.0012	-9.330	0.0019	5
	5-6		6-7		6-8		3-6		
HD 81192	0.190	0.001	-0.002	0.001	-0.067	0.004	0.92	--	

Anon 1 : 8'.3 N, 5'.1 W of NGC 3031 (M81) nucleus
Anon 2 : 2.3 S, 0.3 W of Feige 32
Anon 3 : 6.0 N, 0.1 E of Feige 95
Anon 4 : 1.2 N, 9.3 W of NGC 6239 nucleus
Anon 5 : 7.9 N, 6.6 W of NGC 6239 nucleus, probably BD +43°2653
* 3 may be converted to an approximate visual magnitude by adding +13.50

3.2 Stellar Observations

Table 11 contains colors and the instrumental magnitude in band 3 for all stars observed with the EMI photocell except the fainter stars in Table 10. However, Rho Bootis and 110 Herculis are repeated from Table 10. Spectral and luminosity classes are given for all the stars. The notation "HV" after the spectral class indicates that the star was taken from the list of high velocity stars given by Keenan and Keller (8).

THESE STARS PROVIDED EXAMPLES OF POPULATION II GIANTS. HD 122563, ALTHOUGH NOT LISTED BY KEENAN AND KELLER, IS AN EXTREME EXAMPLE OF A POPULATION II GIANT. THE GIANTS NOT MARKED "HV" OR "P" ARE MORE OR LESS NORMAL POPULATION I OBJECTS. TABLE 12 GIVES THE COLORS AND SPECTRAL CLASSES FOR ALL STARS OBSERVED IN THE RED. BOTH TABLES 11 AND 12 ARE IN ORDER OF RIGHT ASCENSION.

TABLE 11

STELLAR COLORS DETERMINED WITH THE BLUE PHOTOCELL

STAR	SPECTRUM	1 - 3	2 - 3	3 - 4	3
μ CAS.	G5VP	1.16	0.56	0.45	-8.32
53 CAS.	B8 IB	0.51	0.20	0.27	-8.02
HD 81192	G7III+ HV	1.69	0.77	0.62	-6.84
θ U.MA.	F6III	0.91	0.36	0.30	-10.37
π LEO	M2III	3.26	1.35	1.24	-8.38
ζ LEO	F0III	0.88	0.25	0.18	-10.15
+51°1696	G0SD	0.86	0.43	0.40	-3.63
HD 103095	G8SD	1.26	0.59	0.50	-6.98
HD 108910	K3+III HV	2.93	1.21	0.98	-6.27
31 COM.	G0III	1.19	0.54	0.44	-8.51
β COM.	G0V	1.06	0.45	0.36	-9.21
HD 122563	G0III	1.34	0.64	0.64	-7.10
HD 124752*	K0V	1.63	0.71	0.56	-4.89
α BOO.	K2IIIP	2.42	1.05	0.82	-13.25
θ BOO.	F7V	0.94	0.40	0.31	-9.48
ρ BOO.	K3III	2.67	1.11	0.85	-9.61
σ BOO.	F2V	0.73	0.28	0.23	-9.15
HD 128902	K2III HV	2.96	1.25	1.01	-7.35
+26°2606	F4SD	0.64	0.30	0.31	-3.82
HD 134063	G5III+ HV	1.65	0.78	0.60	-5.55
HD 134439	K0SD	1.26	0.60	0.52	-4.37
5 SER. A	F8III-IV HV	1.03	0.44	0.32	-8.50
HD 140283	F5SD	0.69	0.32	0.33	-6.29
λ SER.	G0V	1.05	0.43	0.46	-9.00
δ OPH.	M1III	3.27	1.33	1.08	-10.30
γ HER.	A9III	0.89	0.25	0.13	-9.90
η DRA.*	G8III	1.74	0.75	0.58	-10.60
HD 148349	M2+III: HV	3.42	1.43	1.25	-7.81
η HER.	G4III	1.70	0.75	0.57	-9.87
48 HER.	K1II-III HV	2.38	1.04	0.81	-6.66
γ DRA.	K5III	3.20	1.31	1.03	-10.82
HD 168322	G8III HV	1.82	0.79	0.63	-7.21

Star	Spectrum	1 - 3	2 - 3	3 - 4	3
110 Her.	F6V	0.89	0.35	0.28	-9.33
κ Cyg.	K0III	1.87	0.79	0.60	-9.52
σ Dra.	K0V	1.64	0.67	0.50	-8.72
16 Cyg. A	G2.5V	1.22	0.52	0.40	-7.50
16 Cyg. B	G4V	1.24	0.54	0.42	-7.24
HD 186776	M3III hv	3.09	1.28	1.04	-6.69
55 Cyg.	B3Ia	0.41	0.22	0.30	-8.72
HD 199191	G8III hv	1.74	0.78	0.61	-6.19
61 Cyg. A	K5V	2.30	0.96	0.87	-8.01
61 Cyg. B	K7V	2.48	1.04	1.03	-7.06
HD 201891	F9sd	0.81	0.36	0.33	-6.15
10 Lac.	O9V	-0.25	-0.16	-0.20	-8.91

* Measures include light of a faint companion

The majority of the stars in Table 11 were measured only once. The following stars were measured more than once: θ U.Ma., HD 103095, 31 Com., HD 124752, +26°2606, HD 134063, HD 134439, all measured twice, HD 128902 and 10 Lac. measured three times, and Rho Boo. and 110 Her. measured five times.

TABLE 12

Stellar Colors Determined with the Red Photocell

Star	Spectrum	3 - 6	5 - 6	6 - 7	6 - 8
HD 81192	G7III+ hv	0.92	0.24	-0.00	-0.07
π Leo	M2III	2.17	0.87	0.13	0.20
ζ Leo	F0III	0.05	-0.08	-0.12	-0.30
HD 103095	G8sd	0.63	0.18	-0.03	-0.13
HD 108910	K3+III hv	1.67	0.48	0.07	0.06
31 Com.	G0III	0.45	0.05	-0.06	-0.16
β Com.	G0V	0.35	0.02	-0.09	-0.19
HD 122563	G0III	0.97	0.24	0.00	-0.03
θ Boo.	F7V	0.15	-0.02	-0.10	-0.25
ρ Boo.	K3III	1.23	0.28	0.02	0.04
σ Boo.	F2V	-0.01	-0.05	-0.11	-0.30
HD 128902	K2III hv	1.54	0.46	0.08	0.15
+26°2606	F4sd	0.15	-0.00	-0.07	-0.21
HD 134063	G5III+ hv	0.77	0.20	-0.01	-0.04
HD 134439	K0sd	0.62	0.13	-0.05	-0.08
λ Ser.	G0V	0.55	0.01	-0.10	-0.26

Star	Spectrum	3 - 6	5 - 6	6 - 7	6 - 8
δ Oph.	M1III	2.05	0.71	0.09	0.18
γ Her.	A9III	-0.13	-0.12	-0.14	-0.32
10 Lac.	O9V	-	-0.31	-0.23	-0.59

HD 81192, the standard red reference and extinction star, was measured 20 times. In addition β Com. was measured twice, and Zeta Leo, HD 108910, 31 Com., and Sigma Boo. were measured twice in 6-7 and 6-8.

3.3 Extragalactic Observations

Table 13 gives the colors and band 3 magnitudes for all galaxies observed with the EMI photocell. The colors have been placed on an absolute energy system as discussed in Section 2.5, however, the corrections indicated in Table 8 have not been applied. The NGC number, or other identification is given for each system along with the Hubble structural type taken from the Humason, Mayall, and Sandage (2) redshift catalog wherever possible. One type, given in parentheses, was determined by the author. The galaxy "Haro 22" was taken from a list of blue galaxies given by Haro (9). The aperture employed for each measurement is given in minutes of arc, and unless otherwise indicated the diaphragm was centered on the nucleus. The last column of Table 13 contains remarks, including references to notes following the table. Certain additional information about the galaxies is given in Table 15 in Part IV.

TABLE 13

Extragalactic Colors Determined with the Blue Photocell

Object	Type	Field	1 - 3	2 - 3	3 - 4	3	Remarks
NGC 205	Ep	1.02′	1.14	.50	.54	-2.16	
		0.36	1.07	.46	.40	-0.46	
NGC 221	Ep	1.02	1.61	.74	.66	-4.22	M32
		0.36	1.61	.74	.69	-3.38	
NGC 224	Sb	3.18	1.80	.80	.73	-6.90	M31
		1.82	1.83	.83	.70	-6.19	
		1.02	1.85	.83	.73	-5.30	
		0.60	1.84	.83	.73	-4.40	
		0.36	1.87	.85	.74	-3.57	

Object	Type	Field	1 - 3	2 - 3	3 - 4	3	Remarks
NGC 598	Sc	1.02	0.70	.35	.45	-1.98	M33, Note 1
NGC 2903	Sc	3.18	1.09	.52	.54	-3.85	
		1.82	1.11	.51	.57	-3.20	
		1.02	1.06	.51	.60	-2.51	
		0.60	1.01	.48	.56	-1.90	
		0.36	0.88	.42	.55	-1.34	
Haro 22	:	0.60	0.55	.37	.10	1.34	
NGC 3031	Sb	1.02	1.76	.81	.74	-4.01	M81
		0.36	1.87	.85	.77	-2.88	
NGC 3115	E7	1.82	1.69	.81	.64	-3.70	
		1.02	1.68	.82	.66	-3.36	
		0.36	1.79	.84	.67	-2.55	
NGC 3351	SBb	3.18	1.27	.60	.63	-3.17	M95, Leo group
		1.82	1.33	.66	.66	-2.64	
		1.02	1.30	.66	.64	-2.16	
		0.60	1.15	.61	.62	-1.73	
NGC 3368	Sa	3.18	1.44	.68	.66	-3.62	M96, Leo group
		1.82	1.50	.72	.68	-3.25	
		1.02	1.59	.76	.69	-2.73	
		0.60	1.64	.78	.73	-2.16	
NGC 3510	SBc	0.60	0.68	.34	.25	0.54	Haro 26
		0.35	0.67	.33	.36	1.15	
		0.60	0.57	.33	.12:	1.44	8"0 W, 32"0 N
NGC 3810	Sc	3.18	0.87	.42	.49	-2.64	Leo group
		1.02	0.98	.48	.53	-1.70	
		0.36	1.22	.59	.64	-0.32	
NGC 3998	S0	1.82	1.65	.80	.65	-2.52	U.Ma. cloud
		1.02	1.67	.80	.66	-2.24	
		0.60	1.69	.80	.68	-1.92	
		0.36	1.73	.84	.67	-1.60	
NGC 4216	Sb	1.02	1.78	.82	.74	-2.24	Virgo cluster
		0.36	1.92	.88	.80	-1.44	
		1.82	1.34	.60	.59	-0.88	54"2 E, 136" N
NGC 4245	SBa	1.87	1.47:	.73:	-	-1.74:	
		1.08	1.55	.72	.65	-1.39	
		0.60	1.55	.74	.66	-0.93	
		0.22	1.49	.71	.68	0.03	
NGC 4274	Sa	3.18	1.56	.75	.71	-2.65	
		1.02	1.64	.77	.73	-1.78	

Object	Type	Field	1 - 3	2 - 3	3 - 4	3	Remarks
NGC 4278	E1	3'.18	1.62	.78	.64	-2.89	
		1.82	1.60	.76	.64	-2.69	
		1.02	1.61	.78	.66	-2.39	
		0.60	1.67	.81	.65	-2.05	
NGC 4283	E0	1.02	1.70	.80	.62	-0.97	
NGC 4374	S0	1.82	1.72	.81	.69	-3.30	13".6 S, Note 2
		0.60	1.76	.83	.71	-2.49	Centered
NGC 4406	E4	1.82	1.68	.77	.64	-3.20	M86, Vir. cl.
		0.60	1.74	.79	.66	-2.20	
NGC 4449	I	1.82	0.51	.24	.23	-3.22	Note 3
		0.36	0.46	.20	.23	-1.17	Note 4
Anon	E0	0.60	1.57	.84	.78	0.08	Note 5
NGC 4486	E0	3.18	1.68	.78	.69	-3.88	M87, Vir. cl.
		1.82	1.71	.81	.68	-3.53	
		1.02	1.72	.82	.68	-3.05	
		0.60	1.69	.80	.71	-2.48	
		0.36	1.71	.82	.72	-1.84	
NGC 4501	Sc	3.18	1.37	.64	.65	-3.41	M88, Vir. cl.
		1.82	1.44	.69	.69	-2.92	
		1.02	1.59	.75	.74	-2.25	
		0.60	1.73	.81	.78	-1.57	
		0.36	1.82	.84	.79	-0.99	
NGC 4548	SBb	3.18	1.39	.68	.71	-2.76	Virgo cluster
		1.82	1.51	.69	.61	-2.27	
		1.02	1.61	.77	.73	-1.70	
		0.36	1.67	.77	.70	-0.61	
NGC 4565	Sb	1.02	1.73	.83	.77	-2.12	
		0.36	1.95	.92	.88	-0.72	
		0.60	1.39	.67	.66	0.81	69".2 W, 82".7 N
		1.02	1.09	.54	.58	0.32	174" W, 193" N
NGC 4579	Sb	3.18	1.44	.69	.62	-3.40	Virgo cluster
		1.82	1.48	.70	.58	-2.95	
		1.02	1.58	.75	.68	-2.46	
		0.60	1.60	.78	.68	-1.99	
		0.36	1.61	.79	.71	-1.53	
NGC 4627	:	0.60	1.05	.45	.42	0.58	Note 6
NGC 4631	Sc	1.02	1.03	.46	.54	-0.98	Offset, Note 7
		1.02	0.47	.25	.36	-1.26	Offset, Note 7
		1.02	0.74	.38	.41	-1.53	Offset, Note 7

Object	Type	Field	1 - 3	2 - 3	3 - 4	3	Remarks
NGC 4643	SB0	1'.87	1.65	.76	.69	-2.46	
		0.60	1.72	.81	.68	-1.82	
		0.22	1.74	.83	.70	-0.78	
NGC 4698	Sa	3.18	1.54	.70	.66	-2.60	Virgo cluster
		1.82	1.56	.74	.66	-2.30	
		1.02	1.64	.78	.62	-1.90	
		0.60	1.64	.76	.66	-1.46	
		0.36	1.64	.76	.71	-0.99	
NGC 4699	Sb	3.18	1.41	.67	.66	-3.62	
		1.82	1.48	.72	.64	-3.31	
		1.02	1.55	.75	.66	-3.12	
		0.60	1.60	.76	.66	-2.72	
		0.36	1.65	.76	.67	-2.26	
NGC 4713	Sc	1.82	0.60	.30	.34	-1.64	
		1.02	0.62	.31	.32	-1.12	
NGC 4762	Sa	0.60	1.61	.75	.58	-1.68	Virgo cluster
		1.02	1.37	.63	.66	0.66	65".1 E, 108" N
NGC 4865	E6	0.60	1.64	.84	.64	0.55	Coma cluster
		0.22	1.64	.77	.68	1.03	
NGC 4874	S0	1.08	1.70	.84	.68	-0.50	Coma cluster
		0.60	1.69	.85	.68	-0.01	
		0.35	1.75	.89	.69	0.48	
NGC 4881	E1	0.60	1.53	.86	.60	0.67	Coma cluster
		0.22	1.73	.86	.65	1.34	
NGC 4889	E4	0.60	1.76	.89	.66	-0.56	Coma cluster
		0.22	1.81	.90	.68	0.40	
NGC 4907	SBb	1.08	1.43	.70	.64	0.30	Coma cluster?
		0.60	1.45	.72	.61	0.66	
		0.35	1.65	.79	.71	1.27	
		0.22	1.71	.85	.69	1.75	
IC 4051	E1	1.08	1.68	.84	.63	0.34	Coma cluster
		0.35	1.70	.83	.70	0.98	
NGC 4911	Sb	0.60	1.24	.58	.60	0.22	Coma cluster?
		0.22	1.51	.80	.75	1.54	
NGC 4921	Sa	1.87	1.48	.70	.62	-0.64	Coma cluster?
		1.08	1.57	.78	.67	-0.08	
		0.60	1.64	.82	.68	0.53	
		0.35	1.70	.84	.69	0.99	

Object	Type	Field	1 - 3	2 - 3	3 - 4	3	Remarks
NGC 5005	Sb	1.82[1]	1.41	.68	.62	-3.06	
NGC 5055	Sb	1.02	1.21	.58	.56	-1.33	54"2 N, M63
		1.02	1.14	.57	.62	-0.81	54"2 S
NGC 5194	Sc	1.82	1.09	.52	.56	-3.40	M51
		1.02	1.13	.55	.57	-2.89	
		0.60	1.26	.58	.62	-2.32	
		0.36	1.36	.62	.61	-1.65	
		1.02	0.99	.46	.52	-1.39	46"1 E, 57"0 S
NGC 5195	Ep	1.02	1.69	.80	.80	-2.39	M51 companion
NGC 5248	Sc	3.18	1.02	.47	.56	-2.88	
		1.82	1.09	.52	.56	-2.42	
		1.02	1.14	.57	.60	-1.78	
		0.60	1.14	.55	.64	-1.22	
		0.60	0.84	.37	.46	0.49	57"0 E, 48"8 S
NGC 5363	I	1.02	1.73	.83	.66	-2.40	Note 8
NGC 5457	Sc	1.82	1.14	.54	.52	-2.60	8"1 W, M101
		0.60	1.17	.57	.56	-0.99	Centered
NGC 5560	(SBc)	1.02	1.14	.56	.61	-0.40	
NGC 5566	SBa	1.82	1.56	.74	.64	-2.28	
		0.60	1.66	.80	.67	-1.60	
		0.36	1.70	.79	.71	-1.28	
NGC 5576	E4	1.02	1.56	.76	.63	-1.90	
NGC 5633	Sb	1.02	0.94	.43	.50	-0.83	
		0.36	1.05	.53	.51	0.12	
NGC 5850	SBb	1.08	1.69	.81	.66	-1.08	
		0.35	1.75	.82	.71	-0.18	
NGC 5907	Sb	0.60	1.60	.76	.73	-0.59	
		1.02	1.37	.67	.57	-0.67	19"0 E, 51"5 S
		1.02	1.16	.54	.56	-0.21	46"1 E, 111" S
		1.02	0.86	.38	.47	0.26	84"1 E, 198" S
NGC 6239	(Sc)	1.82	0.71	.36	.31	-0.98	
		1.02	0.72	.39	.32	-0.74	
		0.36	0.64	.39	.35	0.40	
NGC 6503	Sc	1.82	1.06	.51	.56	-2.64	
		0.60	1.23	.59	.62	-1.23	

Note 1. Centered on brightest patch, slightly SE of photographic center.

NOTE 2. M84, VIRGO CLUSTER

NOTE 3. CENTERED ON THE OVERALL STRUCTURE

NOTE 4. CENTERED ON STELLAR-LIKE NUCLEUS SLIGHTLY E OF THE GENERAL CENTER OF THE GALAXY

NOTE 5. VIRGO CLUSTER DWARF ELLIPTICAL GALAXY, 7' N, 4'.4 W OF NGC 4486

NOTE 6. SMALL GALAXY JUST N OF NGC 4631. THIS GALAXY RESEMBLES AN ELLIPTICAL GALAXY EXCEPT THAT IT HAS NO SIGNIFICANT NUCLEUS.

NOTE 7. SINCE THIS GALAXY SHOWS NO DISTINCT NUCLEUS, OFFSETS HAVE BEEN MADE FROM A STAR NEAR THE EDGE OF THE GALAXY AND DIRECTLY N OF THE CENTER. TAKEN IN THE ORDER LISTED IN THE TABLE THE OFFSETS ARE 54"2 E; 103" W, 48"8 S; 78"6 E, 27"1 S. ALTHOUGH NO REAL NUCLEUS IS SEEN, THE MEASURE 54" E OF THE OFFSET STAR MAY INCLUDE LIGHT FROM THE OUTER PART OF A CENTRAL BULGE. BOTH OTHER REGIONS MEASURED INCLUDE BRIGHT VISUAL PATCHES, PROBABLY H II REGIONS.

NOTE 8. A FAIRLY BRIGHT STAR NEAR THE NUCLEUS IS INCLUDED IN THE MEASURES.

TABLE 14 CONTAINS ALL EXTRAGALACTIC OBSERVATIONS OBTAINED IN THE RED. THE MATERIAL IS ARRANGED AS IN TABLE 13 WITH THE ADDITION OF THE COLOR 3–6 WHICH TIES TOGETHER THE BLUE AND RED OBSERVATIONS. IN ORDER TO FORMULATE 3–6 IT WAS NECESSARY TO INTERPOLATE AMONG BAND 3 MAGNITUDES TO DERIVE THE VALUE OF 3 CORRESPONDING TO THE FIELD SIZE USED TO MEASURE 6. THIS PROBLEM AROSE BECAUSE OF THE DIFFERENT SCALES OF THE 60-INCH AND 100-INCH TELESCOPES, AND THE FACT THAT ALL GALAXIES MEASURED IN THE RED AT THE 100-INCH HAD BEEN MEASURED IN THE BLUE AT THE 60-INCH. HOWEVER, FOR THE DIAPHRAGMS EMPLOYED IN MEASUREMENT, A GIVEN FIELD SIZE AT THE 60-INCH TELESCOPE CORRESPONDS CLOSELY TO THE FIELD SIZE OF THE NEXT LARGER DIAPHRAGM AT THE 100-INCH TELESCOPE. THUS THE INTERPOLATION CORRECTIONS WERE SMALL AND IT IS UNLIKELY THAT SERIOUS ERRORS ARE PRESENT IN 3–6 DUE TO THE INTERPOLATION. THE STELLAR 3–6 COLORS, GIVEN IN TABLE 12 ARE OF COURSE INDEPENDENT OF DIAPHRAGM SIZE.

TABLE 14

EXTRAGALACTIC COLORS DETERMINED WITH THE RED PHOTOCELL

OBJECT	TYPE	FIELD	5–6	6–7	6–8	3–6	6*	REMARKS
NGC 224	SB	1'.08	.53	.09	.21	1.36	-6.74	M31
		0.60	.54	.11	.24	1.34	-5.75	
		0.35	.54	.12	.25	1.32	-4.83	

Object	Type	Field	5-6	6-7	6-8	3-6	6*	Remarks
NGC 2903	Sc	1'.08	.36	.10	.19	0.98	-3.55	
		0.60	.38	.11	.19	0.99	-2.89	
		0.35	.39	.09	.21	1.00	-2.30	
NGC 3115	E7	1.08	.40	.10	.20	1.31	-4.71	
		0.60	.40	.08	.20	-	-4.38	
		0.35	.42	.08	.19	1.51	-4.04	
NGC 3351	SBb	1.08	.40	.08	.17	1.13	-3.33	M95, Leo group
		0.60	.41	.10	.15	1.18	-2.91	
		0.35	.35	.07	.18	-	-2.43	
NGC 3810	Sc	1.08	.27	.03	.13	0.89	-2.66	Leo group
		0.60	.25	.08	.23	-	-2.07	
		0.35	.37	.10	.12	1.14	-1.41	
NGC 4486	E0	1.08	.40	.10	.19	1.12	-4.22	M87, Vir. cl.
		0.60	.40	.10	.22	1.13	-3.61	
		0.35	.38	.11	.20	1.10	-2.90	
NGC 4631	Sc	1.08	.23	.16	.30:	0.80:	-2.38	**
NGC 5248	Sc	1.08	.35	.10	.20	1.01	-2.84	
		0.60	.33	.09	.17	1.10	-2.33	
		0.35	.32	.11	.20	-	-1.80	

* 4.83 has been subtracted from the original instrumental magnitudes in band 6, in accordance with Table 6. Thus 3-6 colors may be formed directly from magnitudes in Tables 13 and 14 except for diaphragm size differences. ** 78".7 E, 27".2 S from reference star. See Table 13.

3.4 Observational Errors

Observational errors may be divided into two categories, internal random errors of measurement on each individual galaxy or star, and tie-in systematic errors between different galaxies or galaxies and stars or between different nights. Some information is available for estimating the random errors of measurement on individual galaxies by comparing the first and last measurement made with each diaphragm size. The first and last measures were almost always taken with the ultraviolet filter when using the EMI photocell; thus at least two determinations of 1-3 are available for each diaphragm size on nearly every galaxy. Figure 1 shows the average deviation of individual determinations from the mean, plotted as a function of band 3 magnitudes for measurements at the 60-inch telescope. Measures made at the 100-inch telescope are of course more accurate at a given magnitude. To make the 100-inch measurements comparable to 60-inch data the 100-inch measurements have been plotted 1.1 magnitudes brighter than observed. 100-inch measurements may be identified in Table 13 by using the field sizes and Table 4.

Figure 1 shows that, as expected, the random errors increase at the faint limits of measurement; brighter than magnitude -1 however 1-3 measurement errors are consistently less than 0.02 magnitude. Extra deflections were taken for the faintest systems, so it is doubtful if random errors as great as 0.05 magnitude exist in 1-3 at any magnitude. 3-4 random errors should be about the same as in 1-3 since deflections in 1 and 4 were quite similar in most cases. Errors in 2-3 should be appreciably less than in 1-3 because of the increased sensitivity in bands 2 and 3. Random errors in 2-3 probably do not exceed 0.02 or 0.03 magnitude at any amgnitude. Relatively little information is available for estimating errors in the red observations; however, what repeat observations are available rarely show deviations of individual measures from the mean larger than 0.02 magnitude in any of the colors 5-6, 6-7, or 6-8.

Tie-in systematic errors between galaxies and stars and between different nights are much more difficult to determine than random errors. Except for a few cases in the red, no repeat measurements were made on galaxies using the same field diaphragm. Reference stars were referred to frequently but provide no check on residual errors after reduction since the standards provided the basis for extinction determination. For five or six galaxies some observations using different diaphragm sizes were obtained on two separate nights. On the basis of these observations, assuming smooth color gradients with radius, night to night systematic errors rarely exceed 0.03 or 0.04 magnitude in all colors. It is doubtful if any exceed 0.1 magnitude.

Systematic errors for magnitudes in band 3 or band 6 are larger than systematic errors in the colors. This is the case primarily because magnitude extinction is much more variable than color extinction and harder to derive accurately because outside atmosphere instrumental magnitudes cannot be assumed to be constant for long periods of time. Differential magnitudes between various diaphragm sizes are presumably nearly as reliable as the colors, but the actual values of individual magnitudes are definitely less accurate. No direct determination of magnitude errors is available, but it is doubtful if any errors as large as 0.1 magnitude occur since no nights were found to have really poor or greatly

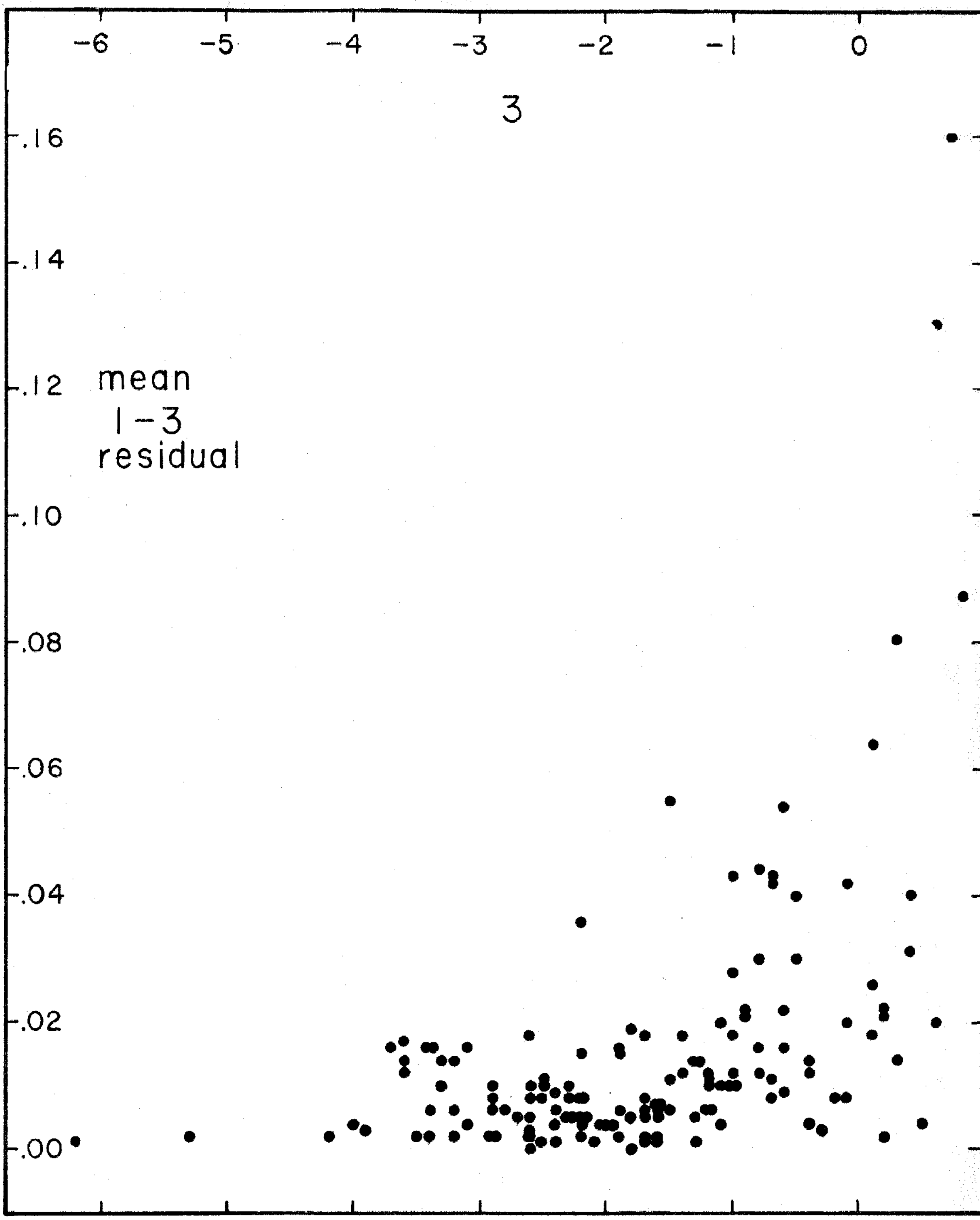

FIGURE 1

THE AVERAGE DEVIATION OF A SINGLE 1-3 DETERMINATION FROM THE MEAN AS A FUNCTION OF BAND 3 INSTRUMENTAL MAGNITUDE

VARIABLE EXTINCTION. IN VIEW OF THE LOWER ACCURACY OF MAGNITUDE DETERMINATIONS THE COLOR 3-6 RELATING THE MEASURES WITH THE TWO PHOTOCELLS IS THE LEAST RELIABLE COLOR. CORRELATIONS OF 3-6 WITH OTHER COLORS IMPLY THAT FEW IF ANY DISCREPANCIES AS LARGE AS 0.1 MAGNITUDE ARE PRESENT IN THE 3-6 COLORS.

IV COLOR CORRELATIONS

4.1 Comparison of Stellar and Extragalactic Colors

As an introduction to analysis of the colors presented in the previous chapter consider first a comparison between stellar and extragalactic colors. For the time being variations of color with such parameters as radius, inclination, velocity, and galactic latitude are neglected. Figures 2 through 6 present five of the possible color-color diagrams of the stellar and extragalactic observations. In the first three figures the color 1-3 is plotted as ordinate against the progressively longer wave length colors 2-3, 3-4, and 3-6. In the last two figures 5-6 is used as ordinate with 6-7 or 6-8 as abscissa. In each figure stellar observations are plotted to the left. Lines have been drawn to represent particular types of stars, viz. main sequence stars, normal giants, high velocity giants, and subdwarfs, whenever separation into distinct groups is sufficiently clear. The lines distinguishing the different types of stars are repeated in the right portion of each figure where the extragalactic color observations are plotted. Different symbols have been used for the basic extragalactic structural types.

In Figures 2 and 3 the separation of the stars into distinct groups is quite clear. Particularly interesting is the separation of the high velocity giants from the normal giants in the same manner as the subdwarfs deviate from the main sequence. The same division into population I and II groups appears to be present in Figure 4, although relatively few 3-6 colors are available and 3-6 is not as accurate as the other colors. The high velocity giant point deviating most extremely in Figures 3 and 4 is the star HD 122563 which shows extreme population II spectral characteristics. Figure 5 has a very short color base line so it is not surprising that the stars show no significant separation into groups. Figure 6 suggests a slight splitting into groups placing the main sequence stars, subdwarfs, and high velocity giants more or less together and apart from the population I giants.

In each of the color-color relationships the extragalactic colors are seen to lie in a fairly distinct sequence displaced from, but nearly parallel to, the stellar pattern. The displacement is readily explained as a natural consequence of the composite nature of the galaxies.

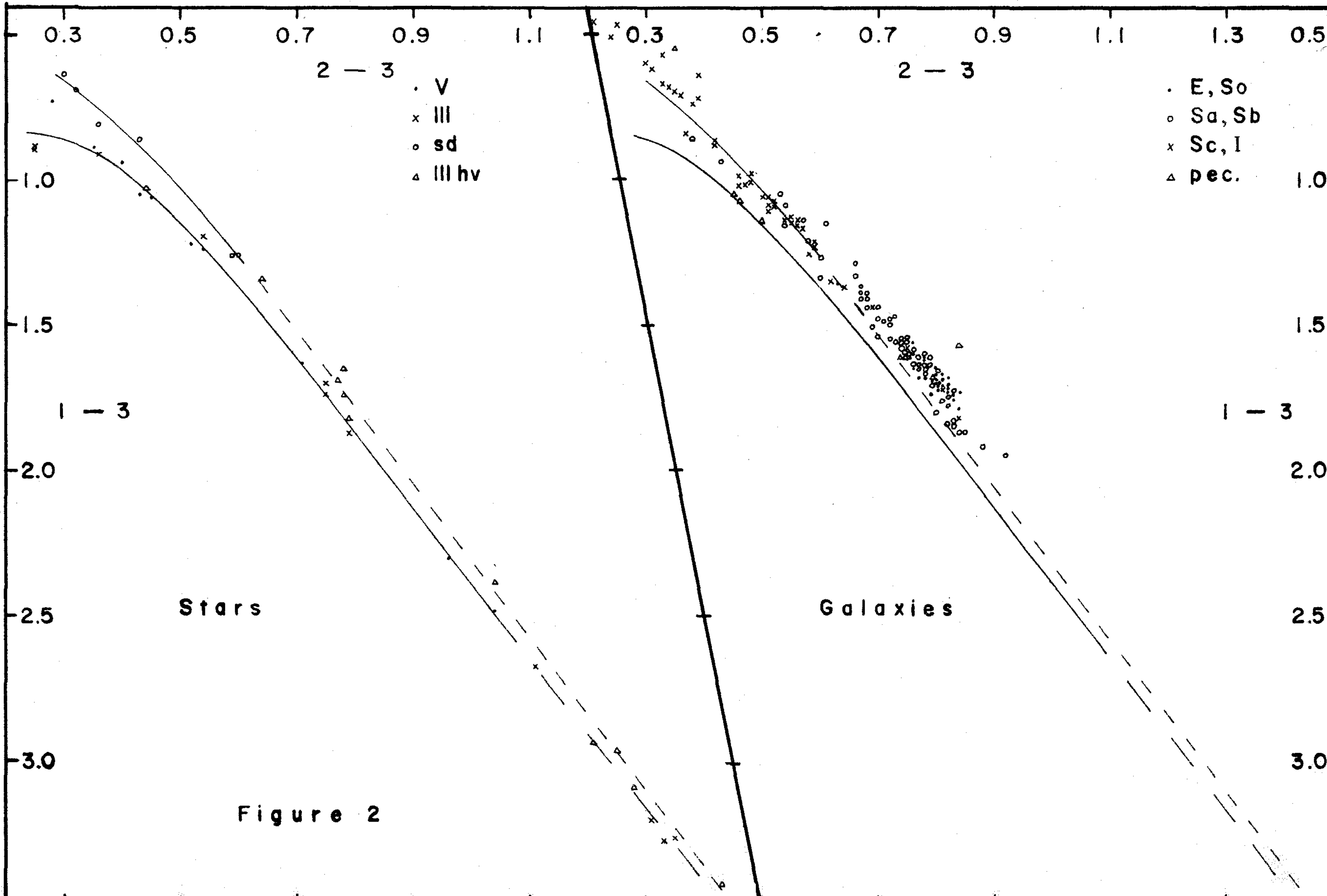

0.3
0.5
0.7
0.9
1.1
1.3
2 — 3
1 — 3
1.0
1.5
2.0
2.5
3.0
0.5
· V
× III
∘ sd
△ III hv
Stars
· E, So
∘ Sa, Sb
× Sc, I
△ pec.
Galaxies

Figure 2

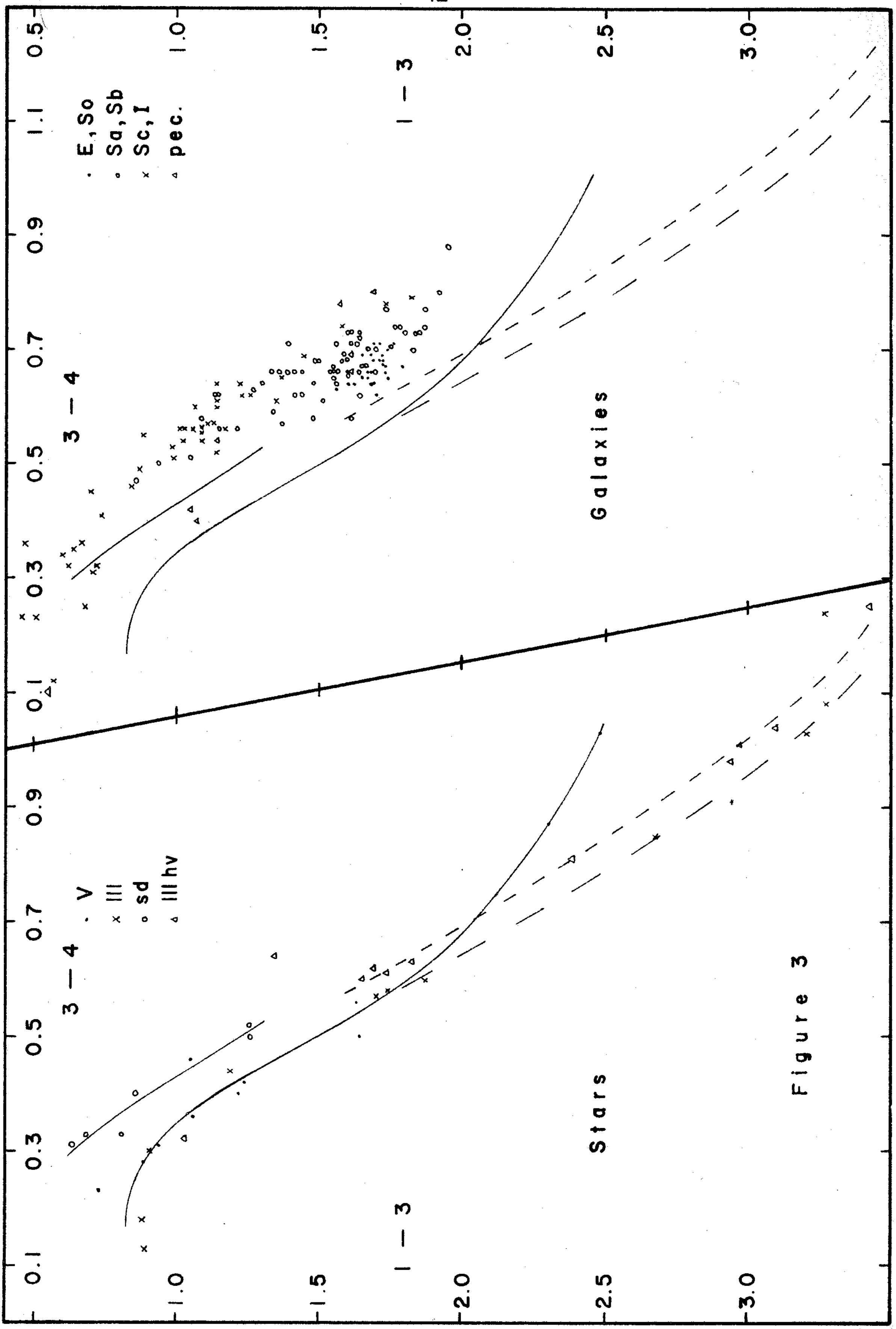
Galaxies
3 — 4
1 — 3
E, So
Sa, Sb
Sc, I
pec.
Stars
3 — 4
1 — 3
V
III
sd
III hv
0.1
0.3
0.5
0.7
0.9
1.1
0.5
1.0
1.5
2.0
2.5
3.0

Figure 3

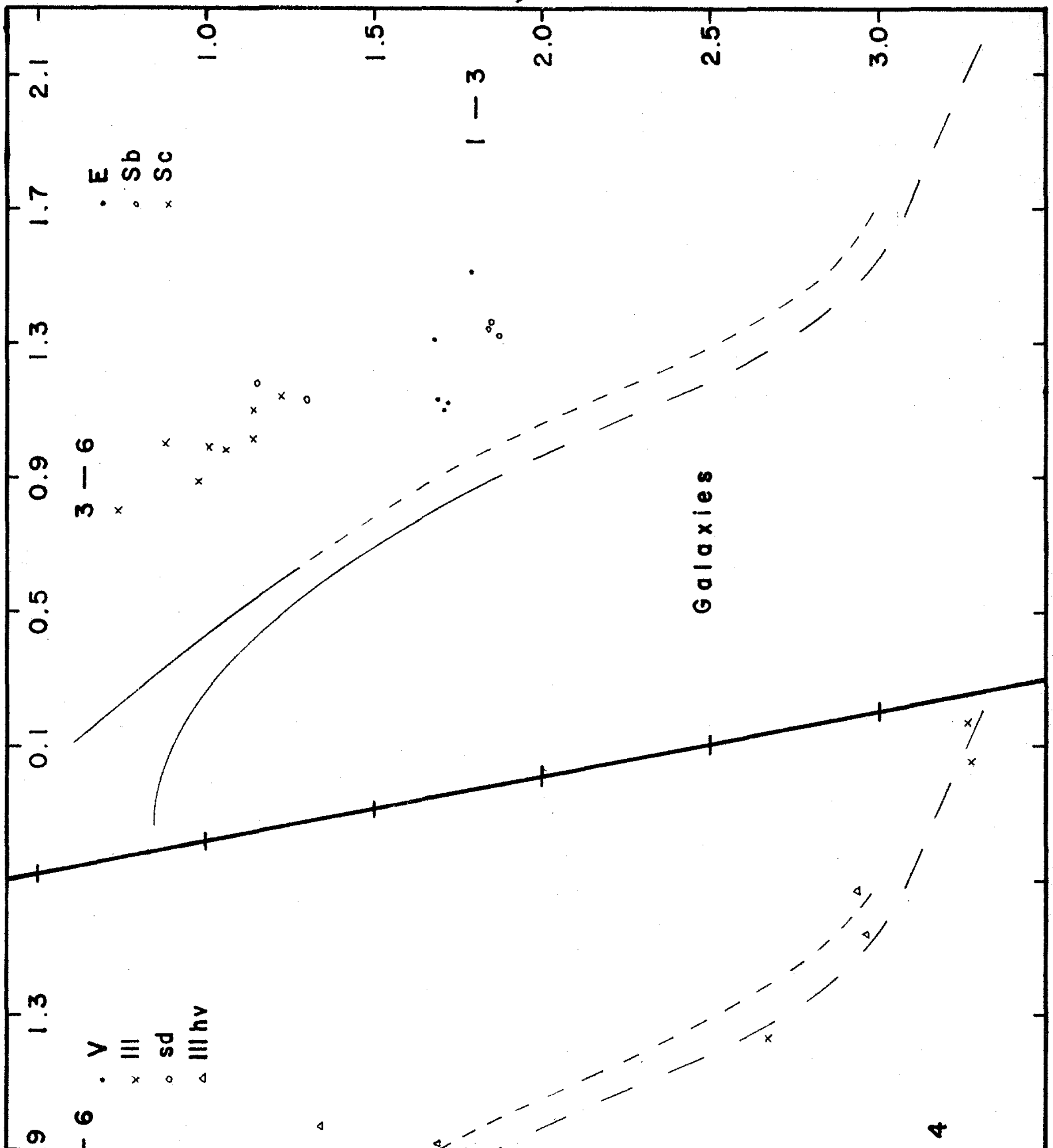
Galaxies
3 — 6
1 — 3
E
Sb
Sc
Stars
3 — 6
1 — 3
V
III
sd
III hv
0.5
0.1
0.5
0.9
1.3
1.7
2.1
1.0
1.5
2.0
2.5
3.0

Figure 4

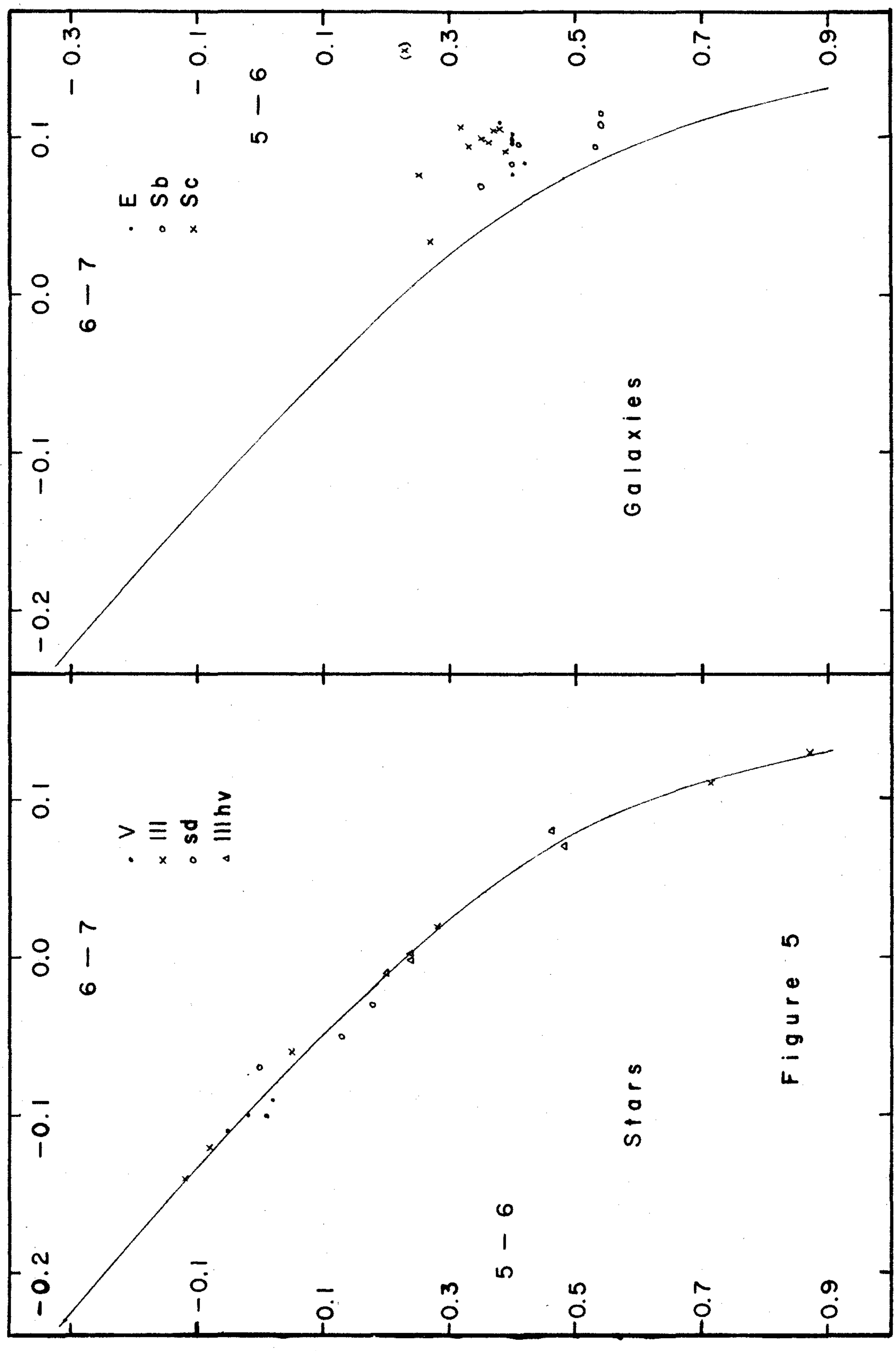
Galaxies
Stars
6 — 7
5 — 6
· E
∘ Sb
× Sc
· V
× III
∘ sd
▵ IIIhv
-0.3
-0.1
0.1
0.3
0.5
0.7
0.9
-0.2
-0.1
0.0
0.1
(x)

Figure 5

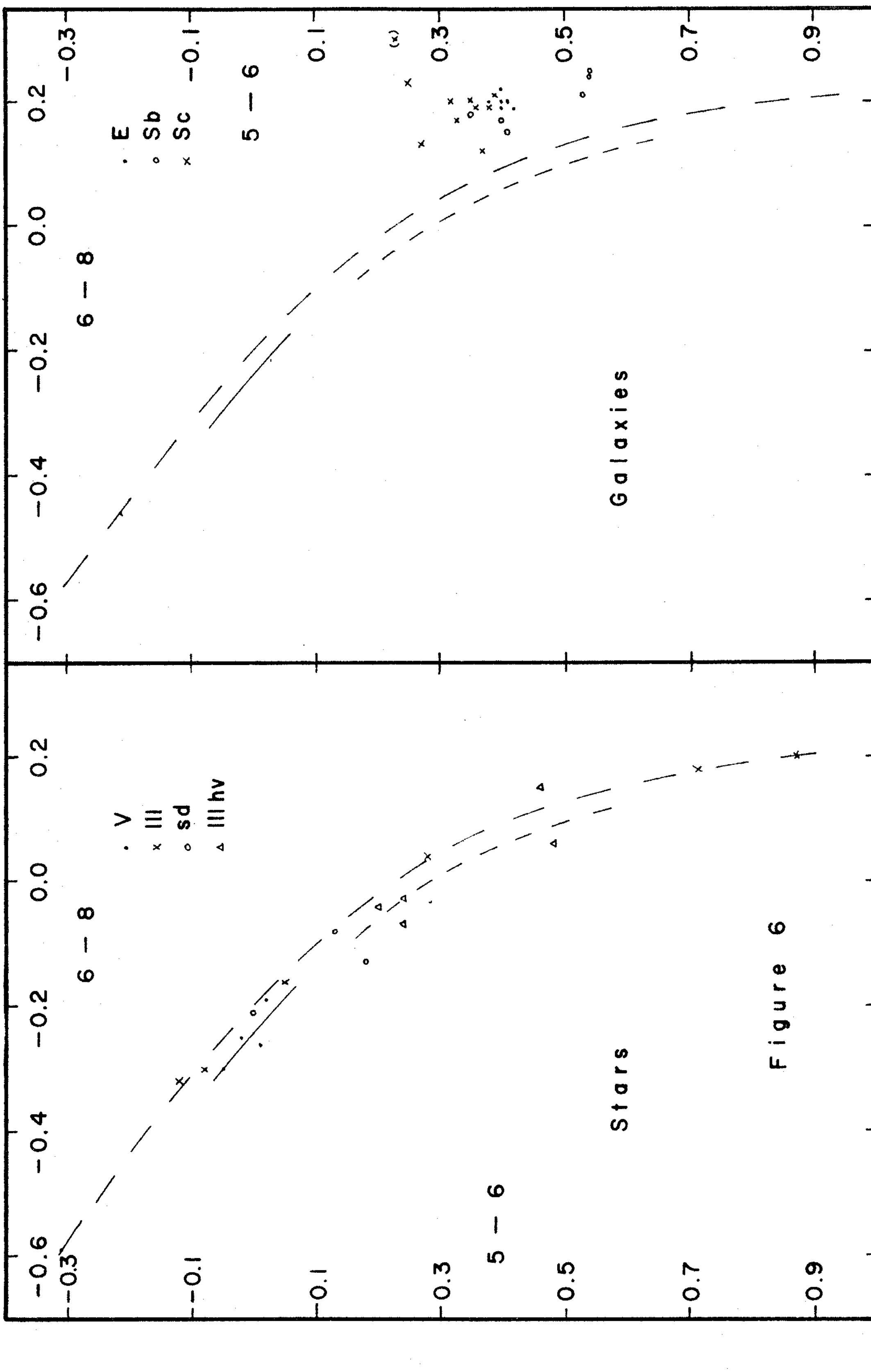

Figure 6

Consider, for example, that a certain type of galaxy has an energy curve resembling a G4III star over the spectral region from band 1 to band 3; thus 1-3 for the galaxy is equal to 1-3 for a G4III star. Now as we examine the galaxy's energy distribution further to the red, energy contributions from stars of later and later spectral type become increasingly important. Thus the galaxy will yield a color 3-4 which resembles a star of spectral type later than G4III, say K1III. Passing still further to the red we would find that 3-6 for the galaxy resembled 3-6 of a K3III star. Thus when we plot one color against another for the galaxy, the longest wave length color is found to be too red to correspond to a star which matches the galaxy in the shorter wave length color. This is just what is observed and illustrated in Figures 2 through 6. Note that as progressively longer color base lines are employed, the difference in the spectral type of the stars matching the two colors increases; hence the deviation of the galaxy colors from the colors of any one type of star grows. This effect shows clearly in progressing from Figure 2 to Figure 4 and from Figure 5 to Figure 6 (note change in scales). About the reddest color one would expect to observe in a galaxy, neglecting reddening by interstellar or intergalactic material, should be representative of the latest spectral type giants. Figure 6 shows that the 6-8 colors of the galaxies do indeed begin to resemble the M giant star colors. Further consideration is given to the composite colors of the galaxies in Part V of this thesis.

In addition to demonstrating the composite structure of galaxies, Figures 2 through 6 show the well known effect that structural type is correlated with color. The Sc and SBc spirals are clearly bluer than the Sa or Sb spirals. Also note that the elliptical galaxies show a relatively small spread in color. Further details of this and other color dependences are given in subsequent sections of this thesis.

4.2 Grouping of Data

In order to investigate certain correlations, such as the variation of color with inclination, redshift velocity, and galactic latitude, it is important to separate the galaxies into groups as homogeneous as possible. Since some of the very correlations we are seeking serve as a basis for distinguishing groups we cannot of course really separate the problem of grouping from the question of correlations.

Since many galaxies show marked radial color variation, the first question that must be resolved is what color to assign to a galaxy before comparing it with any other systems. One satisfactory answer is to use the color integrated over the entire galaxy out to some limiting isophote as has been done extensively be Holmberg (10). Unfortunately such total integrated colors cannot be derived from the observations made for this thesis because of the limitations on field diaphragm sizes. Many of the systems measured have outlying structure well outside the field of the largest diaphragm acceptable by the photoelectric equipment. Thus measures made with large diaphragms provide information of radial color variation, but give little data for anything but relatively coarse correlations between systems.

A second alternative, and the one followed in this study, is to use colors derived with small diaphragms, and assume that the light comes dominantly from the galaxy's nucleus. Nuclear measurements have been found to yield surprisingly good correlations considering that only certain fixed diaphragm sizes were employed in measurement, hence the smallest field measured varies somewhat as to how much of the whole galaxy it contains. The success of correlations may be partially explained by the fact that nuclei are generally much brighter than outer regions of galaxies, hence over a fairly wide range of apertures isolating the central regions the nuclear light is dominant. It would be dangerous to assume that very small and very large galaxies could be compared directly without serious systematic effects entering. However, with few exceptions, the systems observed do not vary widely in apparent size.

Nuclear colors have several advantages over total integrated colors. First, the nuclei are certainly more homogeneous in stellar content than entire galaxies, and are probably less disturbed by internal reddening except when systems are highly inclined. Secondly, spectroscopic information, such as the spectral classifications given by Morgan and Mayall (1), generally refers to the nucleus. Thirdly, relative size and form of extragalactic nuclei are important factors in structural classification. Thus there is ample justification for investigating correlations using the best estimate of nuclear colors.

Galaxies were categorized into homogeneous groups by means of preliminary correlations of spectral type, structural type, and inclination with nuclear color. With rare exceptions the smallest diaphragm measure was used as a measure of nuclear color for all galaxies considered. The first step consisted of separation into structural types and within these into spectral types using the Morgan and Mayall spectral classification, thus on criteria independent of measured colors. For systems without published spectral types, provisional types were assigned by means of the correlation between color and spectral type discussed in Section 4.6. The colors were then plotted against the inclination parameter 1 - b/a where a and b are the major and minor dimensions. The inclination effect on color is particularly important in grouping the Morgan and Mayall type K systems as is shown in Section 4.3. On the basis of these correlations nine fairly distinct groups were formed with most galaxies falling into three classes. One additional group of miscellaneous peculiar objects, or objects without suitable nuclear measurements completes the grouping. Radial color variation studies later suggested a few minor modifications of the original groupings. These modifications are of importance only for radial color studies and are discussed in Section 4.7. Group numbers for these galaxies are followed by "p".

Table 15 lists all the observed galaxies giving the group assignment; a brief description of the groups follows the table. Also given, for use in correlations, are the structural type, the Morgan-Mayall spectral type, the inclination factor 1 - b/a, the observed redshift velocity from the Humason, Sandage, and Mayall redshift catalog, and the cosecant of the galactic latitude. Structural types have been taken from the redshift catalog except for values enclosed in parentheses, which have been assigned by the author or taken from other sources. Spectral types given without any distinguishing marks are directly from data published by Morgan and Mayall (1). Types marked with an asterisk are from an older list kindly made available to the author by Dr. Morgan. These values are probably somewhat less reliable than the main list. Finally, spectral types in parentheses have been determined by the author from the correlation relation between nuclear color and spectral type. The axis ratio b/a generally has been taken from the Shapley-Ames catalog (11); for systems not given, b/a was determined from photographs. A few Shapley-Ames b/a ratios were rejected as not representative of actual inclinations. This applied primarily to certain barred spirals. Redshift velocities in Table 15 are given in units of 10^3 km/sec.

TABLE 15

GROUP MEMBERSHIP AND CORRELATION PARAMETERS

OBJECT	GROUP	TYPE	SP.	1-B/A	CSC β	VEL.
NGC 205	10	EP		.62	2.79	-.24
221	10	EP		.19	2.67	-.21
224	10	SB	K	.75	2.79	-.27
598	10	SC	F	.33	1.94	-.19
2903	2P	SC	AF	.54	1.39	.64
HARO 22	10	:	(A)	.17		
NGC 3031	9	SB	K	.38	1.49	-.06
3115	7	E7	K	.75	1.62	.65
3351	3P	SBB	(?)	.00	1.19	.69
3368	6	SA	(K)	.43	1.19	.93
NGC 3510	1	SBC	A*	:	1.08	.72
3810	4	SC	F	.33	1.08	.97
3998	8	S0	K	.24	1.14	1.11
4216	9	SB	K	.86	1.89	.03
4245	5P	SBA	(GK)	.40	1.01	.89
NGC 4274	6	SA	(K)	.71	1.01	.77
4278	7	E1	(K)	.10	1.01	.62
4283	7	E0	(K)	.00	1.01	1.07
4374	8	S0	(K)	.10	1.04	.95
4406	7	E3	(K)	.24	1.04	-.37
NGC 4449	10	I	A	:	1.05	.21
ANON	10	E0		.00	1.04	1.49
NGC 4486	7	E0	K	.00	1.04	1.29
4501	9	SC(SB)	(K)	.50	1.02	2.12
4548	9P	SBB	(K)	.10	1.03	.43
NGC 4565	9	SB	K	.93	1.00	1.22
4579	6	SB	(K:)	.11	1.04	1.75
4627	10	(EP)		.30	1.00	
4631	10	SC	A	.90	1.00	.59
4643	8	SB0	K	.00	1.11	1.43
NGC 4698	6	SA	(K)	.67	1.06	1.03
4699	6	SB(SA)	K	.46	1.24	1.51
4713	1	SC	AF	.29	1.08	.66
4762	6	SA	K	.89	1.04	.87
4865	6	E6	(K)	.57	1.00	4.64
NGC 4874	8	S0	(K)	.00	1.00	7.17
4881	7	E1	(K)	.00	1.00	6.69
4889	7	E4	(K)	.40	1.00	6.42
4907	9P	SBB	(K)	.09	1.00	5.87
IC 4051	7	E1	(K)	.09	1.00	4.93

Object	Group	Type	Sp.	1-b/a	csc β	Vel.
NGC 4911	5	Sb	(GK)	.12	1.00	8.01
4921	6	Sa	(K)	.00	1.00	5.46
5005	5	Sb	FG(GK)	.70	1.02	1.01
5055	10	Sb	FG	.62	1.04	.50
5194	4	Sc	F	.00	1.08	.44
NGC 5195	10	Ep		.25	1.08	.54
5248	3	Sc	FG*	.56	1.08	1.18
5363	7	I(E4)	K	.38	1.13	1.14
5457	3	Sc	FG*	.00	1.15	.25
5560	3	(SBc)	(FG)	:	1.19	:
NGC 5566	6	SBa	(K)	.44	1.19	1.46
5576	5	E4	(GK)	.43	1.19	1.53
5633	3	Sb	FG	.44	1.13	2.32
5850	9p	SBb	K	.19	1.37	2.32
5907	6	Sb	(K:)	.95	1.29	.55
NGC 6239	1	(Sc)	A*	.60	1.59	.96
6503	4	Sc	F*	.80	1.94	.03

Group 1: This group is distinguished by systems with Morgan-Mayall spectral class A. The group has three members, two Sc and one SBc galaxies; two are of spectral class A, and one if AF although very much bluer than the other AF system observed.

Group 2: This group contains one galaxy, the AF type Sc galaxy NGC 2903.

Group 3: Spectral type FG galaxies characterize this group. The five members include two Sc systems and one each of SBc, Sb and SBb.

Group 4: Three Sc spectral type F systems make up this group. It is interesting that although earlier in spectral type than the FG group, the F galaxies are distinctly redder. The F galaxies also tend to show much more rapid radial color changes.

Group 5: Four galaxies are contained in Group 5. They have little in common except color which is much redder than Groups 1 to 4 but still distinctly bluer than the large number of K galaxies. One system has an FG classification but is very much redder than the other three FG systems. The group contains two Sb systems an SBa system and the exceptionally blue elliptical NGC 5576. These systems have tentatively been called GK systems, but it may be that they form no homogeneous group.

Group 6: This group, which can be called the Sa group, is the largest homogeneous subdivision. It contains the bluest of the K galaxies, and all the Sa and SBa galaxies with the possible exception of the one peculiar SBa in Group 5. In addition it contains three Sb galaxies and one elliptical. These were assigned to this group on the basis of inclination effects which have a remarkable subgrouping effect on the K galaxies.

Group 7: This group is characterized by elliptical galaxies which make up eight of the nine members. The ninth member is the irregular K system NGC 5363. This one system has a fairly bright foreground star very near the nucleus; this star may contribute to the classification as irregular. Except for slight irregularities the system closely resembles an E4 galaxy. Group 7 contains only K systems and all the giant ellipticals except the two in Groups 5 and 6.

Group 8: This is the S0 and SB0 group with three S0 systems and one SB0. The group contains only K systems.

Group 9: This is the Sb group and has seven members. Six b spirals are equally divided between normal and barred and the seventh system is the exceptionally red Sc, NGC 4501. Holmberg (10) classifies NGC 4501 as a late type Sb and this classification is probably much more likely than Sc in view of the radically different nuclear color from any other Sc.

Group 10: The 11 galaxies not included in Groups 1 to 9 have been lumped together in a miscellaneous and peculiar group. Five of the systems are peculiar or dwarf ellipticals which do not in themselves form a homogeneous group. The peculiar blue and very small galaxy Haro 22 is also in this group. Both M31 and M33 are placed in Group 10, partially because they have negative galactic latitude, but primarily because their large size makes them difficult to compare with the smaller objects. There is no doubt that M31 is a Group 9 system. Although M33 is assigned an F classification the one available color more closely fits an A galaxy. The final three systems in Group 10 are the FG, Sb galaxy NGC 5055 for which no nuclear measure was obtained, and the irregular NGC 4449 and edge-on Sc NGC 4631 where no obvious nuclei were seen for measurement. Both of the latter systems have type A spectra and colors like Group 1 galaxies.

Thus with the possible exception of Group 5 all the normal galaxies with nuclear color measurements can be classified into fairly distinct groups. In order of number, the dominant characteristic of each group is; class A, class AF, class FG, class F, "blue" K, Sa, E, S0, and Sb.

4.3 Dependence of Color on Galactic Latitude, Velocity and Inclination

The classification of galaxies into groups fairly effectively removes the dependence of nuclear color on structural and spectral type. It thus becomes possible within individual groups to look for correlations of nuclear color with the galaxy's position, orientation, and motion in space. This analysis is limited to data collected with the EMI photocell because very little material is available in the red. Galaxies were deliberately selected for this thesis program to minimize dependence of color on redshift and galactic position. This was done by measuring only objects with small redshifts and relatively high galactic latitude. It is of interest, however, to show that slight residual effects remain.

Because the variation of color with velocity and galactic latitude is small, a plot of nuclear colors against the inclination parameter 1 - b/a shows immediately all significant inclination effects. Such a diagram reveals that only the three largest groups - 6, 7, and 9 show significant and rather remarkable dependence of color on inclination (see Figure 7). The material available for the smaller groups is too scanty to make precise statements, but apparently no major effects are present.

Within observational accuracy, nuclear color in Groups 6, 7, and 9 varies linearly with inclination. To evaluate velocity, galactic latitude and inclination effects for the three groups a least-squares solution was carried out, using observation equations of the form

$$(\text{color})_{ij} = C_{oij} + X_{ij}(1 - b/a) + Y_i \csc\beta + Z_i V \quad . \qquad (30)$$

The subscript i refers to the particular color involved, while j refers to the group. C_o is the nuclear color reduced to zero inclination, zero velocity, and to outside the galaxy. X, Y and Z are reddenings produced by a shift of 90° in inclination, absorption between the sun and the galactic pole, and a recession velocity of 1000km/sec. Y and Z depend upon only the particular color index considered while C_o and X depend upon the group as well. Judging from the colors of Group 6, 7, and 9

SYSTEMS, THEIR ENERGY CURVES ARE ALL VERY SIMILAR, HENCE THERE IS NO REASON TO EXPECT Z TO VARY SIGNIFICANTLY BETWEEN GROUPS.

TABLE 16

SOLUTIONS OF EQUATION 30 FOR GROUPS 6, 7 AND 9

QUANTITY	SOLN.	PE	SOLN.	PE	SOLN.	PE
	1 - 3		2 - 3		3 - 4	
C_{o6}	1.64	.018	.78	.009	.69	.009
C_{o7}	1.67	.010	.79	.005	.66	.009
C_{o9}	1.64	.008	.76	.006	.68	.011
X_6	-.03	.030	-.04	.016	.03	.017
X_7	.14	.026	.06	.013	.01	.029
X_9	.32	.014	.14	.010	.19	.019
Y	.008	.018	.003	.010	*	
Z	.007	.002	.011	.001	*	

* THE ORIGINAL SOLUTION GAVE NEGATIVE VALUES, SO Y AND Z WERE SET EQUAL TO ZERO AND NEW VALUES OF C_o AND X COMPUTED.

IT IS IMMEDIATELY APPARENT FROM TABLE 16 THAT NO SIGNIFICANT DEPENDENCE OF COLOR ON GALACTIC LATITUDE IS PRESENT, ALTHOUGH AT LEAST 1-3 AND 2-3 SHOW THE CORRECT SIGN FOR Y. VELOCITY DEPENDENCE OF COLOR IS SIGNIFICANT BUT SMALL, AND IMPORTANT ONLY FOR THE COMA CLUSTER GALAXIES. THE ORIGINAL SOLUTION FOR VELOCITY EFFECTS IN 3-4 YIELDED Z = -0.0005 WITH A PROBABLE ERROR OF ABOUT 0.002, HENCE FOR ALL PRACTICAL PURPOSES Z = 0.000 FOR 3-4. UNLESS GREAT CARE IS TAKEN TO MEASURE THE SMALL DISTANT GALAXIES OVER THE SAME NUCLEAR REGIONS AS MEASURED IN THE NEARBY LARGE SYSTEMS, RADIAL COLOR VARIATIONS MAY BE COUPLED TO REDSHIFT EFFECTS. SUCH SYSTEMATIC Z ERRORS MAY BE PRESENT HERE TO SOME DEGREE.

FIGURE 7 DISPLAYS THE INCLINATION EFFECT ON NUCLEAR COLOR FOR GROUPS 6, 7 AND 9. THE OBSERVED COLORS, REDUCED TO ZERO VELOCITY AND TO THE GALACTIC POLE USING TABLE 16 DATA, ARE PLOTTED AGAINST 1 - B/A; LINES

HAVE BEEN DRAWN TO REPRESENT THE LEAST-SQUARES FIT. THE FIGURE CLEARLY DEMONSTRATES THAT THE THREE GROUPS WHILE HAVING INSIGNIFICANTLY DIFFERENT NUCLEAR COLORS WHEN FACE-ON, HAVE STRIKINGLY DIFFERENT INCLINATION EFFECTS. AS INCLINATION INCREASES THE SA NUCLEI, IF ANYTHING, BECOME VERY SLIGHTLY BLUER, WHILE THE NUCLEI OF ELLIPTICALS BECOME SLIGHTLY REDDER AND THE SB NUCLEI BECOME MARKEDLY REDDER. THE REMARKABLE SEPARATION BETWEEN SA AND SB SYSTEMS FOUND HERE IS TO BE CONTRASTED WITH THE INCLINATION EFFECT IN TOTAL INTEGRATED COLOR ACCORDING TO HOLMBERG (10). HOLMBERG FINDS NO DISTINCTION BETWEEN SA AND SB- COLORS WITH BOTH TYPES BECOMING REDDER AS INCLINATION INCREASES. SB+ SYSTEMS SHOW A SLIGHTLY SMALLER EFFECT, BUT NOT GREATLY DIFFERENT. THE COLORS FOUND BY HOLMBERG SHOW AN APPRECIABLE DISPERSION ABOUT THE MEAN INCLINATION RELATIONS. ALTHOUGH HOLMBERG HAS NOT YET PUBLISHED HIS INVESTIGATIONS OF INTERNAL COLOR DISTRIBUTION IN GALAXIES, HE STATES IN A FOOTNOTE IN HIS PAPER ON INTEGRATED COLORS (10, PAGE 47) THAT MEAN NUCLEAR COLORS ARE INDEPENDENT OF INCLINATION EXCEPT AT EXTREME VALUES. THIS IS IN DIRECT CONTRADICTION TO THE RESULTS FOUND HERE, BUT LACKING FURTHER INFORMATION NO DETAILED COMPARISON OF DATA CAN BE MADE.

SINCE THE FACE-ON NUCLEAR COLORS OF GROUP 6 AND 9 DO NOT DIFFER SIGNIFICANTLY, THE STELLAR CONTENTS OF THE NUCLEI ARE PRESUMABLY QUITE SIMILAR AND IN ANY CASE CAN HAVE NOTHING TO DO WITH THE OBSERVED INCLINATION EFFECTS. HOWEVER, IF THE DISTINCT INCLINATION RELATIONS FOUND IN THIS THESIS ARE IN FACT TRUE THE GROUPS MUST BE CONSTRUCTED, AT LEAST IN SOME PORTIONS, ON RATHER DIFFERENT MODELS. WHILE THE SAMPLE IS SMALL AND MAY BE INFLUENCED BY SELECTION EFFECTS THESE RESULTS ARE INCOMPATIBLE WITH A CONTINUOUS SEQUENCE OF TYPES BLENDING INTO ONE ANOTHER. IT IS ALSO PROBABLE THAT GIVEN A MEASURE OF THE INCLINATION AND THE GROUP MEMBERSHIP A RATHER PRECISE COLOR CAN BE PREDICTED. THIS COULD MAKE THE SPIRALS AS VALUABLE AS THE ELLIPTICALS FOR DISTANT COLOR-REDSHIFT RELATIONS PROVIDING ONE CAN CLASSIFY THE SYSTEMS AND THE NUCLEI CAN BE SATISFACTORILY ISOLATED FOR MEASUREMENT.

THREE POSSIBLE EFFECTS MIGHT CONTRIBUTE TO THE VARIATION OF COLOR WITH INCLINATION. REDDENING BY INTERNAL ABSORPTION IS THE MOST IMPORTANT EFFECT, WHILE BLUEING CAN BE OBSERVED WHEN INCREASING INCLINATION COMPRESSES THE GALAXY ALONG THE MINOR AXIS SO THAT RELATIVELY BLUE REGIONS MOVE INTO THE FIELD OF VIEW NEAR THE NUCLEUS. A THIRD EFFECT MAY BE PRODUCED BY DIFFRACTION OF LIGHT FROM THE NUCLEUS IN AN OPTICALLY THIN

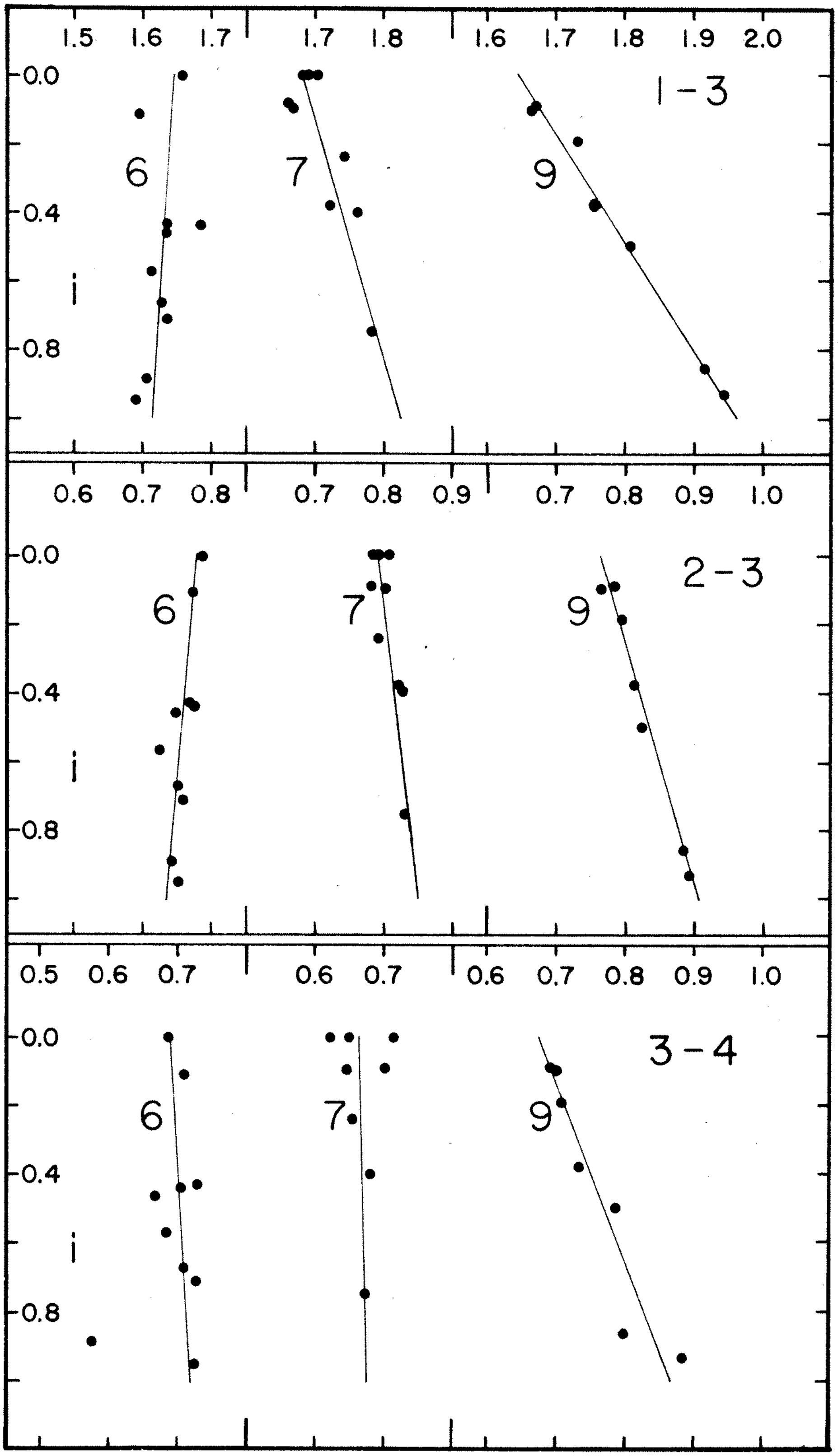

FIGURE 7

NUCLEAR COLOR VERSUS $i = 1 - b/a$ FOR GROUPS 6, 7, AND 9

LAYER OF SMALL DIELECTRIC PARTICLES IN THE REGION IMMEDIATELY AROUND THE NUCLEUS AS DISCUSSED BY ELVIUS (12).

ONLY THE INTERNAL ABSORPTION EFFECT CAN PRODUCE THE REDDENING OBSERVED IN THE SB GALAXIES WITH INCREASING TILT. A CHECK ON THE ASSIGNMENT OF THE TILT EFFECT TO ABSORPTION IS PROVIDED BY THE RATIO OF THE X VALUES IN TABLE 16. IF THE EFFECT IS REALLY SELECTIVE ABSORPTION, THE X RATIOS SHOULD MATCH THE RATIOS OF COLOR EXCESS, BETWEEN THE γ_1 POINTS, FROM THE INTERSTELLAR ABSORPTION CURVE GIVEN BY WHITFORD (13). ASSUMING, OF COURSE, THAT THE LAW OF REDDENING IS SIMILAR TO THAT FOUND FOR OUR OWN GALAXY. TABLE 17 LISTS THE OBSERVED X RATIOS FOR GROUP 9 AND THE ONE BEST DETERMINED RATIO FOR GROUP 7. THE RATIOS COMPUTED FROM THE WHITFORD INTERSTELLAR REDDENING CURVE ARE GIVEN FOR COMPARISON.

TABLE 17

COLOR EXCESS RATIOS

RATIO	WHITFORD	7	9
E_{1-3}/E_{2-3}	1.71	2.4	2.24
E_{1-3}/E_{3-4}	1.24	-	1.66
E_{2-3}/E_{3-4}	0.73	-	0.74

INSPECTION OF TABLE 17 REVEALS THAT BETWEEN BANDS 2 AND 4 THE GROUP 9 TILT EFFECT CAN BE EXPLAINED ENTIRELY BY INTERNAL ABSORPTION. THE ULTRAVIOLET INTENSITY, HOWEVER, FALLS OFF SOMEWHAT TOO FAST TO FIT THE ABSORPTION LAW. NEVERTHELESS IT IS APPARENT THAT INTERNAL ABSORPTION WILL ACCOUNT FOR THE LARGE PART OF THE TILT EFFECT. THERE IS NO EVIDENCE THAT BLUE STARS IN THE OUTER PORTIONS OR DIFFRACTION EFFECT ENTER SIGNIFICANTLY SINCE BOTH PROCESSES WOULD AGGRAVATE THE ULTRAVIOLET DEFICIENCY. IF THE ABSORPTION LAW WERE TO DIFFER SLIGHTLY FROM THAT FOUND IN OUR OWN GALAXY, THE ULTRAVIOLET IS THE MOST LIKELY PLACE TO SEE SUCH A DIFFERENCE SINCE THE TOTAL ABSORPTION IS THE LARGEST THERE.

ALTHOUGH INCLINATION EFFECTS IN THE ELLIPTICALS, GROUP 7, ARE SMALL, THEY APPEAR TO BE SIMPLY SCALED DOWN VERSIONS OF THE GROUP 9 PHENOMENA. THE BEST DETERMINED X RATIO FOR GROUP 7 AGREES WITH THE GROUP 9 RATIO WITHIN THE UNCERTAINTIES IN X. THE PRESENCE OF λ3727 [O II] EMISSION IN SOME ELLIPTICALS IMPLIES THAT THEY ARE NOT ENTIRELY FREE OF INTERSTELLAR

MATERIAL, HENCE THE SMALL TILT EFFECT IS NOT UNREASONABLE. THUS IT WOULD SEEM THAT BOTH SB AND ELLIPTICAL GALAXIES HAVE ABSORBING MATERIAL PENETRATING QUITE DEEPLY INTO THE NUCLEAR REGIONS, ALTHOUGH THE AMOUNT OF MATERIAL INVOLVED FOR THE ELLIPTICALS IS RELATIVELY SMALL.

THE SITUATION IN THE SA GALAXIES IS ENTIRELY DIFFERENT FROM THE SB SYSTEMS. IN THE SHORTER WAVE LENGTH COLORS INCREASING TILT PRODUCES A SLIGHT BLUEING, ALTHOUGH THE UNCERTAINTY IN X IS ABOUT AS LARGE AS THE EFFECT. IT FOLLOWS THAT INTERNAL ABSORPTION EFFECTS IN THE NUCLEAR REGIONS MUST BE QUITE DIFFERENT BETWEEN SA AND SB GALAXIES, OR AT LEAST THE ABSORPTION MUST AFFECT A MUCH SMALLER NUMBER OF THE STARS IN THE SA NUCLEI. IT IS POSSIBLE THAT THE LARGER NUCLEAR BULGE OF THE SA GALAXIES PLACES MUCH OF THE NUCLEAR LIGHT OUTSIDE THE SUPPOSEDLY LOW-LYING DUST LAYER. THE REDUCED ABSORPTION REDDENING MIGHT THEN BE SUFFICIENTLY COMPENSATED FOR BY THE ADDITION OF BLUER STARS FROM THE OUTER REGIONS TO PRODUCE THE OBSERVED COLOR VARIATION. IF THIS IS NOT THE CASE THEN THE SA NUCLEI AND MUCH OF THE REGION IMMEDIATELY AROUND MUST BE NEARLY ENTIRELY FREE OF DUST

NONE OF THE POSSIBLE EXPLANATIONS OF THE TILT EFFECT ON COLOR ARE PARTICULARLY UNREASONABLE; THE SURPRISING ASPECT HOWEVER IS THAT THE SA AND SB SYSTEMS FIT TWO DISTINCTLY DIFFERENT PATTERNS WITH NO SIGNIFICANT SCATTER BETWEEN. IF MORE EXTENSIVE OBSERVATIONS CONFIRM THIS THE GENERALLY ASSUMED CONTINUITY BETWEEN SA AND SB SYSTEMS CANNOT BE VALID.

IT SEEMS VERY UNLIKELY THAT DIFFRACTION EFFECTS ENTER SIGNIFICANTLY INTO THE TILT PHENOMENA FOR ANY OF THE GROUP 6 OR 9 GALAXIES. THE PHENOMENON IS QUITE RESTRICTED TO FAIRLY STEEP INCLINATIONS AND REGIONS QUITE CLOSE TO THE BRIGHT CENTRAL NUCLEUS. IN THE SA AND SB SPIRALS THE NUCLEAR BULGE EXTENDS OVER MUCH OF THE CRITICAL REGION AND PROBABLY FAIRLY WELL DROWNS OUT ANY EFFECT THAT MIGHT BE PRESENT. IN THE VICINITY OF THE RELATIVELY SMALL NUCLEI OF SC SPIRALS THE EFFECT SHOULD BE MOST EASILY DETECTED IF PRESENT AT ALL. NONE OF THE COLOR GROUPS INCLUDING SC SYSTEMS SHOW SIGNIFICANT TILT-COLOR EFFECTS, BUT THE MATERIAL IN EACH GROUP IS VERY LIMITED.

4.4 MEAN COLORS OF NUCLEI IN DIFFERENT GROUPS

TABLE 18 GIVES THE MEAN COLORS, WITH PROBABLE ERRORS, FOR THE NUCLEI OF THE GALAXIES IN THE NINE BASIC GROUPS. ALSO GIVEN IS THE NUMBER OF SYSTEMS IN EACH GROUP. ALL OBSERVED 1-3 AND 2-3 COLORS WERE REFERRED TO

ZERO REDSHIFT AND TO THE GALACTIC POLE, USING THE MATERIAL IN TABLE 16, BEFORE FORMING THE MEANS. TECHNICALLY THE VALUE OF Z, THE VELOCITY COLOR DEPENDENCE, WILL VARY WITH DIFFERENT ENERGY DISTRIBUTIONS, BUT THE EFFECT IS SMALL AND HAS BEEN NEGLECTED. EXCEPT FOR THE COMA CLUSTER GALAXIES, VELOCITY CORRECTIONS ARE QUITE SMALL ANYWAY. IN ADDITION TO VELOCITY AND GALACTIC LATITUDE CORRECTIONS, INCLINATION CORRECTIONS HAVE BEEN APPLIED TO ALL COLORS IN GROUPS 6, 7, AND 9. FOR THESE GROUPS THE COLORS WOULD BE THE SAME AS C_o IN TABLE 16 EXCEPT THAT THE C_o VALUES INCLUDE THE SMALL ADDITIONAL ABSORPTION CORRECTION TO REDUCE TO OUTSIDE THE GALAXY.

TABLE 18

MEAN NUCLEAR COLORS

GROUP	1 - 3	PE	2 - 3	PE	3 - 4	PE	N
1	.64	.009	.33	.016	.34	.006	3
2	.88		.42		.55		1
3	1.12	.020	.55	.013	.58	.020	4
4	1.23	.008	.58	.002	.63	.006	3
5	1.47	.020	.71	.010	.67	.020	4
6	1.65	.018	.78	.009	.69	.009	10
7	1.68	.010	.79	.005	.66	.009	9
8	1.72	.008	.82	.002	.69	.006	4
9	1.65	.008	.76	.006	.68	.011	7

4.5 DEPENDENCE OF NUCLEAR COLOR ON NEBULAR TYPE

THE CORRELATION OF NUCLEAR COLORS 1-3, 2-3, AND 3-4 WITH STRUCTURAL TYPE IS SHOWN IN FIGURE 8. GROUP 10 SYSTEMS ARE OMITTED FROM THE FIGURE. ALL COLORS HAVE BEEN CORRECTED FOR VELOCITY AND GALACTIC LATITUDE EFFECTS, AND FOR INCLINATION EFFECTS WHERE APPROPRIATE.

THE FIGURE SHOWS ABOUT WHAT WOULD BE EXPECTED JUDGING FROM OLDER CORRELATIONS OF COLOR AND STRUCTURAL TYPE. THE ELLIPTICALS, SO, AND SA SYSTEMS SHOW RELATIVELY LITTLE COLOR VARIATION WHILE THE SB SYSTEMS BEGIN TO INCLUDE SOME RELATIVELY BLUE GALAXIES, AND THE SC SYSTEMS ARE CONSIDERABLY BLUER. IT IS INTERESTING TO NOTE THAT AFTER REMOVAL OF THE INCLINATION EFFECT THE ELLIPTICALS, SO NUCLEI, SA NUCLEI, AND MOST SB NUCLEI SHOW VERY LITTLE DISPERSION IN COLOR. FOR SEVERAL OF THE BLUEST SB SYSTEMS REALLY SMALL DIAPHRAGM MEASUREMENTS ARE NOT AVAILABLE. SMALLER

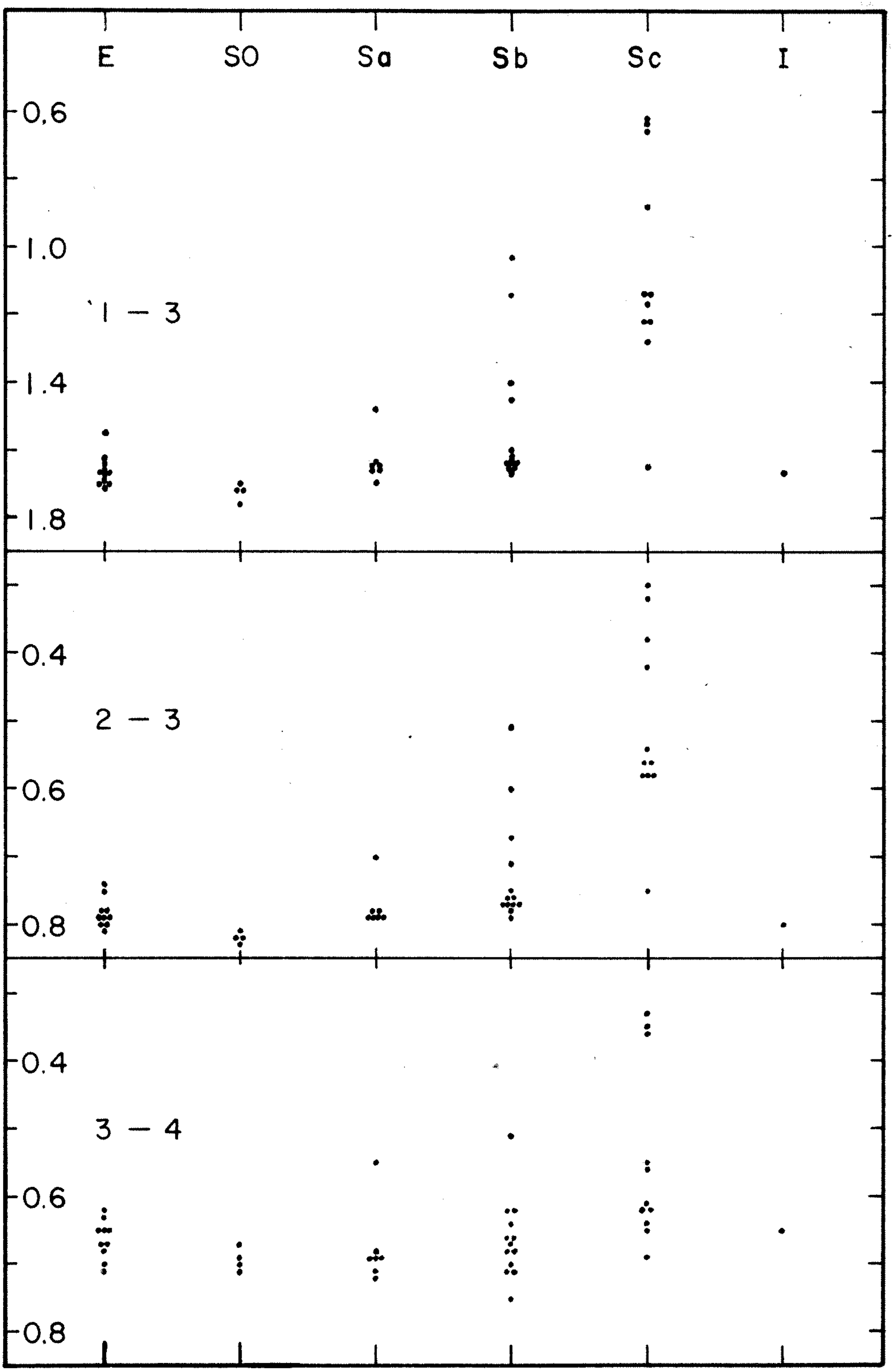

Figure 8

Nuclear color as a function of structural type

APERTURE MEASURES MIGHT BRING SOME OF THESE POINTS CLOSER TO THE MAIN GROUP. WITH THE EXCEPTION OF THE THREE BLUEST Sc GALAXIES (GROUP 1) THERE IS NOT MUCH SEPARATION OF 3-4 WITH STRUCTURAL TYPE. THE SPREAD OF COLOR WITH NEBULAR TYPE BECOMES STILL LESS IN THE RED JUDGING FROM WHAT FEW OBSERVATIONS ARE AVAILABLE.

4.6 NUCLEAR COLOR AS A FUNCTION OF SPECTRAL TYPE

OF THE VARIOUS OBSERVABLES CONNECTED WITH EXTRAGALACTIC SYSTEMS, INTEGRATED COLOR AND SPECTRAL CLASS PROVIDE MOST OF THE INFORMATION AVAILABLE CONCERNING THE ACTUAL STELLAR CONTENT OF ALL BUT THE VERY NEAREST GALAXIES. AS BOTH COLOR AND SPECTRAL CLASS ARE FIXED BY THE SAME DOMINANT STELLAR TYPES, WE CAN EXPECT, AND DO INDEED FIND, A GOOD COLOR-SPECTRUM CORRELATION. OLDER INVESTIGATIONS HAVE SHOWN GENERAL COLOR-SPECTRAL TYPE CORRELATIONS, BUT HAVE SUFFERED FROM TWO MAJOR DIFFICULTIES. FIRST, BECAUSE OF THE COMPOSITE NATURE OF GALAXIES, SPECTRA CANNOT BE EASILY CLASSIFIED ON A HOMOGENEOUS SYSTEM. THUS, UNTIL RECENT CAREFUL STUDY BY MORGAN AND MAYALL (1) NO REALLY PRECISE SPECTRAL CLASS INFORMATION WAS AVAILABLE. SECONDLY, FEW HIGH PRECISION COLOR OBSERVATIONS EXIST WHICH REFER TO JUST CENTRAL NUCLEAR REGIONS OF GALAXIES. SPECTROGRAMS GENERALLY REFER TO NUCLEAR REGIONS; CONSEQUENTLY A GOOD CORRELATION STUDY REQUIRES COLORS OF JUST CENTRAL PORTIONS. PHOTOMETRY IN THIS THESIS REPRESENTS A STEP TOWARD SUPPLYING SUCH MEASURES.

FIGURES 9 AND 10 PRESENT THE NUCLEAR COLOR-SPECTRAL CLASS CORRELATIONS FOUND. THE FIRST FIGURE SHOWS THE COLORS OBSERVED WITH THE EMI PHOTOCELL WHILE THE SECOND FIGURE PRESENTS THE RED DATA. THE INTERSYSTEM COLOR 3-6 IS OF DUBIOUS QUALITY, HENCE NOT SHOWN. THE NUCLEAR COLORS IN FIGURE 9 HAVE BEEN CORRECTED FOR REDSHIFT, GALACTIC LATITUDE AND INCLINATION EFFECTS. THE RED OBSERVATIONS IN FIGURE 10 ARE PLOTTED DIRECTLY, WITHOUT ANY CORRECTIONS, FROM TABLE 14. ONLY OBJECTS WITH DIRECT DETERMINATIONS OF SPECTRAL CLASS ARE SHOWN. THE ONE F SYSTEM, NGC 3810, OBSERVED IN THE RED IS RELATIVELY FAINT; CONSEQUENTLY THE OBSERVATIONS ARE NOT OF HIGH ACCURACY, PARTICULARLY 6-8. ALSO, NONE OF THE A SYSTEMS WITH WELL DEFINED NUCLEI WERE OBSERVED IN THE RED. THE ONE A SYSTEM THAT WAS OBSERVED, NGC 4631, IS AN IRREGULAR EDGE-ON Sc SHOWING NO SIGNIFICANT NUCLEUS. FURTHERMORE, EVEN THE OBSERVATIONS OF NGC 4631 ARE UNCERTAIN BECAUSE OF INTERRUPTION BY CLOUDS DURING MEASUREMENT.

IN THE FIGURES SPECTRAL TYPES HAVE BEEN SPACED EQUALLY EXCEPT FOR

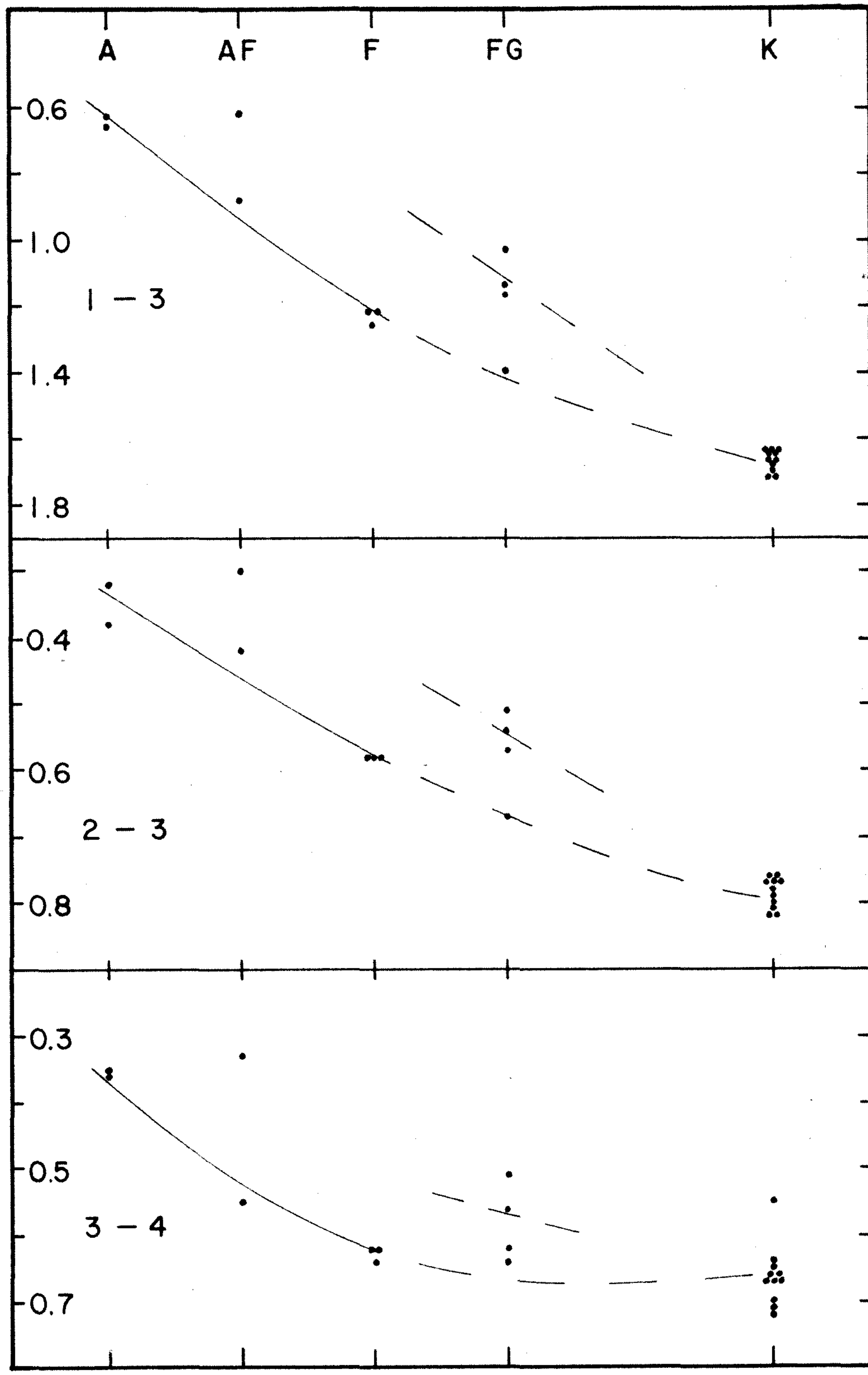

Figure 9

Nuclear color as a function of spectral class

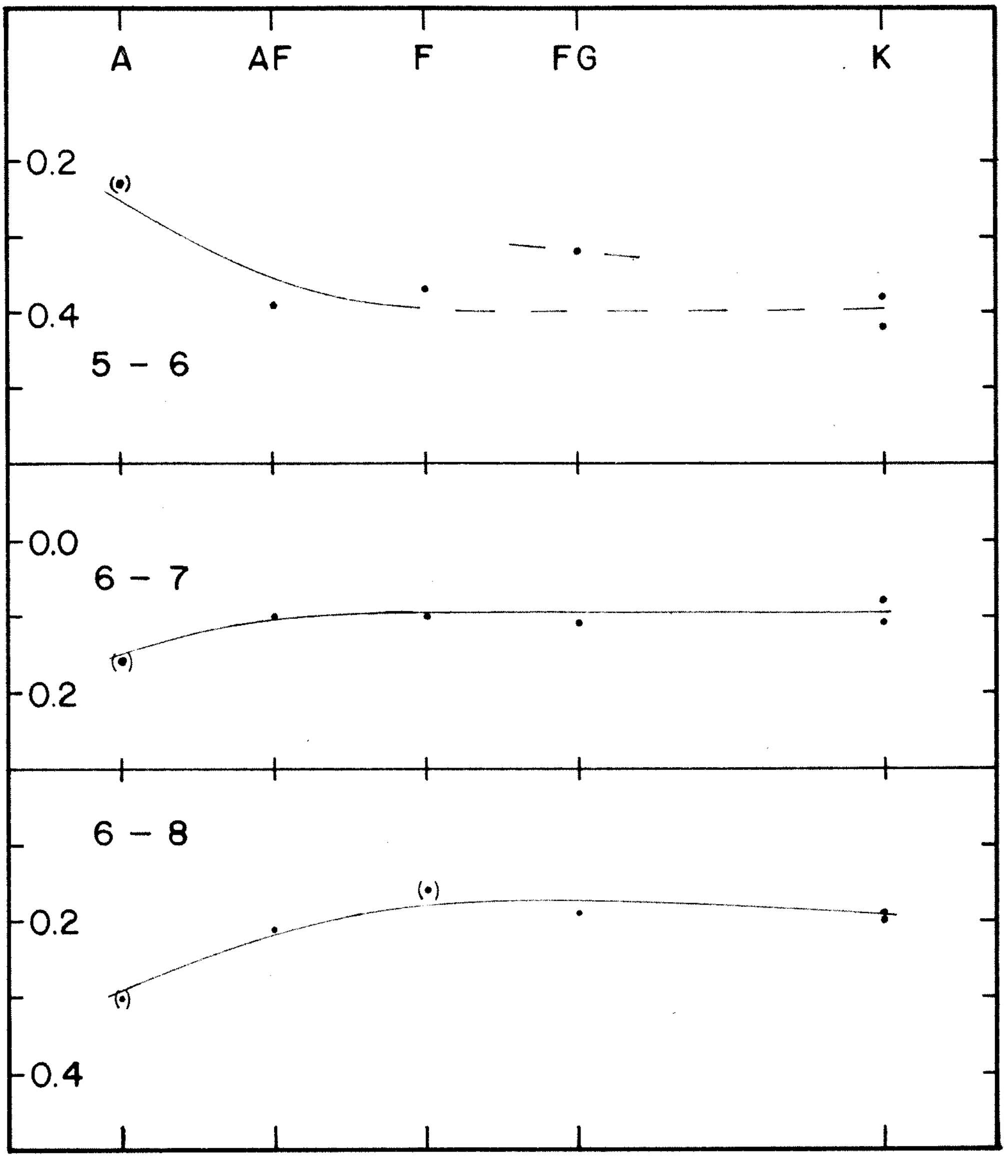

FIGURE 10

NUCLEAR COLOR AS A FUNCTION OF SPECTRAL CLASS. POINTS FOR WHICH THE INFORMATION IS RELATIVELY UNCERTAIN ARE ENCLOSED IN PARENTHESES.

K WHICH HAS BEEN ARBITRARILY SEPARATED FROM FG BY DOUBLE SPACING IN VIEW OF THE LARGER SPECTRAL CLASS INTERVAL. FOR THE COLORS 6-7 AND 6-8 THE OBSERVATIONS ARE READILY FIT BY A SINGLE SMOOTH LINE. FOR THE OTHER COLORS HOWEVER, PARTICULARLY THE ULTRAVIOLET, TO FIT ALL POINTS WOULD REQUIRE EITHER A DISCONTINUITY OR A RATHER SHARP KINK IN PASSING FROM CLASS F TO FG. THE OBSERVATIONS SHOW THAT, WITH ONE EXCEPTION, FG SYSTEMS HAVE BLUER NUCLEI THAN F GALAXIES DESPITE THEIR LATER SPECTRAL TYPE. THE ONE FG GALAXY THAT IS REDDER THAN THE F OBJECTS IS NGC 5005. THIS GALAXY, OBSERVED WITH ONLY ONE RATHER LARGE DIAPHRAGM, WOULD PROBABLY BE STILL REDDER IF OBSERVED WITH A SMALLER DIAPHRAGM.

IN FIGURE 9, AND THE FIRST PART OF 10, CORRELATION LINES HAVE BEEN DRAWN SEPARATELY THROUGH THE F GALAXIES AND THE BLUE FG SYSTEMS RATHER THAN INTRODUCING A SHARP TWIST IN A SINGLE RELATION FITTING BOTH TYPES. THERE APPEARS TO BE SOME DEFINITE EVIDENCE FAVORING TWO DISTINCT RELATIONS. IN ADDITION TO BEING SET APART BY THE COLOR-SPECTRAL CLASS INVERSION THE F AND FG GALAXIES SHOW MARKEDLY DIFFERENT RADIAL COLOR VARIATIONS. THE F GALAXIES SHOW A VERY STEEP RADIAL COLOR GRADIENT COMPARED TO THE FG SYSTEMS FOR WHICH COLOR VARIES SLOWLY WITH RADIUS. ALSO THE DEVIANT FG GALAXY AND ONE EXCEPTIONALLY BLUE AF GALAXY AT LEAST SUGGEST THE OVERLAP OF TWO PARALLEL GROUPS. THE PRESENT INFORMATION IS CERTAINLY NOT CONCLUSIVE IN DEMONSTRATING THE EXISTENCE OF TWO DISTINCT OVERLAPPING RELATIONS, BUT IT IS SUGGESTIVE.

IF THE DUALITY IS REAL IT IS INTERESTING TO SPECULATE ON ITS CAUSE. FIGURES 2 AND 3 ILLUSTRATE THE FAIRLY WELL KNOWN FACT THAT SUBDWARFS AND HIGH VELOCITY GIANTS BECOME PROGRESSIVELY BRIGHTER THAN THEIR POPULATION I COUNTERPARTS THROUGH THE BLUE AND VIOLET. THIS EXCESS BLUEING IS PRESUMABLY DUE TO A REDUCED METAL CONTENT RESULTING IN LESS LINE BLANKETING. THUS ONE CAN SPECULATE THAT THE LOWER CORRELATION LINE IN FIGURE 9 REFERS TO SYSTEMS DOMINATED BY POPULATION I STARS WITH TYPICALLY SOLAR METAL ABUNDANCES. THE BLUER SYSTEMS MIGHT THEN INCLUDE A STRONG COMPONENT OF STARS WITH LOWER METAL CONTENT. A CAREFUL STUDY OF THE SPECTRA OF F AND FG GALAXIES, COMBINED WITH ADDITIONAL COLORS AND A SEARCH FOR POSSIBLE OVERLAP CASES, SHOULD PERMIT A CHECK OF THIS HYPOTHESIS. SOME GROUP 5 GALAXIES ARE POSSIBLE OVERLAP CASES, PARTICULARLY NGC 5005 WHICH BEARS AN FG CLASSIFICATION. NGC 4713 IS AN EXCEPTIONALLY BLUE POTENTIAL OVERLAP CASE.

THERE IS DEFINITE EVIDENCE THAT AT LEAST SOME OF THE K GALAXIES ARE TO BE ASSOCIATED WITH THE HIGH METAL CONTENT SYSTEMS, CONSEQUENTLY THEY

HAVE BEEN TENTATIVELY TIED TO THE LOWER RATHER THAN UPPER LINE IN FIGURE 9. MORGAN AND MAYALL NOTE IN THEIR PAPER (1) THAT THE NUCLEUS OF M31 IS DEFINITELY NOT DOMINATED BY WEAK LINE GIANTS BUT RATHER BY GIANTS WITH APPARENTLY NORMAL METAL CONTENT. ADDITIONAL EVIDENCE FAVORING DOMINANCE OF POPULATION I IN K SYSTEMS HAS BEEN GIVEN BY BAUM (14). HE FINDS THAT THE COLORS OF GIANT ELLIPTICALS ARE MORE REPRESENTATIVE OF OLD POPULATION I (AS FOUND IN THE GALACTIC CLUSTER M67) THAN OF PURE POPULATION II.

THUS, IN SUMMARY, IT SEEMS POSSIBLE THAT OVER THE ENTIRE SPECTRAL RANGE FROM A TO K THERE MAY BE A SEQUENCE OF EXTRAGALACTIC NUCLEI BUILT ON A DOMINANTLY POPULATION I PATTERN. A SEPARATE GROUP OF SYSTEMS CHARACTERIZED BY POPULATION II MAY EXIST AS WELL AND INCLUDE AMONG ITS MEMBERS MOST OF THE OBSERVED FG GALAXIES.

4.7 THE VARIATION OF COLOR WITH RADIUS

HAVING GROUPED THE GALAXIES WITHOUT CONSIDERATION OF RADIAL COLOR GRADIENT, IT WAS VERY INTERESTING TO FIND THAT WITH VERY FEW EXCEPTIONS THE GROUPS WERE HOMOGENEOUS IN COLOR GRADIENT. INVESTIGATION OF RADIAL EFFECTS WAS LIMITED TO SYSTEMS MEASURED WITH MORE THAN ONE DIAPHRAGM SIZE, SYSTEMS NOT TOO STEEPLY INCLINED, AND SYSTEMS NOT TOO SMALL OR VERY LARGE. COMA CLUSTER MEMBERS WERE NOT INCLUDED BECAUSE THEY ARE SMALL AND RELATIVELY FAINT. IT SHOULD BE MENTIONED, HOWEVER, THAT WITHIN THE ACCURACY LIMITATIONS OF COMA CLUSTER OBSERVATIONS RADIAL EFFECTS ARE IN GOOD AGREEMENT WITH VARIATIONS PRESENT IN BRIGHTER GALAXIES. RADIAL COLOR EFFECTS IN THE RED WERE SMALL AND UNCERTAIN, CONSEQUENTLY THIS SECTION DEALS ONLY WITH EMI PHOTOCELL OBSERVATIONS.

IN ORDER TO COMPARE RADIAL COLOR GRADIENTS EVEN WITHIN INDIVIDUAL GROUPS IT IS NECESSARY TO REMOVE THE EFFECT OF DIFFERING ANGULAR SIZES. PUBLISHED SIZES, SUCH AS GIVEN IN THE SHAPLEY-AMES CATALOG, OR BY HOLMBERG (10), WERE FOUND TO BE TOO DEPENDENT UPON OUTLYING FAINT WISPS OF STRUCTURE TO GIVE A CONSISTENT MEASURE OF THE SCALE TO BE APPLIED TO COLOR VARIATIONS NEAR THE NUCLEUS. CONSEQUENTLY, DIAMETERS REFERRING TO THE MAIN STRUCTURE OF THE GALAXIES WERE TAKEN FROM 48-INCH SCHMIDT TELESCOPE PLATES. IN DETERMINING MAJOR AND MINOR DIMENSIONS, OUTLYING FAINT WISPS AND LARGE FAINT SPIRAL ARM EXTENSIONS WERE NEGLECTED. WITHIN GROUPS THE RELATIVE SIZES FOUND ARE PROBABLY QUITE CONSISTENT SINCE THE SYSTEMS ARE MORE OR LESS ALIKE STRUCTURALLY. IT SHOULD BE EMPHASIZED, HOWEVER, THAT DIAMETERS SO DERIVED CANNOT BE USED TO COMPARE SUCH DIFFERENT SYSTEMS AS

ELLIPTICALS AND SPIRALS. DIAMETERS ADOPTED FOR VARIOUS SYSTEMS ARE GIVEN IN TABLE 19 WHICH LISTS GALAXIES ACCORDING TO GROUP MEMBERSHIP. ONLY GALAXIES USED FOR RADIAL STUDIES ARE LISTED. DIMENSIONS ARE GIVEN IN UNITS OF 1/50 INCH AS MEASURED DIRECTLY ON 48-INCH SCHMIDT PLATES (1MM = 67"), SINCE ONLY RELATIVE VALUES HAVE ANY SIGNIFICANT MEANING.

FOR EACH GROUP, COLOR AND MAGNITUDE WERE PLOTTED AGAINST RELATIVE RADIUS (APERTURE SIZE DIVIDED BY THE MEAN DIAMETER IN TABLE 19). IT WAS IMMEDIATELY APPARENT THAT EXCEPT FOR GROUP 9 AND NGC 3351 IN GROUP 3, RADIAL COLOR CURVES WITHIN EACH GROUP WERE QUITE SIMILAR IN SHAPE. DUE TO SMALL SYSTEMATIC TIE-IN ERRORS BETWEEN GALAXIES, ACTUAL INTRINSIC COLOR DIFFERENCES, ERRORS IN RELATIVE SIZES USED, AND SLIGHT EFFECTS DUE TO TILT, VELOCITY AND GALACTIC LATITUDE, THE PLOT OF RELATIVE RADIUS AGAINST COLOR, AS WOULD BE EXPECTED, SHOWED SMALL CONSTANT SHIFTS BETWEEN GALAXIES WITHIN GROUPS. IN ORDER TO SHOW THE SHAPE OF RADIAL COLOR AND MAGNITUDE VARIATIONS AS WELL AS POSSIBLE, THE DISPLACEMENTS WERE REMOVED BY ADDING SMALL CONSTANT CORRECTIONS TO ALL COLOR AND MAGNITUDE MEASURES ON EACH GALAXY. THE AVERAGE CORRECTION WAS 0.03 IN 1-3, 0.01 IN 2-3, AND 0.02 IN 3-4; THE MAXIMUM CORRECTION WAS 0.08. INTERPRETED AS AN UPPER LIMIT TO SYSTEMATIC ERRORS BETWEEN SYSTEMS THE CORRECTIONS ARE IN AGREEMENT WITH THE ERRORS ESTIMATED IN PART III.

FIGURES 11 THROUGH 15 ILLUSTRATE RADIAL COLOR AND MAGNITUDE VARIATIONS FOR THE GROUPS IN TABLE 19. ON THE BASIS OF THESE CURVES, COLORS OF A SERIES OF CONCENTRIC RINGS WERE COMPUTED BY SUBTRACTING OUT THE PORTION INSIDE EACH RING. THE RESULTS OF THESE COMPUTATIONS, SOMEWHAT SMOOTHED, ARE GRAPHED IN FIGURES 16 THROUGH 19. EACH FIGURE HAS TWO PARTS; 1-3 IS PLOTTED AGAINST 2-3 AT THE TOP AND AGAINST 3-4 ON THE BOTTOM, MAKING THEM SIMILAR TO FIGURES 2 AND 3. LINES HAVE BEEN DRAWN TO REPRESENT THE RUN OF COLOR WITH RELATIVE RADIUS, VALUES OF WHICH ARE INDICATED AT POINTS ALONG EACH LINE. IN EACH FIGURE CERTAIN ZONES HAVE BEEN DRAWN TO ENCLOSE THE INTEGRATED COLOR MEASURES, ACCORDING TO FIGURE 2 AND 3, OF THE ELLIPTICALS, SA AND SB SYSTEMS, AND THE SC GALAXIES. TWO GROUPS OF SC SYSTEMS HAVE BEEN DISTINGUISHED SEPARATING AT WHAT APPEARS TO BE A NATURAL BREAK IN FIGURES 2 AND 3 AT 1-3 = 0.8. UTILIZING FIGURES 11 THROUGH 19 WE CAN MAKE THE FOLLOWING OBSERVATIONS CONCERNING RADIAL COLOR EFFECTS.

TABLE 19

DATA EMPLOYED IN RADIAL COLOR INVESTIGATIONS

Group	NGC	Size
1	3510	0.5x5.7
	4713	2.0x3.0
	6239	1.2x2.3
2p	2903	4.2x7.9
3	5248	2.3x4.5
	5457	15 x 15
	5633	0.9x1.2
3p	3351	4.0x4.5
4	3810	4.0x6.0
	5194	9.2x9.2
5p	4245	1.9x2.4
6	3368	3.2x5.0
	4579	3.0x4.9
	4699	3.9x5.7
	5566	1.6x2.9
7	3115	1.2x4.8
	4278	1.1x1.3
	4406	1.2x1.1
	4486	1.9x1.9
8	3998	2.2x2.9
	4374	1.6x1.9
	4643	3.0x3.0
9(SB)	3031	9.0x2.1
	4501	3.2x6.7
9(SBb)*	4548	3.0x4.4
	5850	3.7x4.1

* Called 9p in Table 15

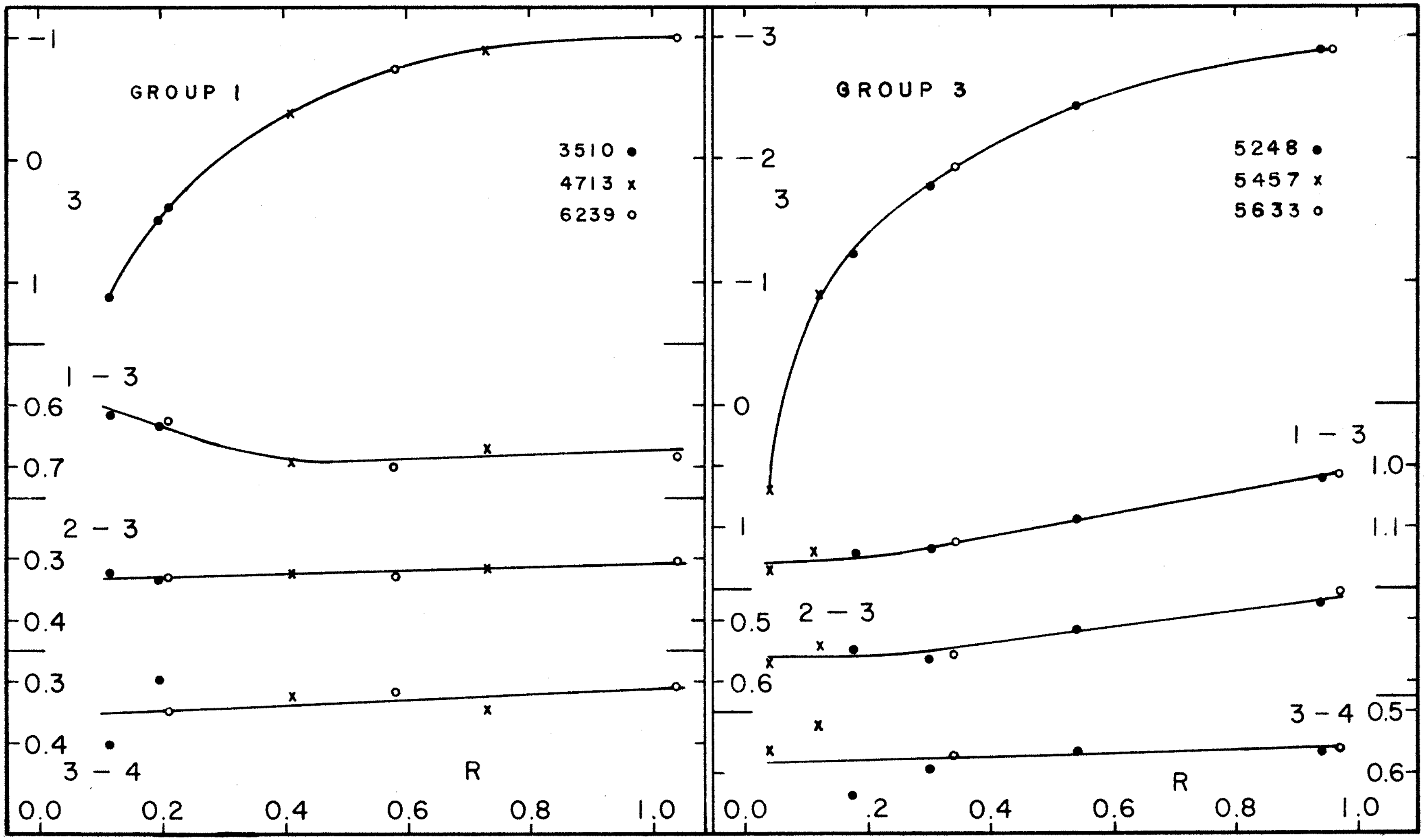

FIGURE 11

COLOR AND BAND 3 MAGNITUDE AS A FUNCTION OF RELATIVE RADIUS R FOR GROUP 1 AND 3 GALAXIES

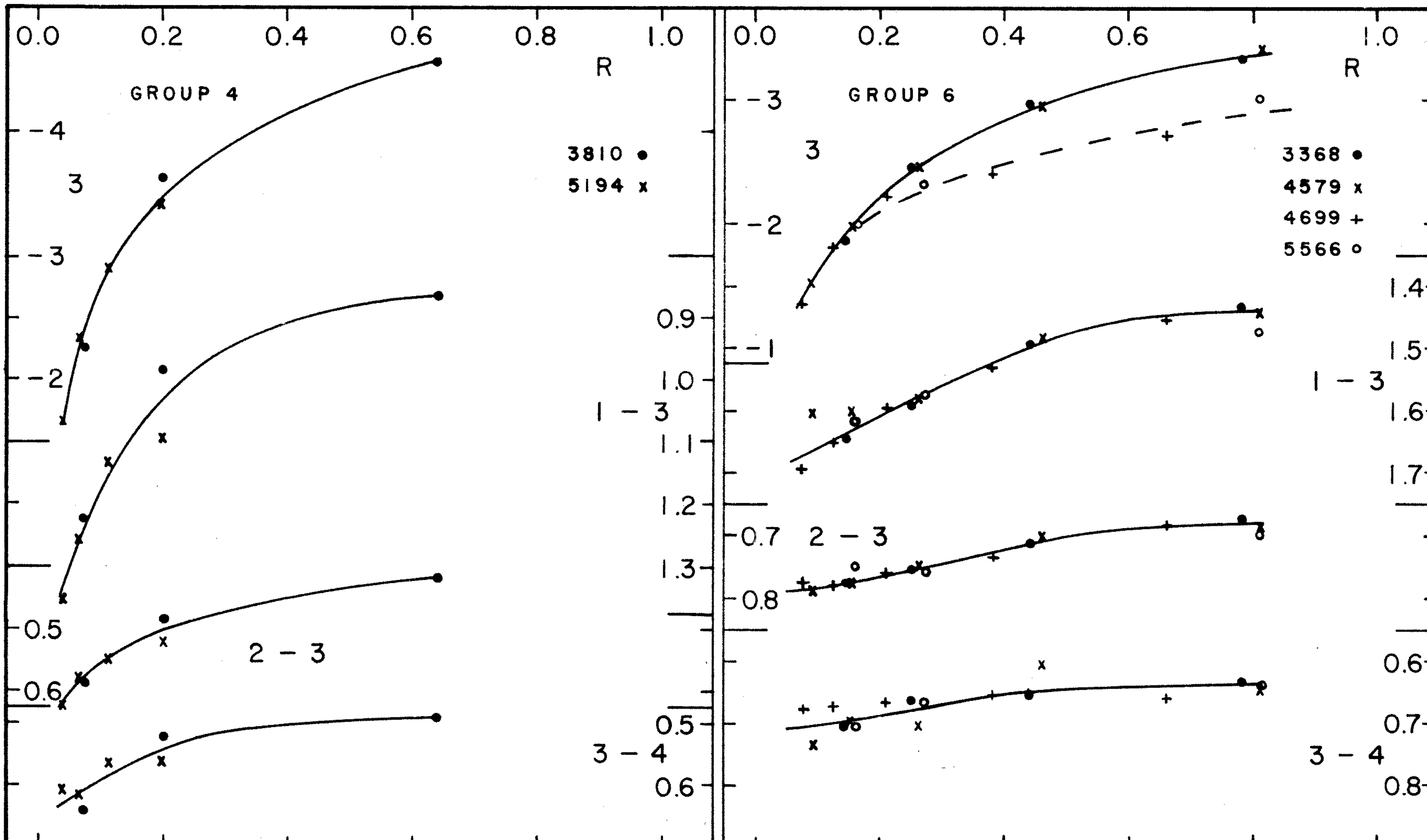

FIGURE 12

COLOR AND BAND 3 MAGNITUDE AS A FUNCTION OF RELATIVE RADIUS R FOR GROUP 4 AND 6 GALAXIES

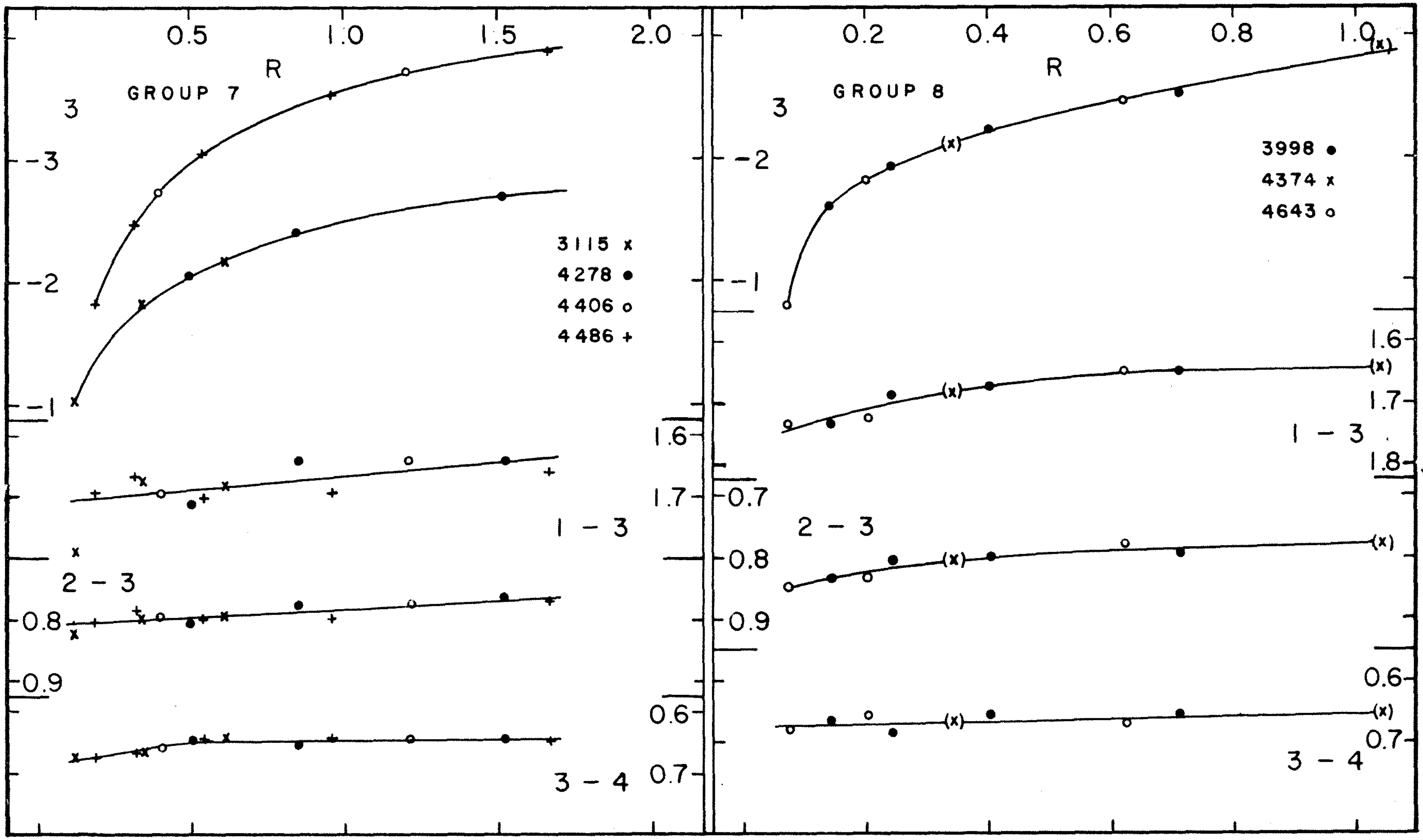

Figure 13

Color and band 3 magnitude as a function of relative radius R for Group 7 and 8 galaxies

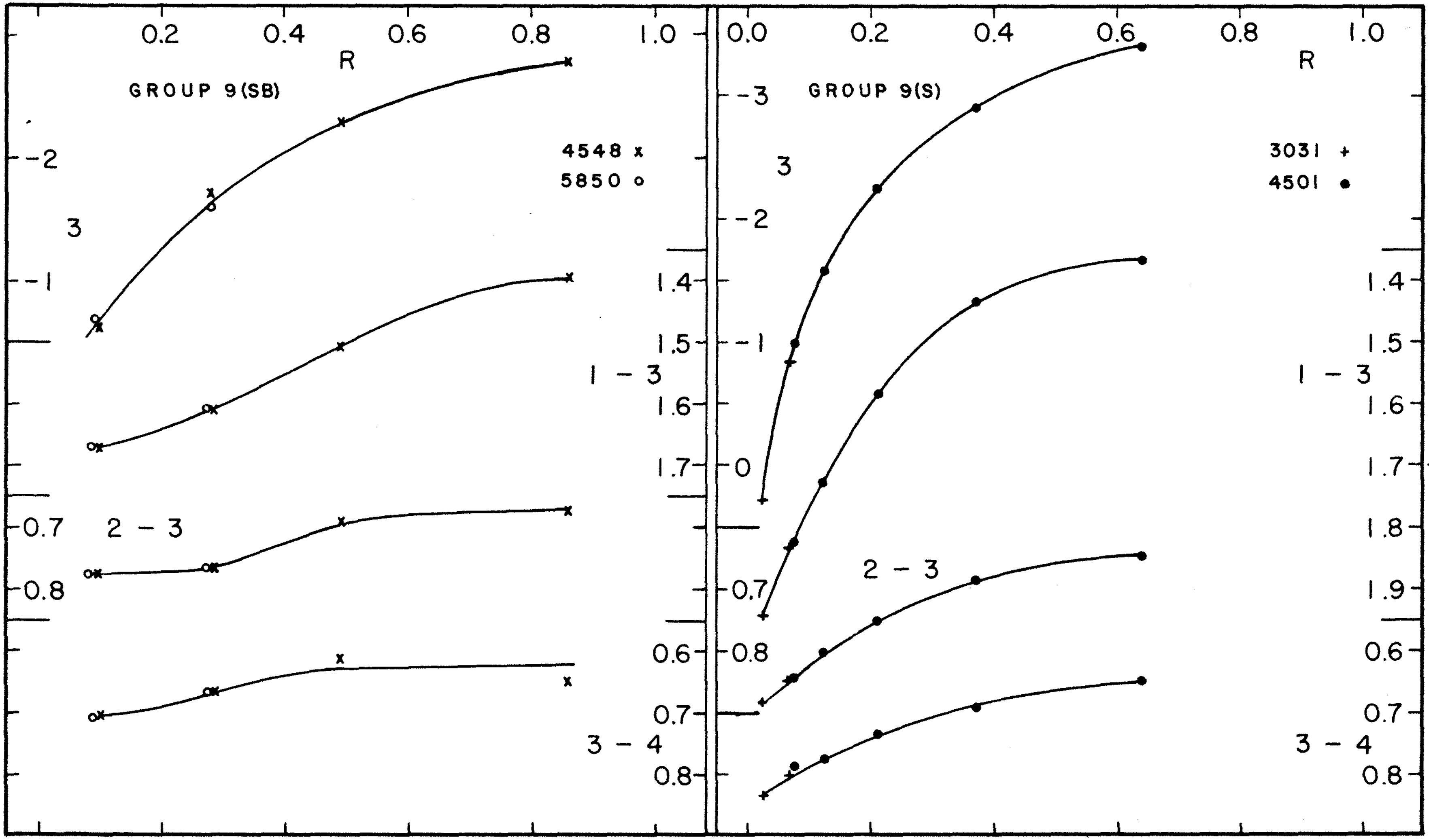

Figure 14

Color and band 3 magnitude as a function of relative radius for Group 9SB and 9S galaxies

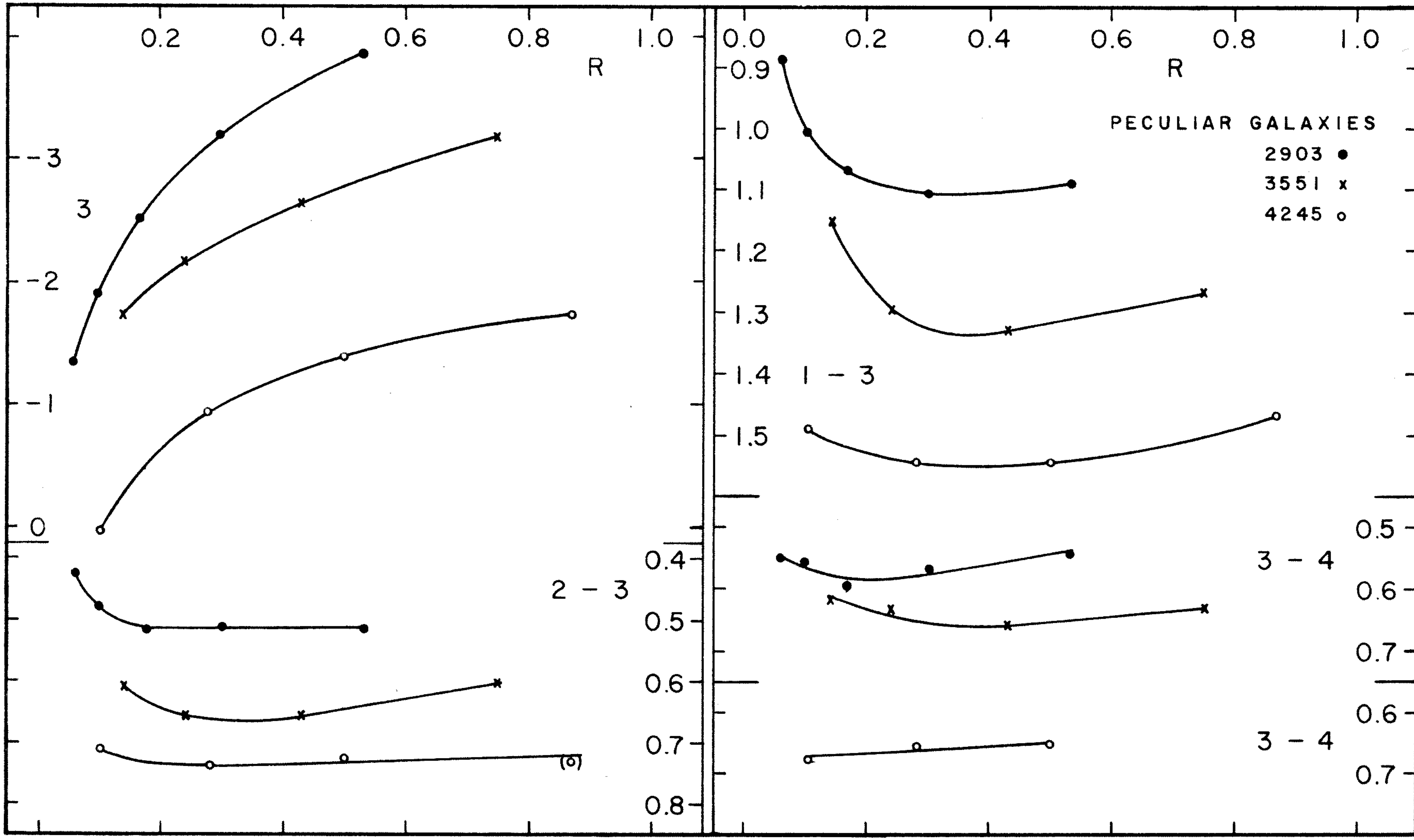

FIGURE 15

COLOR AND BAND 3 MAGNITUDE AS A FUNCTION OF RELATIVE RADIUS R FOR THREE GALAXIES SHOWING BLUEING TOWARD THE CENTER

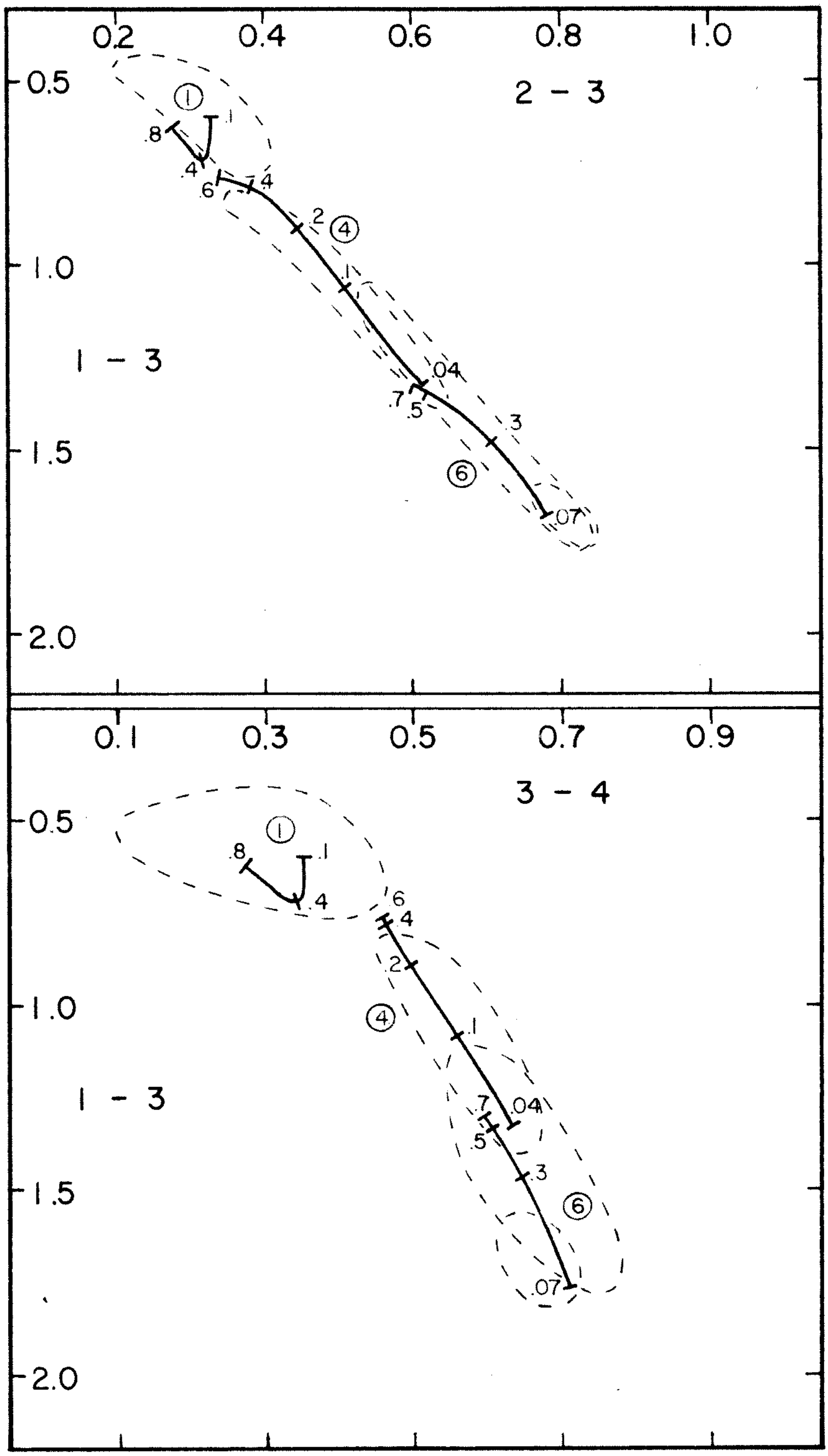

FIGURE 16

COLOR-COLOR RELATIONSHIPS FOR CONCENTRIC RINGS ABOUT THE NUCLEI OF GROUP 1, 4, AND 6 GALAXIES. VALUES OF RELATIVE RADIUS ARE GIVEN ALONG EACH CURVE. THE DASHED ZONES ENCLOSE THE INTEGRATED COLOR MEASUREMENTS FOR GALAXIES OF DIFFERENT STRUCTURAL TYPE.

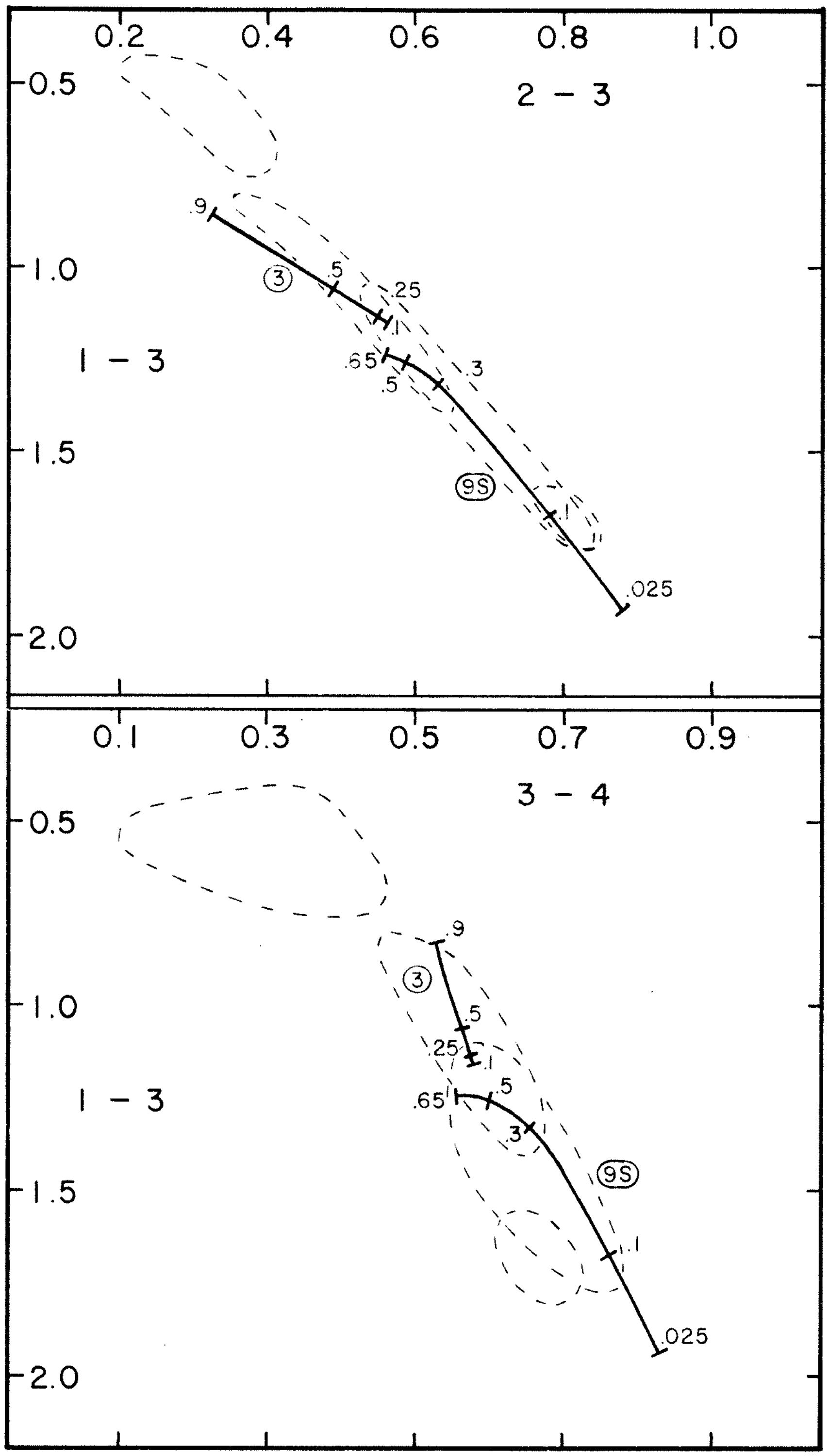

Figure 17

Same as Figure 16, illustrating Groups 3 and 9S

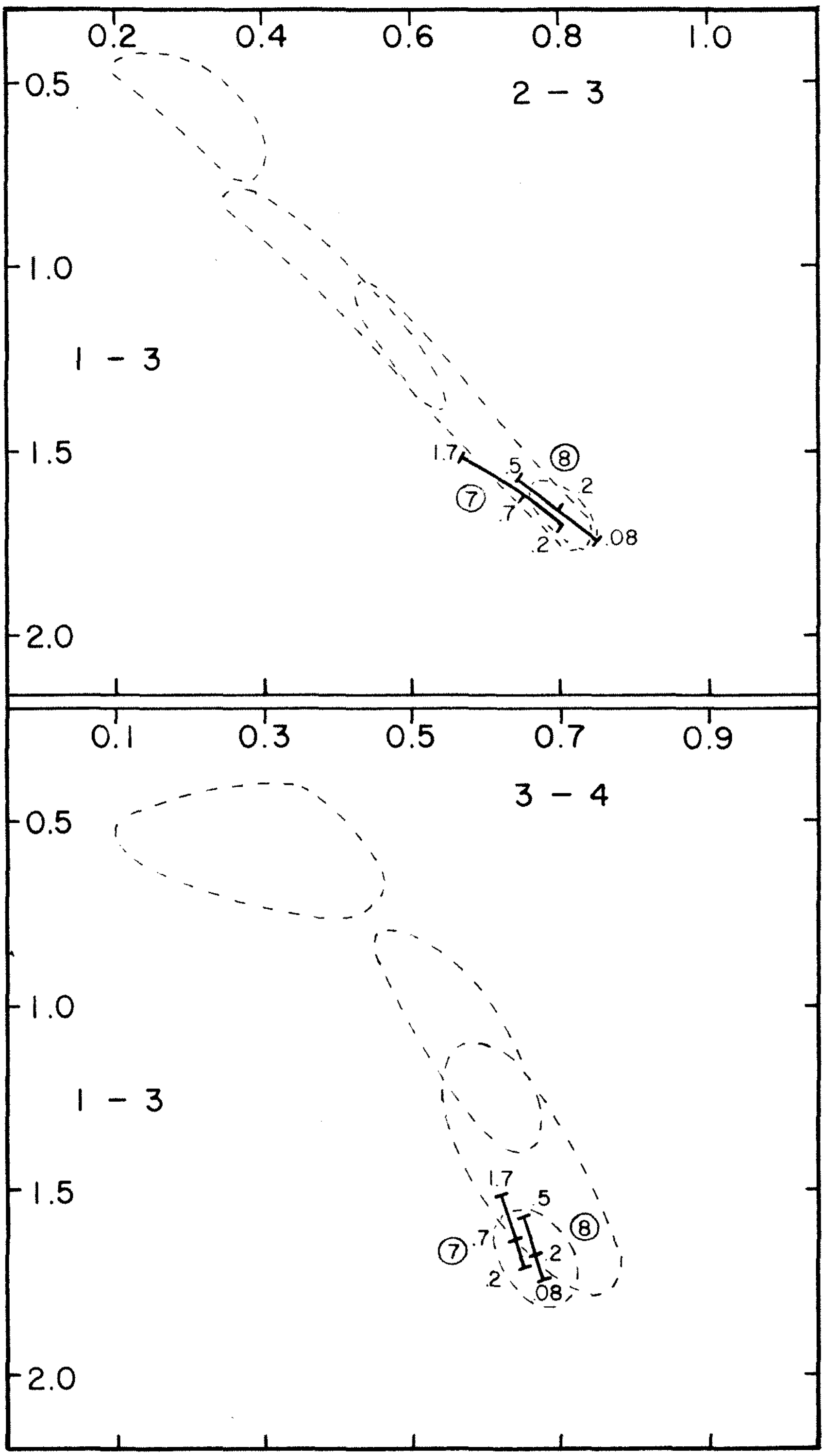

FIGURE 18

SAME AS FIGURE 16, ILLUSTRATING GROUPS 7 AND 8

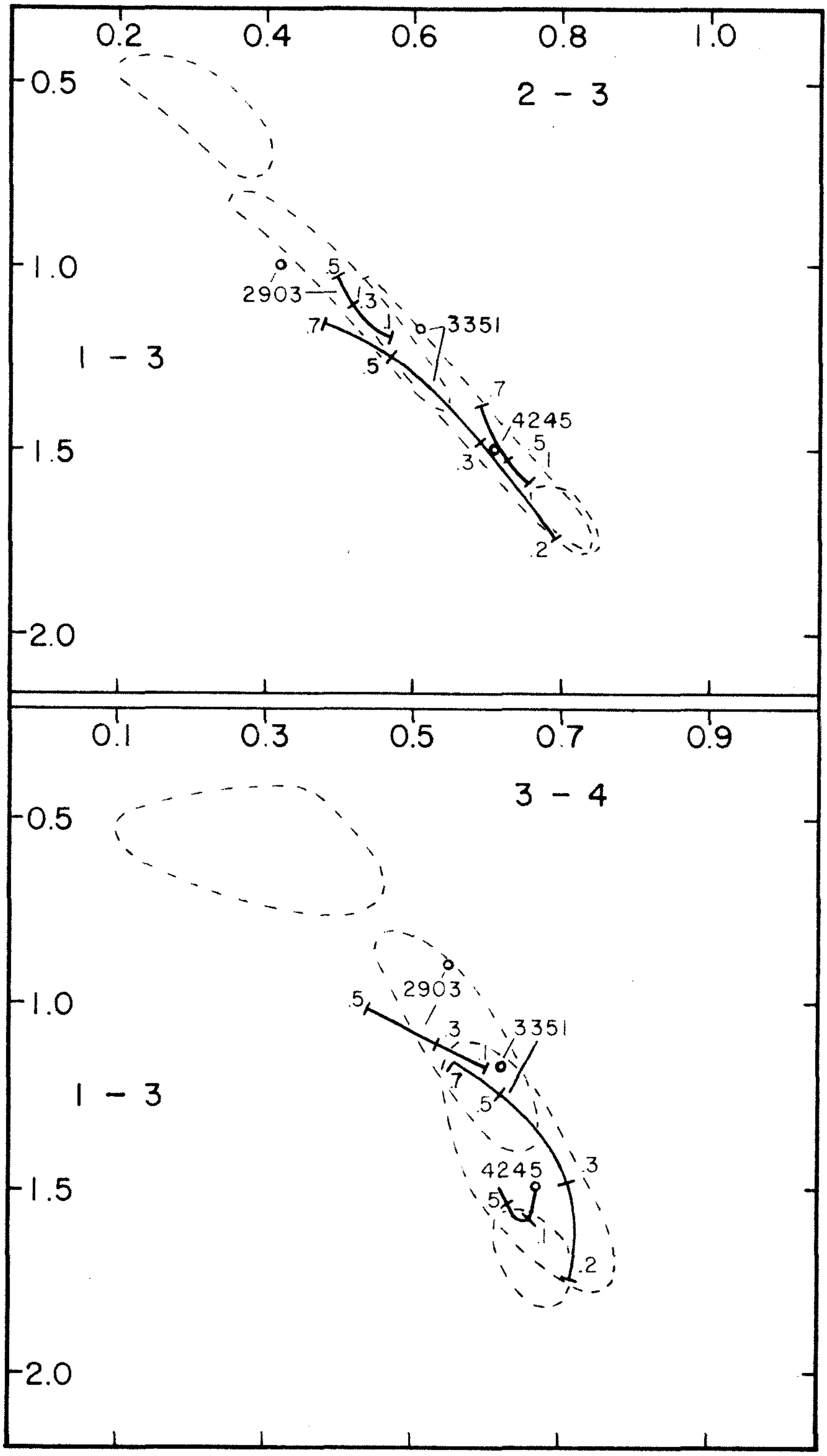

Figure 19

Same as Figure 16, illustrating three galaxies with peculiar blue nuclei. Open circles denote the smallest aperture measurement on each system.

Group 1: Radial integrated color variations for these systems are small with the existence of a very red nucleus definitely not indicated. There is some evidence that the nuclear region brightens in the ultraviolet. All the Group 1 systems are relatively faint, consequently the results for this group are not highly accurate. It is apparent from Figure 16 that the Group 1 systems populate only the "blue Sc" region. Such irregular galaxies as NGC 4449 also lie in the area. The extreme blueness of these galaxies demonstrates that they must be relatively weakly populated with red and yellow giants in comparison with the blue early-type main sequence, giant, and supergiant stars. Further evidence for domination by young blue stars is given by Morgan and Mayall (1) from analysis of spectra.

Group 2: The one galaxy in this group, NGC 2903, shows a strong blueing toward the nucleus. Discussion of NGC 2903 is postponed to later in conjunction with two other blue-centered systems.

Group 3: Three of the five systems in Group 3 are suitable for radial color studies. One other system, called 3p in Table 19, shows a blue center and is lumped with NGC 2903 for discussion later. The three systems investigated agree closely that radial color variations are relatively gradual with the center reddest. The color curves tend to flatten toward the center suggesting a fairly large homogeneous central region. Concentric ring color variations shown in Figure 17 demonstrate several interesting points. One of the most interesting effects is the tendency for ring colors to lie in the same regions occupied by the integrated colors. The color of any given ring thus resembles the color of the entire galaxy inside some slightly larger ring. This effect appears in all the groups showing significant radial color variations. We can explain this observation if we consider spiral galaxies to consist of one group of reddish, presumably old, stars concentrated in the nucleus and decreasing in density outwards, plus a group of bluer stars, presumably younger, which avoid the nucleus and increase in density outwards. The integrated color within some radius will then be representative of certain relative proportions of the two populations; at some particular radius the local population ratio will have the same

VALUE SO THE LOCAL COLOR WILL RESEMBLE THE INTEGRATED COLOR. THE PRESENCE OF MORE THAN TWO DISTINCTLY DIFFERENT POPULATIONS IN APPRECIABLE NUMBERS WILL RESULT IN ISOLATED RINGS RESEMBLING THE INTEGRATED COLORS ONLY IN CERTAIN SPECIAL CASES. THUS WE CAN INTERPRET THE OBSERVATIONS AS FAVORING ONLY TWO DOMINANT POPULATIONS.

A SECOND OBSERVATION WE CAN MAKE FROM FIGURE 17 IS THAT THE BLUEST RINGS ARE STILL NOT AS BLUE AS GROUP 1 SYSTEMS AT ANY RADIUS. HOWEVER, THE RING COLORS SUGGEST THAT GROUP 3 SYSTEMS BECOME BLUER IN THE OUTER REGIONS INCREASINGLY RAPIDLY AND MIGHT HAVE COLORS AS BLUE AS GROUP 1 SYSTEMS OUTSIDE THE REGIONS STUDIED. FOR GROUP 4, 6, AND 9 GALAXIES THE OUTER PORTIONS APPEAR TO LEVEL OFF IN COLOR. TO ASCRIBE TOO MUCH SIGNIFICANCE TO THIS DIFFERENCE ON THE BASIS OF THE PRESENT DATA WOULD BE QUITE DANGEROUS SINCE THE OUTER RING COLORS ARE NOT WELL DETERMINED. THE REGIONS DO NOT CONTRIBUTE MUCH OF THE TOTAL LIGHT OBSERVED, SO SLIGHT ERRORS IN THE COLORS MEASURED WITH LARGE DIAPHRAGMS ARE CONSIDERABLY MAGNIFIED IN REMOVING THE CENTRAL REGIONS TO COMPUTE RING COLORS.

GROUP 4: OF THE THREE GROUP 4 SYSTEMS, NGC 6503 IS TOO STEEPLY INCLINED TO BE SAFELY COMPARED WITH THE OTHER TWO GALAXIES. THE TWO GALAXIES SUITABLE FOR RADIAL INVESTIGATIONS ARE SHARPLY SET APART FROM GROUP 3 SYSTEMS BY STEEP COLOR GRADIENTS NEAR THE NUCLEUS AND A RAPID LEVELING OFF OF COLOR IN THE OUTER REGIONS. THE COLOR AT SMALL RADII APPEARS TO BE APPROACHING A VALUE MARKEDLY REDDER THAN THE MEAN "SMALL DIAPHRĀGM" COLOR, GIVEN IN SECTION 4.4, WHICH REFERS TO A RELATIVE RADIUS OF ABOUT 0.075. IT SEEMS POSSIBLE THAT THE VERY CENTER OF THE GROUP 4 SYSTEMS COULD BE AS RED AS THE ELLIPTICAL GALAXIES. THE VERY STEEP COLOR GRADIENT IN THE CENTER SUGGESTS THAT THE STELLAR COMPOSITION VARIES RAPIDLY WITH RADIUS COMPARED WITH THE GROUP 3 GALAXIES. THIS RAISES A NUMBER OF QUESTIONS SUCH AS JUST WHAT REGION A SPECTROGRAM REFERS TO, CONSEQUENTLY WHAT COLOR MEASURE SHOULD BE COMPARED WITH A SPECTRAL CLASS. IF, FOR EXAMPLE, A SPECTROGRAM OF A GROUP 4 GALAXY WERE DOMINATED BY LIGHT FROM BETWEEN RADII .1 AND .2 THE SPECTRAL TYPE COULD BE EARLIER THAN THAT OF A GROUP 3 GALAXY, EVEN THOUGH THE GROUP 4 GALAXY HAS A

REALLY REDDER NUCLEUS. THIS CERTAINLY MAKES IT DANGEROUS TO OVERINTERPRET THE EFFECTS FOUND IN SECTION 4.6 WHERE NUCLEAR COLOR WAS COMPARED WITH SPECTRAL CLASS. CLEARLY ONE NEEDS TO OBTAIN SPECTROGRAMS OF SPECIFICALLY RESTRICTED REGIONS WHEN DEALING WITH GALAXIES WITH RAPID RADIAL COLOR CHANGES.

AS WITH GROUP 3 THE OUTERMOST RINGS DO NOT GET AS BLUE AS GROUP 1 GALAXIES. THE GROUP 4 GALAXIES APPEAR TO LEVEL OFF IN REGARD TO RING COLOR OUTSIDE OF RELATIVE RADIUS AS SMALL AS 0.2. THIS IS CERTAINLY IN MARKED CONTRAST WITH GROUP 3 WHICH SHOWS VIRTUALLY NO COLOR CHANGE WITHIN SUCH A SMALL RELATIVE RADIUS.

NGC 6503, ALTHOUGH TOO INCLINED FOR DIRECT COMPARISON WITH MORE NEARLY FACE-ON SYSTEMS, HAS QUITE A STEEP COLOR GRADIENT DEFINITELY IN AGREEMENT WITH ITS GROUP 4 MEMBERSHIP. THE COLOR CURVE TENDS TO BE SLIGHTLY FLATTER, ABOUT THE SAME NUCLEAR COLOR BUT A REDDER LARGE DIAPHRAGM COLOR. THIS IS IN ACCORD WITH INCLINATION EFFECTS FOUND HERE FOR NUCLEAR COLORS, AND BY HOLMBERG (10) FOR INTEGRATED COLORS.

GROUP 5: THE ONLY MEMBER OF THIS GROUP SUITABLE FOR RADIAL COLOR STUDIES, NGC 4245, SHOWS A BLUE NUCLEUS AND IN COMBINATION WITH NGC 2903 AND NGC 3351 IS DISCUSSED LATER.

GROUP 6: FOUR GROUP 6 GALAXIES WERE CONSIDERED SUITABLE FOR RADIAL COLOR STUDIES. THE REMAINING SYSTEMS ARE TOO INCLINED ALTHOUGH THEY PROVIDE NO CONTRADICTION TO RESULTS FOUND FOR MORE NEARLY FACE-ON SYSTEMS. THEY TEND TO HAVE THE SAME NUCLEAR COLORS BUT MARKEDLY REDDER LARGE DIAPHRAGM COLORS THAN THE FACE-ON SYSTEMS, IN AGREEMENT WITH INCLINATION EFFECTS IN SECTION 4.6 AND ACCORDING TO HOLMBERG (10). THE MOST NEARLY FACE-ON GROUP 6 GALAXIES SHOW RADIAL COLOR GRADIENTS INTERMEDIATE BETWEEN GROUPS 3 AND 4. THERE IS POSSIBLY A SLIGHT TENDENCY FOR COLOR TO LEVEL OFF NEAR THE NUCLEUS. CONCENTRIC RING COLORS APPEAR TO LEVEL OFF IN THE OUTER PORTIONS AT ABOUT THE NUCLEAR COLORS OF GROUP 4 GALAXIES, AND SIGNIFICANTLY REDDER THAN GROUP 3 NUCLEI. THIS LEVELING OFF OF COLORS DOES NOT MEAN THAT SOME VERY BLUE PATCHES DO NOT EXIST, IT SIMPLY MEANS THAT A GREAT DEAL OF THE LIGHT IN THE OUTER PART OF MOST SPIRALS COMES FROM RELATIVELY RED STARS AND OUTWEIGHS THE BLUE REGIONS. IN EDGE-ON GALAXIES, INDIVIDUAL SETTINGS DEMONSTRATE THAT LOCALLY VERY BLUE PATCHES EXIST.

Consider for example the offset measures of the edge-on Sb spiral NGC 5907, a member of Group 6. The bluest offset 1-3 measure, out near one tip, is about 0.4 magnitude bluer than the leveling-off outer ring color in a face-on system. It is interesting to note that this bluest locally measured color for the edge-on system resembles closely the color of outer regions in face-on Group 3 and 4 galaxies. This supports the concept that all the observed colors can be produced by mixing, in varying proportions, two stellar populations, one dominated by young blue stars and the other by older yellow and red giants.

Group 7: Four elliptical nebulae demonstrate slight but very convincing radial color variations. The outermost regions measured appear to be one to two tenths of a magnitude bluer than the nuclei.

Group 8: Three S0 systems appear to resemble quite closely the ellipticals in radial color changes. The S0 galaxies appear to be slightly redder overall than the ellipticals but are apparently bluer than the central portions of Sb nuclei.

Group 9: Analysis of Group 9 systems immediately demonstrated that barred spirals were distinctly different from normal spirals. The barred spirals appear to be virtually identical in radial color change to the Group 6 systems. Since these galaxies are nearly face-on, inclination effects were no assistance in assigning group membership, consequently they were assigned to Group 9 from the structural classification alone. Since they are face-on systems, transfer to Group 6 has virtually no effect on inclination color effects found for either Group 6 or 9 or on mean nuclear colors given in Section 4.4. With removal of the two barred spirals, Group 9 is left rather poorly populated. NGC 4501 indicates a very steep color gradient much as was found in Group 4. Measures in M81 and the central portion of M31 confirm the steep color gradient near the nucleus. NGC 4501 is by no means face-on, and in view of the marked inclination effects in Group 9 the nuclear color is probably too red and the whole curve may be slightly distorted, probably flattened, from what we would observe face-on. The outer portions of NGC 4501 appear to level off in color at about the same value found for Group 6, about 1.2 to 1.3 in 1-3. Tentatively normal Group 9 spirals can

BE PRESUMED TO SHOW MARKED RADIAL COLOR VARIATIONS, BUT WITHOUT FURTHER OBSERVATION OF FACE-ON SYSTEMS THIS IS NOT CONCLUSIVE. MORGAN AND MAYALL (1) NOTE THAT THE SPECTRUM OF THE M31 NUCLEUS CLOSELY RESEMBLES THE SPECTRUM OF THE OUTER REGIONS. THIS IS NOT CONSISTENT WITH TOO GREAT A RADIAL COLOR CHANGE, ALTHOUGH COLOR IS PROBABLY MORE SENSITIVE TO SMALL CHANGES IN STELLAR MEMBERSHIP, SAY A FRACTION OF A SPECTRAL SUBCLASS, THAN ARE THE HIGHLY COMPOSITE SPECTRA.

BLUE CENTERED GALAXIES: FIGURES 15 AND 19 ILLUSTRATE THE RADIAL COLOR BEHAVIOR OF THREE GALAXIES, EACH QUITE DIFFERENT STRUCTURALLY FROM THE OTHERS BUT ALL SHOWING A COMMON TENDENCY, AT LEAST IN 1-3 AND 2-3, TO BECOME BLUER TOWARD THE NUCLEUS. THE BLUEST GALAXY, NGC 2903, WAS ORIGINALLY PLACED IN A UNIQUE GROUP, 2, PURELY ON THE BASIS OF THE SMALLEST DIAPHRAGM COLOR WHICH PLACED IT INTERMEDIATE BETWEEN GROUPS 1 AND 3 OR 4. THE STRIKINGLY PECULIAR INTEGRATED COLOR CURVES IN FIGURE 15 ARE, IT TURNS OUT, QUITE DECEPTIVE SINCE COMPUTATION OF THE COLORS OF CONCENTRIC RINGS DEMONSTRATES THAT ALL THE BLUEING EFFECT IS CONTAINED WITHIN THE SMALLEST DIAPHRAGM MEASUREMENT. THE SMALLEST RING COLOR, AND THE RADIAL RUN OF CONCENTRIC RING COLORS RESEMBLE THOSE OF GROUP 3 SYSTEMS REMARKABLY WELL.

IN THE SAME MANNER, CONCENTRIC RING COLORS FOR NGC 3351 DEMONSTRATE THAT ALL CENTRAL BLUEING ARISES WITHIN THE SMALLEST DIAPHRAGM. THE SMALLEST RING COLOR AND RAPID RADIAL COLOR VARIATIONS CLOSELY RESEMBLE THOSE OF NGC 4501 IN THE SB GROUP 9. NGC 4245 PRESENTS A SIMILAR PICTURE LOOKING VERY MUCH LIKE A GROUP 6 SYSTEM AFTER REMOVAL OF THE BLUE NUCLEUS.

THE EXISTENCE OF THREE PECULIAR GALAXIES, QUITE DIFFERENT IN COLOR, AND MARKEDLY DIFFERENT IN STRUCTURAL TYPE, YET ALL HAVING THE SAME NUCLEAR PECULIARITY, POSES AN INTERESTING PICTURE. IT SEEMS QUITE REMARKABLE THAT WITH SUCH PECULIAR NUCLEI THE GALAXIES ARE, IN THEIR OUTER PORTIONS, ESSENTIALLY INDISTINGUISHABLE IN COLOR BEHAVIOR FROM GROUPS OF ORDINARY GALAXIES ALREADY DISCUSSED. TENTATIVELY IT SEEMS REASONABLE TO ASSIGN THE GALAXIES TO THE GROUPS INDICATED BY THE RING COLORS, AND CONSIDER THE "BLUE NUCLEUS" PROPERTY A PECULIARITY WHICH MAY AFFECT ANY GROUP, AT LEAST AMONG THE SPIRALS.

4.8 Summary, and Selection Effects

Tentatively the observed galaxies have been distributed into seven more or less distinct groups. Table 20 summarizes the principal characteristics of the groups.

TABLE 20

Principal Characteristics of the Extragalactic Subgroups

Group	Sp	Type	Nucl. Color Inclin. Eff.	Radial Color Gradiant
1	A	Sc	small?	small
3	FG	Sc	small?	small
4	F	Sc	small?	steep
6	K	Sa, SBb?	zero or slight blueing	intermediate
7	K	E	slight reddening	small
8	K	S0	?	small
9	K	Sb	marked reddening	steep?

Face-on Color*

Group	1 - 3	2 - 3	3 - 4	1 - 3	2 - 3	3 - 4
	Nucleus			Outer Regions		
1	.65	.35	.35	.65	.30	.30
3	1.15	.55	.60	.85	.30	.55
4	1.25+	.60+	.65	.80	.35	.45
6	1.65	.80	.70	1.35	.60	.60
7	1.70	.80	.70	1.55	.70	.65
8	1.75	.85	.70	1.60	.75	.65
9	1.65+	.75+	.70+	1.2-?	.6-?	.6-?

* To about nearest 0.05 magnitude

The plus sign on Group 4 and 9 colors means that because of steep radial color gradients the true "stellar" nuclei are much redder than the values given. The tabulated values refer to a relative radius of about 0.075 of the radius of massive spiral structure.

Having presented evidence favoring distinct groups we now should inquire about the reality of the divisions. A selection effect, which might produce artificial groups is present in the Sc galaxies observed. With two exceptions all the Sc spirals observed were systems with Morgan-Mayall classifications. It is not surprising, of course, that spectral type is a group characteristic, but one wonders what would be found if

A SELECTION OF Sc SYSTEMS WERE OBSERVED THAT HAD NOT ALREADY BEEN GUARANTEED MORE OR LESS HOMOGENEOUS. IT IS INTERESTING TO NOTE, HOWEVER, THAT THE TWO AF GALAXIES OBSERVED DO NOT FORM A GROUP, ONE GOING INTO THE A GROUP AND THE OTHER INTO THE FG GROUP WITH A PECULIAR BLUE CENTER. ALSO ONE FG GALAXY DOES NOT FALL IN THE NORMAL FG GROUP. THUS IT IS APPARENT THAT ALTHOUGH SPECTRAL CLASS IS IMPORTANT IN GROUP ASSIGNMENT IT IS CERTAINLY ONLY ONE OF SEVERAL FACTORS. GROUPS 1, 3, AND 4 SEEM QUITE DISTINCT IN THE PRESENT OBSERVATIONS BUT FURTHER INFORMATION MIGHT EASILY DEMONSTRATE THE EXISTENCE OF GALAXIES THE SAME COLOR AS IN GROUPS 3 AND 4 BUT WITH INTERMEDIATE RADIAL COLOR GRADIENTS. NO OBVIOUS SELECTION EFFECTS ARE PRESENT IN THE K GALAXIES SINCE ALL STRUCTURAL TYPES ARE REPRESENTED AND MANY SYSTEMS WITHOUT SPECTRAL CLASSIFICATION WERE INCLUDED. IN MY OPINION THE PRESENT INVESTIGATION STRONGLY SUGGESTS THE EXISTENCE OF SOME DISTINCT SUBCLASSES AMONG EXTRAGALACTIC NEBULAE, BUT BY NO MEANS DOES IT PROVE THEIR EXISTENCE.

V SYNTHETIC GALAXIES

5.1 Energy Curves

Consider now the problem of inferring the stellar content of a galaxy given its energy distribution and the energy distributions of individual stars. Five cases have been selected to represent the range of colors found. Section 5.2 is devoted to discussion of an average K nucleus, while subsequent sections are concerned with progressively earlier spectral class nuclei. Table 21 gives the color indices used to define the five types of nuclei investigated; all colors are reffered to band 3. The upper part of Figure 20 illustrates the energy curves. For bands 1 to 4 colors have been taken from Table 18 excepting that K is an average of Groups 6, 7, and 9. To derive the color indices between 3 and the red or infrared 5-6, 6-7, 6-8, and to a first approximation 3-6, were taken directly from red observations in Table 14. A graph of $1/\lambda$ against magnitude, referred to zero at 3, was prepared for each type of nucleus; smooth curves were drawn separately through the four red and four blue points. These curves usually did not intersect, indicating a discontinuity between bands 4 and 5 due to relatively large errors in 3-6 values used. Since bands 4 and 5 lie close together in $1/\lambda$ the amount of the discontinuity could be read quite accurately, permitting an improved determination of 3-6. Using 3-6 values determined in this manner the red colors in Table 21 were derived from the observed 5-6, 6-7 and 6-8 values.

Table 22 contains stellar colors used in synthesis computations. Except for the M2Ia star the color indices were obtained in the following manner. 1-3, 2-3, 3-4, 5-6, 6-7, and 6-8 for all stars observed were plotted against spectral class and mean lines were drawn to represent the observations. Separate lines were drawn for different luminosity classes when there was a clear distinction. Using these curves, colors were read off for representative stellar types. Preliminary 3-6 values were improved by continuity between bands 4 and 5 as was done for extragalactic colors, to permit tying all the colors directly to band 3. The M2Ia star, α Orionis, in Table 22 was not observed directly by the author. Colors for this star were derived by reading relative magnitudes from a flux scan made available by Dr. Code. Colors so derived were corrected, by use of Table 9, for calibration differences between Code's system and that of this thesis. The 3-6 color of α Orionis was adjusted slightly by continuity considerations after transformation from Code's system. The lower portion of Figure 20 illustrates the stellar energy curves used in synthesis studies.

Table 22 lists the integrated color indices of the galactic cluster M67 and an average globular cluster in addition to stellar colors. The M67 values were derived by summing up the luminosities of member stars using the luminosity function given by Sandage (15) and the color-magnitude diagram given by Johnson and Sandage (16). The globular cluster colors were derived by reading the magnitude differences between Stebbins and Whitford six color measurements for M32 and an average globular cluster, as tabulated by Roberts (17), at the effective wave lengths of the system used for this thesis. These magnitude differences were applied directly to M32 observations in bands 1 to 4 to yield colors on the thesis system. In the red, where no M32 measures were obtained, M32 was assumed to fit smoothly onto the average K nucleus colors. This is a very good approximation since the deviation of M32 from the mean K colors between bands 1 and 4 is significant only for 1-3.

All synthesis computations have been carried out by means of least-squares solutions. If L_G denotes the luminosity of a galaxy and L_i denotes the luminosity of the i'th type of star,

$$L_G = \sum_i A_i L_i \quad . \tag{31}$$

One such equation applies to each observed band. We may write this equation in terms of luminosity ratios, hence color indices, by writing

$$\frac{L_G}{L_{3G}} = \sum_i \left(\frac{A_i L_{3i}}{L_{3G}}\right)\frac{L_i}{L_{3i}} \quad . \tag{32}$$

If all luminosities, including L_{3G}, were known exactly, A_i would simply be the number of type i stars in the galaxy. Since L_{3G} is not known, we simply incorporate it into A_i and interpret the A_i values as relative numbers of stars. Thus we write the equation of condition for least-squares analysis

$$\frac{L_G}{L_{3G}} = \sum_i \alpha_i \left(\frac{L_i}{L_{3i}}\right) \quad . \tag{33}$$

It will be noted that this formulation requires no knowledge of relative

STELLAR LUMINOSITIES PRIOR TO THE DERIVATION OF α VALUES. CONVERSION OF α VALUES TO RELATIVE NUMBERS OF DIFFERENT TYPES OF STARS DOES OF COURSE INVOLVE KNOWLEDGE OF RELATIVE LUMINOSITIES.

TABLE 21

EXTRAGALACTIC COLORS USED FOR SYNTHESIS

TYPE	3 - 1	3 - 2	3 - 4	3 - 5	3 - 6	3 - 7	3 - 8
K	-1.66	-0.78	0.68	0.87	1.27	1.37	1.47
FG	-1.12	-0.55	0.58	0.75	1.08	1.18	1.27
F	-1.23	-0.58	0.62	0.79	1.11	1.21	1.27
AF	-0.88	-0.42	0.55	0.69	1.08	1.18	1.28
A	-0.64	-0.33	0.34	0.45	0.68	0.84	0.98

TABLE 22

STELLAR COLORS USED FOR SYNTHESIS

TYPE	3 - 1	3 - 2	3 - 4	3 - 5	3 - 6	3 - 7	3 - 8
O9V	0.25	0.16	-0.20	-0.28	-0.59	-0.83	-1.18
A9III	-0.89	-0.25	0.13	0.13	0.01	-0.13	-0.31
G2III	-1.26	-0.57	0.44	0.51	0.56	0.49	0.38
GLOB.CL.	-1.24	-0.54	0.42	0.51	0.66	0.63	0.54
M67	-1.78	-0.82	0.70	0.87	1.13	1.12	1.08
M2III	-3.25	-1.34	1.16	1.49	2.36	2.47	2.56
M2IA	-3.61	-1.94	1.36	1.77	2.67	2.80	2.98

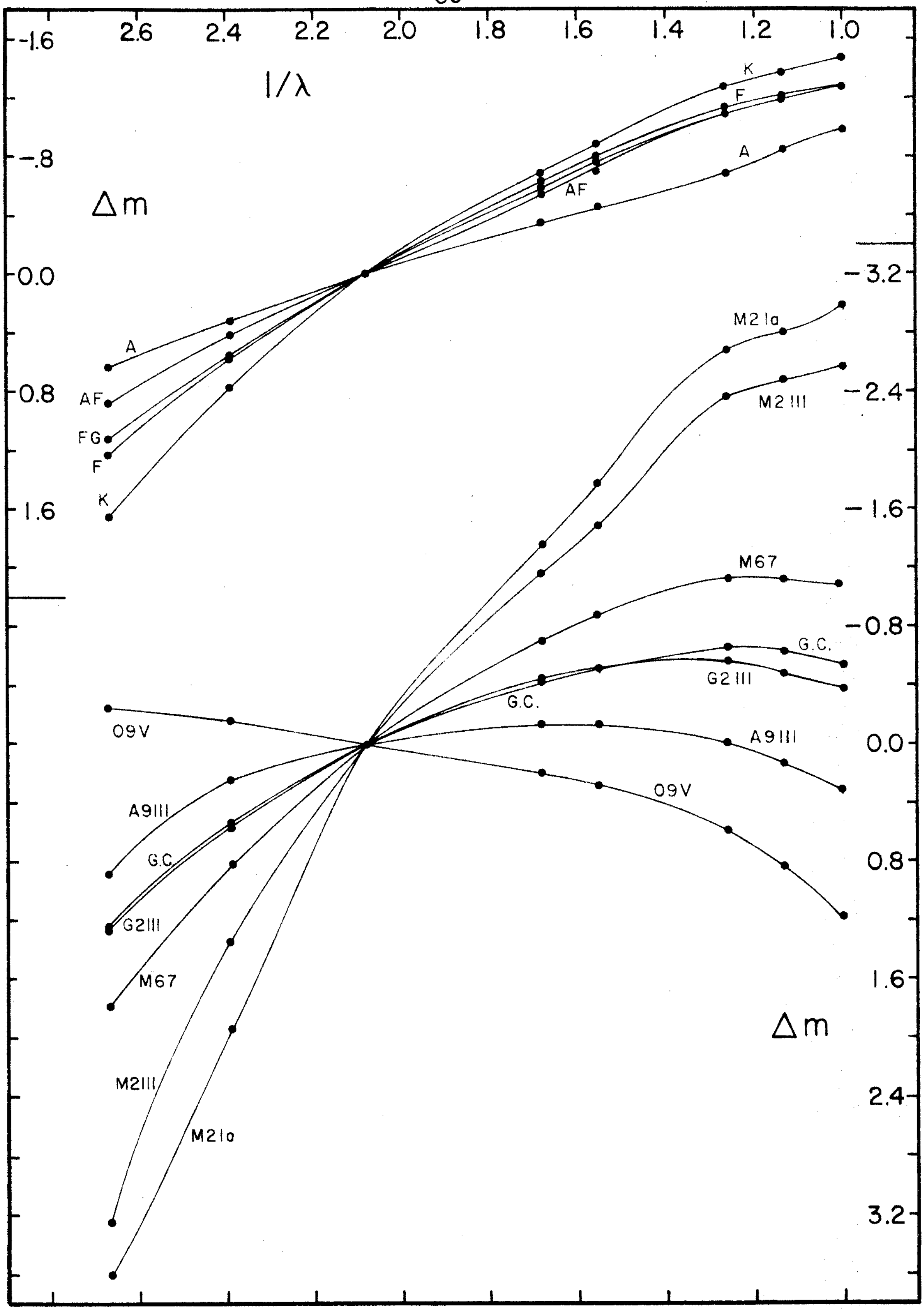

FIGURE 20

ENERGY CURVES OF GALAXIES (TOP) AND STARS (BOTTOM) USED IN SYNTHESIS

5.2 K Nuclei

K nuclei, representative of ellipticals and the Sa and Sb spirals, are very common stellar aggregates in space. Spectroscopic observations and spectral types inferred from colors generally agree that no apprecia-ble number of stars earlier than late F or early G contribute to the observed light. This immediately suggests an old stellar population from which the stars more massive than type F have been removed by evolu-tion. The two classical examples of such old populations in our galaxy are the globular clusters and the galactic cluster M67. Neither old population II, as found in globular clusters, nor old population I, as found in M67, closely matches the integrated color of a K nucleus. Roberts (17) has shown that the energy curve of the elliptical galaxy M32 can be produced by adding a great many K and M dwarfs to the normal popu-lation of globular clusters. This addition also brings the mass-luminos-ity ratio into order of magnitude agreement with M32 observations. There are, however, a number of serious objections to this model. Globular cluster stars tend to have weaker metallic lines, giving the impression of earlier spectral type, than stars of the same effective temperature with solar metal abundances. In a highly composite galaxy spectrum, if low metal content stars dominated, the spectrum would almost certainly be classified as F or G at the latest. If enough K and M dwarfs were present to make the spectral class as late as K the characteristics of dwarfs should show clearly in the spectra, particularly toward the red. Spectral observations indicate that giant stars dominate the spectrum far out into the red with no significant indication of dwarfs.

One might possibly add enough population II K and M giants to a globular cluster to produce the observed K galaxy energy distribution and spectral type. However, this would require a distribution of stars along the globular cluster giant branch quite at variance with modern evolution concepts. Probably the strongest evidence against the presence of large numbers of globular cluster giants is provided by spectroscopic data. Morgan and Mayall (1) note that the M31 nucleus definitely is not domi-nated by weak line giants of the type found in many globular clusters.

In view of the clear cut arguments against pure population II the more profitable line of domination by population I is followed here. Com-parison of K system colors with M67 reveals that K systems are brighter in both the ultraviolet and infrared. This is to be compared with globular cluster colors which are everywhere bluer than K galaxies. It is obvious that the blue deficiency in M67 cannot be compensated for by adding late-type dwarf stars. The addition of such stars may be important in the far red. To obtain the added blueing at short wave lengths in K systems we have several choices. One obvious solution would be to add some main sequence A and early F stars, implying the presence of an appreciable number of stars younger than the M67 population. This would provide the observed blueing but would disagree with spectroscopic evidence which shows no trace of hydrogen line absorption.

A second alternative would be to add an excess number of G giant stars. The first entry in Table 23 gives the solution of equation 33 for a three point synthesis based upon colors of M67, and G2III and M2III stars. The solution gives a very good fit to the K energy distribution between bands 1 and 6, but the fit deteriorates markedly if bands 7 and 8 are included. It appears that the far red of K galaxies brightens too fast to be matched by M2III colors. If we neglect the last two red points the M and G giant plus M67 fit is certainly good. The weight the solution assigns to the G star source is a little large in view of the fact that Morgan and Mayall find gG8 to gK3 stars dominate K spectra in the neighborhood of band 2. The result is in fairly good agreement, however, with flux scans by Code where G2III stars approximate the ultraviolet region of M32 quite well. M32 appears to be slightly bluer in the ultraviolet than normal K systems considered here, but the difference is small.

One argument that may be leveled against the model of M67 plus excess G giants arises from evolution considerations. Since the giant stage of evolution is relatively brief there must be a source of supply for G giants. Evolution in M67 has progressed to the point where G subgiants plus K and probably M giants are being produced. Production of significant numbers of G giants requires a main sequence break-off point somewhat bluer than in M67, somewhere in the A or early F stars. If this were the case we would have the same argument against the model as applied to the model of M67 plus a young main sequence. We would expect to find some trace of hydrogen lines in the spectra.

One final model which can add relatively blue stars to an M67 population yet avoid addition of A and F stars involves a mixture of population I and II. The second solution of equation 33 given in Table 23 represents such a synthetic fit using the colors of a globular cluster in

PLACE OF THE G2III COMPONENT OF THE OTHER SOLUTION. THE MATCH IS VIRTUALLY IDENTICAL TO THE G2 GIANT MODEL EXCEPTING THAT THE CONTRIBUTION OF M67 LIGHT IS INCREASED SLIGHTLY AT THE EXPENSE OF BOTH OTHER SOURCES. THIS MODEL IS INTERESTING IN A NUMBER OF RESPECTS. MOST IMPORTANT IT PROVIDES A RELATIVELY GOOD FIT TO BOTH SPECTRAL AND COLOR OBSERVATIONS AND REQUIRES NO DEVIATION FROM MODERN EVOLUTION CONCEPTS. THE MODEL IMPLIES THAT ABOUT HALF OF THE OBSERVED ULTRAVIOLET LIGHT ARISES FROM POPULATION II SOURCES; IN THE RED, POPULATION II STARS CONTRIBUTE LESS THAN A QUARTER OF THE LIGHT AND LESS THAN HALF AS MUCH AS THE OLD POPULATION I STARS REPRESENTED BY M67. IT WOULD BE INTERESTING, ALTHOUGH PERHAPS NOT FEASIBLE, TO CARRY OUT A COLOR-MAGNITUDE ANALYSIS FOR THE BRIGHTEST RED AND YELLOW GIANTS IN M31 AND M32 TO SEE IF ONE CAN DETERMINE THE POPULATION RATIO BY DIRECT OBSERVATION.

TABLE 23

K SYNTHESIS SOLUTIONS

	L_1	L_2	L_3	L_4	L_5	L_6	α
M2III	.007	.041	.141	.411	.557	1.242	.14
M67	.092	.225	.477	.906	1.062	1.349	.48
G2III	.118	.223	.376	.564	.603	.630	.38
SOLN.1	.217	.489	.994	1.881	2.222	3.221	
K	.217	.488	1.000	1.871	2.228	3.221	
SOLN1 - K	.000	.001	-.006	.010	-.006	.000	
M2III	.006	.034	.118	.343	.465	1.036	.12
M67	.105	.256	.542	1.030	1.207	1.534	.54
GLOB. CL.	.107	.203	.335	.491	.565	.650	.33
SOLN.2	.218	.493	.995	1.864	2.237	3.220	
K	.217	.488	1.000	1.871	2.228	3.221	
SOLN.2 - K	.001	.005	-.005	-.007	.009	-.001	

ONE PROBLEM IN SYNTHESIS OF K COLORS REMAINING TO BE CONSIDERED CONCERNS THE MATCHING OF FAR RED COLORS. IF BANDS 7 AND 8 ARE INCLUDED IN EITHER OF THE SOLUTIONS DISCUSSED ABOVE, THE WEIGHT OF THE M2III SOURCE INCREASES SHARPLY AND THE GENERAL FIT TO THE K ENERGY DISTRIBUTION BECOMES POOR THROUGHOUT THE RED. IN PARTICULAR THE SOLUTION PREDICTS TOO MUCH LIGHT IN BANDS 4 THROUGH 6 AND IS DEFICIENT IN BAND 8. THE OBVIOUS SOLUTION IS THAT STARS REDDER THAN M2III BECOME IMPORTANT IN THE FAR RED. COLORS FOR THE M2IA STAR α ORIONIS, AVAILABLE BY TRANSFORMATION FROM FLUX SCANS MADE BY DR. CODE, GIVE A SLIGHTLY IMPROVED FIT BUT DO NOT COMPLETELY

REMOVE THE DIFFICULTIES. BECAUSE OF RELATIVELY LARGE UNCERTAINTY IN TYING TOGETHER THE RED AND BLUE OBSERVATIONS IT MAY BE DANGEROUS TO OVERINTERPRET THE RED EXCESS. HOWEVER, RESIDUALS IN TABLE 23 INDICATE A RELATIVELY GOOD FIT IN PASSING FROM BAND 4 TO 5 SUGGESTING FITTING ERRORS ARE NOT LARGE.

IF THE RED EXCESS IS REAL THE LIGHT MIGHT COME FROM A RELATIVELY FEW LATE M GIANTS, A LARGE NUMBER OF LATE-TYPE DWARFS, OR A COMBINATION OF BOTH. THERE IS NO DOUBT THAT M67 IS DEFICIENT IN DWARFS, DUE TO PREFERENTIAL ESCAPE OF LOW MASS STARS, COMPARED TO A GALAXY. HOWEVER, ADDITION OF ENOUGH LATE-TYPE DWARFS TO PRODUCE THE OBSERVED K RED ENERGY CURVE WOULD VERY LIKELY PRODUCE OBSERVABLE EFFECTS AT SHORTER WAVE LENGTHS. THIS WOULD BE CONTRARY TO SPECTROSCOPIC OBSERVATION OF STRICT GIANT DOMINATION. IT FOLLOWS THAT DWARF STARS ALONE CANNOT SATISFY BOTH THE COLOR AND SPECTROSCOPIC DATA. NEVERTHELESS THE FAR RED IS THE BEST PLACE TO SEE DWARFS IF THEY CAN BE SEEN AT ALL. IT MIGHT BE INTERESTING TO ATTEMPT SOME FAR INFRARED SPECTRA, USING I-Z PLATES, TO COMPARE THE NUCLEI OF M31 AND M32 WITH SOME LATE M GIANTS.

TO SUMMARIZE, K NUCLEI CAN BE REPRESENTED BY A DOMINANT POPULATION I AGGREGATE PLUS AN EXCESS NUMBER OF G STARS. A MORE SATISFACTORY SOLUTION COMBINES AN M67 POPULATION WITH A WEAKER POPULATION II ASSEMBLY. IN THE FAR RED SOME ADDITIONAL RED GIANTS ARE REQUIRED. A SIZEABLE LATE DWARF POPULATION MIGHT CONTRIBUTE SOME LIGHT IN THE FAR RED. THROUGHOUT THE SPECTRUM, WITH THE POSSIBLE EXCEPTION OF THE FAR RED, GIANT STARS ARE DOMINANT. THE MODEL MIXING POPULATION I AND II STARS REQUIRES NO STARS YOUNGER THAN FOUND IN M67 AND GLOBULAR CLUSTERS.

5.3 F AND FG NUCLEI

IN THIS SECTION WE CONSIDER F AND FG SYSTEMS TOGETHER SINCE THEY DO NOT DIFFER MUCH IN COLOR. A SUGGESTION ABOUT WHAT STELLAR COMPOSITION TO EXPECT IS AFFORDED BY THE OBSERVATION, MENTIONED IN SECTION 4.7, THAT F AND FG NUCLEI RESEMBLE IN COLOR THE OUTER PARTS OF K SPIRALS. THIS MEANS THAT IF OUR GALAXY IS ASSUMED TO BE A K SYSTEM THERE MAY BE A STELLAR POPULATION SIMILAR TO THAT IN F AND FG NUCLEI NEAR THE SUM. SOLAR NEIGHBORHOOD STUDIES SHOW A FAIRLY STRONG OLD POPULATION I COMPONENT PLUS A WEAKER POPULATION II COMPONENT REPRESENTED BY THE SUBDWARFS. IN ADDITION THERE ARE SOME YOUNG MAIN SEQUENCE STARS. THUS LOCALLY WE HAVE A STELLAR DISTRIBUTION MUCH LIKE THE SECOND SOLUTION (MIXED POPULATION I AND II)

PROPOSED FOR K NUCLEI, PLUS A YOUNG MAIN SEQUENCE. THUS AS A FIRST MODEL FOR F ANF FG NUCLEI WE CONSIDER THE ADDITION OF SOME YOUNG BLUE STARS TO K COLORS. THE FIRST TWO ENTRIES IN TABLE 24 GIVE THE SOLUTIONS OF EQUATION 33 FOR MODELS ADDING O9 AND A9 STARS TO K NUCLEI. THE TABLE DEMONSTRATES THAT THE FG ENERGY CURVE IS FIT VERY WELL WHILE THE F COLORS ARE MATCHED SLIGHTLY LESS SATISFACTORILY.

IN THE SECTION DEALING WITH THE CORRELATION BETWEEN NUCLEAR COLOR AND SPECTRAL TYPE IT WAS SUGGESTED THAT FG SYSTEMS MIGHT HAVE MORE POPULATION II THAN F GALAXIES IN ORDER TO EXPLAIN THE COLOR-SPECTRAL CLASS INVERSION IN PASSING FROM F TO FG TYPES. THIS IDEA PROVIDES THE BASIS FOR THE LAST TWO SOLUTIONS OF EQUATION 33 GIVEN IN TABLE 24. IF WE ACCEPT THE MODEL THAT K NUCLEI CONSIST OF M67 + GLOBULAR CLUSTER + RED STARS, IN THE PROPORTIONS INDICATED IN TABLE 23, WE CAN SUBTRACT THE POPULATION II GLOBULAR CLUSTER CONTRIBUTION TO OBTAIN A NEW ENERGY DISTRIBUTION

$$L_{K'} = \frac{L_K - 0.334 L_{\text{GLOB. CL.}}}{1 - 0.334} \quad . \qquad (34)$$

THIS ENERGY DISTRIBUTION IN COMBINATION WITH O9 AND A9 COLORS DOES NOT GIVE A GOOD FIT TO EITHER F OR FG GALAXIES; RESIDUALS INDICATE A NEED FOR SOMETHING INTERMEDIATE BETWEEN THE A9 AND K' COLORS. THIS NEED WAS SATISFIED BY CONSTRUCTION OF A POPULATION I K SYSTEM ACCORDING TO THE RELATION

$$L_{K''} = \frac{L_K - 0.334 L_{\text{GLOB.CL.}} + 0.376 L_{\text{G2III}}}{1 - 0.334 + 0.376} \quad . \qquad (35)$$

THUS THE REMOVAL OF GLOBULAR CLUSTER LIGHT HAS BEEN COMPENSATED FOR BY THE ADDITION OF POPULATION I G GIANT STARS.

IT HAS BEEN FOUND IN PRACTICE THAT SYNTHESIS SOLUTIONS USING MORE THAN THREE FAIRLY DISTINCT ENERGY CURVES OFTEN YIELD UNREASONABLE RESULTS, SUCH AS NEGATIVE WEIGHTS. THIS IS PRESUMABLE BECAUSE THE CLOSER FIT ALLOWED BY MORE DEGREES OF FREEDOM MAKES THE SOLUTION TOO SENSITIVE TO SMALL ERRORS IN THE COLOR OBSERVATIONS. WITH AS FEW DEGREES OF FREEDOM AS POSSIBLE THE SOLUTION IS FIXED BY THE GENERAL SHAPES OF THE ENERGY CURVES. IT IS FOR THIS REASON THAT THE G2III COEFFICIENT IN EQUATION 35 HAS BEEN FIXED RATHER THAN LEAVING IT FREE IN THE SOLUTION OF EQUATION 33. THE G2III WEIGHT ASSUMED HAS BEEN TAKEN FROM THE FIRST SYNTHESIS SOLUTION OF K NUCLEI (M67 + G2III + M2III) IN TABLE 23. SLIGHT VARIATION IN THE G2 WEIGHT HAS NO IMPORTANT EFFECT ON THE SOLUTION OF EQUATION 33.

Using K'' plus O9 and A9 stars the last two entries in Table 24 were computed. The results demonstrate that both F and FG colors can be constructed quite well from a pure population I model. Close inspection of the mean residual $|\bar{\Delta}|$ in each solution reveals that the pure population I model fits the F galaxy very slightly better than the mixed population model. The reverse is true for FG systems. The fitting differences are so slight, however, that they could be entirely accidental. About the most that may be said is that the solutions do not contradict the idea that F systems have less population II than FG galaxies.

TABLE 24

F and FG Synthesis Solutions

	L_1	L_2	L_3	L_4	L_5	L_6	L_7	L_8	α
K	.175	.394	.808	1.511	1.799	2.601	2.852	3.128	.81
A9III	.067	.121	.152	.171	.171	.153	.135	.114	.15
O9V	.088	.081	.070	.058	.054	.040	.032	.023	.07
Soln.1	.330	.596	1.030	1.740	2.024	2.794	3.019	3.265	
F	.322	.586	1.000	1.770	2.070	2.780	3.048	3.221	
Soln.1 – F	.008	.010	.030	–.030	–.046	.014	–.029	.044	$\|\bar{\Delta}\|$=.026
K	.173	.390	.799	1.495	1.780	2.574	2.822	3.095	.80
A9III	.043	.078	.098	.111	.111	.099	.087	.074	.10
O9V	.141	.130	.112	.093	.087	.065	.052	.038	.11
Soln.2	.357	.598	1.009	1.699	1.978	2.738	2.961	3.207	
FG	.357	.603	1.000	1.706	1.995	2.704	2.965	3.221	
Soln.2 – FG	.000	–.005	.009	–.007	–.017	.034	–.004	–.014	$\|\bar{\Delta}\|$=.011
K''	.189	.420	.863	1.610	1.901	2.681	2.921	3.194	.86
A9III	.022	.039	.050	.056	.056	.050	.044	.037	.05
O9V	.131	.121	.104	.087	.080	.060	.048	.035	.10
Soln.3	.342	.580	1.017	1.753	2.037	2.791	3.013	3.266	
F	.322	.586	1.000	1.770	2.070	2.780	3.048	3.221	
Soln.3 – F	.020	–.006	.017	–.017	–.033	.011	–.035	.045	$\|\bar{\Delta}\|$=.023
K''	.187	.416	.853	1.592	1.880	2.651	2.888	3.159	.85
A9III	–.001	–.001	–.001	–.001	–.001	–.001	–.001	–.001	–.00
O9V	.183	.168	.145	.121	.112	.084	.068	.049	.15
Soln.4	.369	.583	.997	1.712	1.991	2.734	2.955	3.207	
FG	.357	.603	1.000	1.706	1.995	2.704	2.965	3.221	
Soln.4 – FG	.012	–.020	–.003	.006	–.004	.030	–.010	–.014	$\|\bar{\Delta}\|$=.012

One other item of interest relates to the comparison of the α values assigned to the O9 and A9 stars. If we assume a luminosity ratio of 100 between O9 and A9 (corresponding to the absolute magnitude difference between about −4 and +1 on the main sequence) we can derive the ratio of the number of O9 stars to the number of A9 stars. For the first three solutions the ratios are 0.009, 0.005, and 0.020 respectively. The fourth solution yields a meaningless negative value for α_{A9}; for all practical purposes the α value is zero. If the blue light in F and FG galaxies actually comes from the main sequence, and if the main sequence luminosity function is the same as found in our galaxy (as given for example by Salpeter (18)) we would expect a ratio between the number of O9 or B0 stars and the number of A9 stars of about 0.001. If much of the blue light in F and FG systems comes from A giants and supergiants, and probably an appreciable portion does, the five magnitude luminosity difference assumed between O9 and A9 is too large. If we assume A supergiants and giants dominate the A light contribution then the α values imply roughly equal numbers of O and early B stars and A supergiants and giants. Color studies alone are probably relatively insensitive to differences between A giants and dwarfs in the integrated colors. Some information about the relative importance of giants and dwarfs among the A contributors can probably be derived from a study of the sharpness of the hydrogen lines in F and FG spectra. The amount of filling in of the hydrogen lines should also give independent information on what fraction of the light at a given wave length actually comes from A stars.

There is no doubt that some stars much bluer than A9 are required to give synthetic solutions that fit F and FG galaxies in the ultraviolet after the red has been matched. Thus there must be a significant number of O and B stars present. Near the effective wave length of band 1 the α values demonstrate that the very blue component contributes about half of the light. It is possible that some effects of the very blue stars can be seen in spectrograms in this region, but there is little likelihood that the blue stars would show at all outside of the ultraviolet.

The overall fit of solution 4 in Table 24 to the FG energy curve is certainly less satisfactory than solution 2 in view of the negative α assigned the A star in solution 4. This may be interpreted, along with the slight reduction of the mean residual, $|\bar{\Delta}|$, as slightly favoring the mixed population model for FG galaxies. The α values provide no evidence for a choice between F galaxy models, excepting that the pure population I model arranges the α weights in the same order as the best FG model.

In summary, both pure population I and mixed population models fit

F and FG galaxies when solutions are found by adding young stars to the old populations of K systems. Weak evidence favors, or at least does not contradict, the hypothesis that F galaxies have nearly pure population I while FG galaxies have mixed populations. This hypothesis might explain the color-spectral class inversion between F and FG nuclei. We should repeat here that the inversion may be accidental, arising from different radial color gradients in F and FG galaxies (see page 77).

The two prime examples of F and FG systems are M51 and M101 respectively. A more extensive study utilizing both additional color measures and spectra of the same restricted regions should enable one to answer some of the questions posed by the comparison of F and FG galaxies. The difference between pure population I and mixed populations may be detected in colors, although the effect is certainly small.

5.4 AF Nuclei

In this section we consider the synthesis of the colors of the peculiar blue nucleus of the AF galaxy NGC 2903. Inspection of the energy curve in Figure 20 reveals that toward the red, NGC 2903 becomes essentially indistinguishable from FG systems. At short wave lengths the AF system is much bluer than FG galaxies. It has been mentioned previously (Section 4.7) that NGC 2903 resembles an FG galaxy in the outer portions, and that all the blueing which distinguishes NGC 2903 from an FG galaxy occurs within the smallest diaphragm used to make observations of the system. Both the similarity of the outer portions and the similarity of the energy curves in the red leads one to ask if the AF colors can be produced by simply increasing the number of young blue stars apparently present in FG galaxies. Interestingly enough it appears that one cannot produce the NGC 2903 nuclear colors in this manner. The first solution of equation 33 in Table 25 illustrates the poor fit obtained when additional O9 stars are added to FG colors. It is apparent that something bluer than O9 is required to achieve a good fit; inclusion of anything intermediate in color between O9 and FG makes the situation worse, yielding negative α values. Since it is doubtful that stars much bluer than O9 exist it follows that something redder than FG is required for combination with blue stars. Synthesis solutions using K'' or K energy distributions plus O9 and A9 stars yielded negative values of α for the A9 source, hence demonstrating that K or K'' colors are not red enough. The only reasonable fit obtained, the second entry in Table 25, combined O9 and A9 colors with a K' energy distribution computed according to equation 34. The fit is by no means perfect, particularly in the ultraviolet where it deviates much like the first solution given in Table 25. Since the synthesis is based upon colors of a single galaxy observed only once, observational errors may cause some of the fitting errors.

The K' energy distribution can be interpreted as the energy distribution of old population I plus an unknown red component. It includes no main sequence earlier than mid to late F and no giants earlier than about K. To synthesize F and FG galaxies it was necessary to add to K' some young O, B, and A stars and an intermediate component, either G giant stars or population II globular cluster stars. The AF synthesis differs in that the intermediate component is missing or weak, and the young blue star weight is somewhat increased. One might possibly explain this observation by saying that the young stars in the NGC 2903 nuclear region are so young that few have had time to evolve into the G giant region. A spectrogram of the nucleus of NGC 2903 taken by Dr. Code suggests from the sharpness and total number of hydrogen lines that many A giants and supergiants are present. A careful study of such spectra should give important independent evidence about the light contributions of G giants.

According to Dr. Code the NGC 2903 spectrogram shows Hβ and mildly strong λ3727 [OII] emission. Hγ is shallow suggesting partial filling in by emission. The emission line observations suggest the presence of H II regions and active star formation. In combination with the color synthesis results and the relative rarity of blue nuclei, the spectral evidence suggests a relatively recent transient phenomenon, possibly an evolutionary stage of a nucleus. A search for additional blue nuclei, and a careful study utilizing both colors and spectra, should answer some of the questions posed by them. Such a study might provide some useful information about stellar evolution. Blue nuclei are probably not uncommon since three out of fifty-seven galaxies observed show the phenomenon. The occurrence of blue nuclei is not a characteristic of any one type of galaxy as is shown by the marked difference in structural type and color of the outer portions among the three observed cases.

Before closing this section and passing on to the rather different A galaxies, it is of interest to summarize some of the reasons for using K or modified K energy distributions in synthesis solutions, rather than

TABLE 25

AF Synthesis Solutions

	L_1	L_2	L_3	L_4	L_5	L_6	L_7	L_8	α
09V	.043	.040	.034	.029	.027	.020	.016	.012	.03
FG	.352	.595	.988	1.685	1.970	2.671	2.928	3.181	.99
Soln.1	.395	.635	1.022	1.714	1.997	2.691	2.944	3.193	
AF	.445	.697	1.000	1.660	1.888	2.704	2.965	3.251	
Soln.1 – AF	–.050	–.044	.022	.054	.109	–.013	–.021	–.058	
09V	.178	.164	.142	.118	.109	.082	.066	.048	.14
A9III	.121	.218	.275	.310	.310	.277	.244	.207	.27
K'	.099	.256	.598	1.240	1.521	2.342	2.637	2.985	.60
Soln.2	.398	.638	1.015	1.668	1.940	2.701	2.947	3.240	
AF	.445	.679	1.000	1.660	1.888	2.704	2.965	3.251	
Soln.2 – AF	–.047	–.041	.015	.008	.052	–.003	–.018	–.011	

using some individual late-type K or M stars. First, we have a reasonable idea of the physical makeup of K aggregates, except perhaps in the far red. Thus studying the modifications necessary to produce other energy distributions is essentially as good as making a synthesis study from stars alone. Secondly, even if we did not understand much about the composition of K aggregates, their common occurrence in space gives one the feeling that they represent a fundamental unit which could be present to various degrees in many systems not purely K. The observation of radial color gradients in K galaxies demonstrates that what we define here as a K nuclear population does indeed appear to mix gradually with other stellar components. Thirdly, the energy curves of all except A type galaxies have a very similar form in the far red. It is directly apparent that whatever satisfies a K energy curve in the far red will, with only small modifications, satisfy FG, F and AF galaxies. Finally, we can understand the K aggregate in terms of modern stellar evolution theory. If most or all galaxies have existed from the "beginning" we would expect to find that at least a portion of each galaxy consists of old stars of the type that characterize K systems.

5.5 A Nuclei

Figure 20 demonstrates that the energy curves of A systems are quite different from energy curves of systems with later spectral class. Not only are A systems strong in the ultraviolet where one would expect, but

THEY ALSO DEVIATE MARKEDLY IN THE FAR RED FROM THE CHARACTERISTIC PATTERN OF REDDER GALAXIES. THERE APPEARS TO BE A SUDDEN UPTURN OF THE ENERGY CURVE IN THE FAR RED, RATHER THAN A LEVELING OFF. IT SHOULD BE MENTIONED AGAIN HERE THAT THE RED A SYSTEM OBSERVATIONS LEAVE MUCH TO BE DESIRED. NONE OF THE SYSTEMS DEFINING THE A ENERGY CURVE BETWEEN BANDS 1 AND 4 WERE OBSERVED IN THE RED. ONE RED OBSERVATION OF AN A SYSTEM WAS TAKEN ON THE EDGE-ON Sc GALAXY NGC 4631. EVEN THIS OBSERVATION SUFFERS SOMEWHAT FROM UNCERTAIN SKY CONDITIONS.

SPECTROSCOPICALLY, MORGAN AND MAYALL (1) FIND THAT A SYSTEMS ARE STRONGLY DOMINATED BY A TO F STARS, AND GENERALLY SHOW EMISSION LINES CHARACTERISTIC OF H II REGIONS. THE FORM OF THE RED ENERGY CURVE SUGGESTS THAT A K COMPONENT, PRESENT IN ALL THE OTHER SYSTEMS CONSIDERED, IS ABSENT OR VERY WEAK. THE SUDDEN UPTURN IN THE FAR RED ENERGY DISTRIBUTION COULD VERY WELL BE THE EFFECT OF M SUPERGIANTS. THUS AN A SYSTEM MODEL HAS BEEN TAKEN FROM **h** AND **χ** PERSEI. TABLE 26 PRESENTS THE SOLUTION OF EQUATION 33 WHEN AN A SYSTEM IS REPRESENTED BY O9, A9, AND M2IA COLORS.

TABLE 26

AN A SYNTHESIS SOLUTION

	L_1	L_2	L_3	L_4	L_5	L_6	L_7	L_8	α
O9V	.252	.232	.200	.167	.155	.116	.093	.068	.20
A9III	.290	.522	.657	.741	.741	.663	.583	.494	.66
M2IA	.004	.019	.113	.396	.578	1.323	1.491	1.760	.11
SOLN.1	.546	.773	.970	1.304	1.474	2.102	2.167	2.322	
A	.555	.738	1.000	1.368	1.514	1.871	2.168	2.466	
SOLN.1 - A	-.009	.035	-.030	-.064	.040	.231	-.001	-.144	

THE FIT IS SEEN TO BE REASONABLE IN THE BLUE, BUT RATHER POOR IN THE RED. OBSERVATIONAL ERRORS PROBABLY CAUSE SOME OF THE POOR RED FIT, BUT IT IS DOUBTFUL IF THEY ACCOUNT FOR ALL THE DEVIATION. A SOMEWHAT REDDER SOURCE THAN M2IA WOULD IMPROVE THE RED FIT. THE DOUBLE PERSEUS CLUSTER CONTAINS M SUPERGIANTS AS LATE AS M4 OR M5. IT WOULD BE INTERESTING TO OBSERVE SOME OF THESE STARS FOR COMPARISON WITH IMPROVED FAR RED MEASURES ON A SYSTEMS. PENDING REVISED RED MEASURES, AN **h** AND **χ** PERSEI MODEL SEEMS TO BE THE BEST DESCRIPTION OF AN A GALAXY.

IT WOULD BE INTERESTING TO OBSERVE A SELECTION OF THE BLUEST GALAXIES FOUND BY HARO (9) TO SEE IF THEY CAN BE REPRESENTED BY AN EVEN STRONGER O and B star population than found in the A galaxies. The O and B star contribution to light in the A galaxies is strong enough that some helium lines might be detected in spectra. The bluest Haro galaxies would almost certainly show helium lines if their very blue color is actually indicative of an extreme preponderance of very young O and B stars.

Except for the replacement of the M2Ia component by K' the AF nucleus of NGC 2903 looks much like the A model. It would be interesting to see if the AF colors could be represented as a combination of FG and A energy distributions once improved red A observations are available. This would be consistent with the outer portions of NGC 2903 resembling an FG galaxy.

The presence of a K component in all but the A galaxies, and probably the very blue Haro galaxies, suggests that the majority of galaxies show no appreciable dispersion in the time of origin of the oldest stars. There appears to be a wide range of possible ages, probably a continuum, among the stellar population bluer than pure K aggregates. The very blue population found in A systems and the AF nucleus of NGC 2903 is certainly very young; the G giant component in F and perhaps FG systems can be interpreted as intermediate in age between the O-B stars and the K component. Since they appear to lack the K component, A systems may represent relatively young galaxies, although a very weak old population could be present and not detectable. Pure or nearly pure population I systems appear to exist, as well as mixed population I and II galaxies. No galaxies consisting of pure population II, at least entirely *old* population II, have been observed.

In conclusion one final point should be made clear. In synthesis solutions certain specific energy sources have been used. The fact that the extragalactic energy distributions have been reproduced more or less satisfactorily from specific sources cannot be taken to imply that galaxies consist of these units. We can however hope that what we use for sources will be *sufficiently representative* of certain portions of a galaxy's content to tell us something. Thus a synthesis solution using an M67 source may give some information about the presence or absence of what we might loosely call old population I. A successful fit does not mean that there are no important differences however. The obvious complexities of galaxies and the relatively low "resolution" of color synthesis studies make it amply clear that we can construct no detailed models of galaxies. We can hope to make some general statements.

REFERENCES

1 MORGAN, W.W. AND MAYALL, N.U. (1957). PUB.A.S.P. 69, 291.

2 HUMASON, M.L., MAYALL, N.U. AND SANDAGE, A.R. (1956). A.J. 61, 97.

3 BAUM, W.A. (1953). A.J. 58, 211, (ABSTRACT).

4 WHITFORD, A.E. (1951). A.J. 56, 51. (ABSTRACT).

5 FEIGE, J. (IN PRESS), AP.J.

6 MINNAERT, M. (1953), THE SUN ED. KUIPER (UNIV. CHICAGO PRESS) CH. 3.

7 ALLEN, C.W. (1953), ASTROPHYSICAL QUANTITIES (UNIV. LONDON, ATHLONE PR.).

8 KEENAN, P.C. AND KELLER, G. (1953), AP.J. 117, 241.

9 HARO, G. (1956), BOL.OBS.TON. Y TAC., NO. 14, P8.

10 HOLMBERG, E. (1958), MEDD.LUNDS ASTR.OBS., SER.II, NO. 136.

11 SHAPLEY, H. AND AMES, A. (1932), ANN.HARV.COLL.OBS. 88, 43.

12 ELVIUS, A. (1956), ANN.OBS.STOCKHOLM 18, NO. 9.

13 WHITFORD, A.E. (1948), AP.J. 107, 102.

14 BAUM, W.A. (1955), A.J. 60, 153, (ABSTRACT).

15 SANDAGE, A.R. (1957), AP.J. 126, 326.

16 JOHNSON, H.L. AND SANDAGE, A.R. (1955). AP.J. 121, 616.

17 ROBERTS, M.S. (1956), A.J. 61, 195.

18 SALPETER, E.E. (1955), AP.J. 121, 161.